National Library
of Canada

Bibliothèque nationale
du Canada

Canadian Theses Service

Service des thèses canadiennes

Ottawa, Canada
K1A 0N4

NOTICE

The quality of this microform is heavily dependent upon the quality of the original thesis submitted for microfilming. Every effort has been made to ensure the highest quality of reproduction possible.

If pages are missing, contact the university which granted the degree.

Some pages may have indistinct print especially if the original pages were typed with a poor typewriter ribbon or if the university sent us an inferior photocopy.

Previously copyrighted materials (journal articles, published tests, etc.) are not filmed.

Reproduction in full or in part of this microform is governed by the Canadian Copyright Act, R.S.C. 1970, c. C-30.

AVIS

La qualité de cette microforme dépend grandement de la qualité de la thèse soumise au microfilmage. Nous avons tout fait pour assurer une qualité supérieure de reproduction.

S'il manque des pages, veuillez communiquer avec l'université qui a conféré le grade.

La qualité d'impression de certaines pages peut laisser à désirer, surtout si les pages originales ont été dactylographiées à l'aide d'un ruban usé ou si l'université nous a fait parvenir une photocopie de qualité inférieure.

Les documents qui font déjà l'objet d'un droit d'auteur (articles de revue, tests publiés, etc.) ne sont pas microfilmés.

La reproduction, même partielle, de cette microforme est soumise à la Loi canadienne sur le droit d'auteur, SRC 1970, c. C-30.

NL-339 (r. 88/04)

Canada

The University of Alberta

Spherically and Cylindrically Symmetric Finite Dynamic Hyperelastic Deformation

by

©

Peter T. Janele

A thesis
submitted to the Faculty of Graduate Studies and Research
in partial fulfilment of the requirements for the degree of

Doctor of Philosophy

Department of Mechanical Engineering

Edmonton, Alberta

Fall, 1988

Permission has been granted to the National Library of Canada to microfilm this thesis and to lend or sell copies of the film.

L'autorisation a été accordée à la Bibliothèque nationale du Canada de microfilmer cette thèse et de prêter ou de vendre des exemplaires du film.

The author (copyright owner) has reserved other publication rights, and neither the thesis nor extensive extracts from it may be printed or otherwise reproduced without his/her written permission.

L'auteur (titulaire du droit d'auteur) se réserve les autres droits de publication; ni la thèse ni de longs extraits de celle-ci ne doivent être imprimés ou autrement reproduits sans son autorisation écrite.

ISBN 0-315-45654-X

The University of Alberta

Release Form

Name of Author: **Peter T. Janele**

Title of Thesis: **Spherically and Cylindrically Symmetric Finite Dynamic Hyperelastic Deformation**

Degree: Doctor of Philosophy

Year this degree granted: Fall 1988

Permission is hereby granted to **The University of Alberta Library** to reproduce single copies of this thesis and to lend or sell such copies for private, scholarly, or scientific research purposes only.

The author reserves other publication rights, and neither the thesis nor extensive tracts from it may be printed or otherwise reproduced without the author's written consent.

Peter Janele

(Student's signature)

Peter T. Janele
615 Munson Mt. Rd.
Penticton, British Columbia
V2A 6J6

Date : August 8, 1988

The University of Alberta
Faculty of Graduate Studies and Research

The undersigned certify that they have read, and recommend to the Faculty of Graduate Studies and Research for acceptance, a thesis entitled

Spherically and Cylindrically Symmetric
Finite Dynamic Hyperelastic Deformation
submitted by
Peter T. Janele

in partial fulfilment of the requirements for the degree of

Doctor of Philosophy.

J.B. Haddow
(Supervisor)
Michael M. Carroll
....
T. Hrudey
A.W. Lipsett

Date : August 8, 1988

Abstract

Some spherically symmetric and cylindrically symmetric elastodynamic problems are considered, namely the finite expansion of thick-walled spherical shells and cylindrical tubes, including compound tubes, and the unloading waves due to a suddenly punched hole in a prestressed sheet. Physically realistic boundary conditions are considered.

Heat conduction is neglected so that the deformation is assumed to be adiabatic. Also, the isentropic approximation is adopted, that is, the effect on the material constitutive equation of the jump in entropy across a shock is neglected. Isothermal and isentropic stress-deformation relations are discussed. A model for strictly entropic elasticity, proposed by Chadwick (1974a), is used to obtain isentropic constitutive equations. Comments on the application and limitations of various strain energy functions are also presented.

Numerical solutions are obtained using a hybrid finite difference-characteristic scheme. This scheme is based on MacCormack's predictor-corrector method, with one of the two additional boundary conditions obtained using the method of characteristics and the other obtained using the Gottlieb-Turkel scheme. The hybrid scheme is attractive due to it's relative ease of implementation, despite complexities of shock formation, wave reflection at material boundaries and transmission and reflection at the interface between dissimilar materials.

The validity of the numerical solutions for nonlinear finite deformation is supported by comparison with various limiting cases for which solutions are available.

Acknowledgements

The author wishes to express appreciation to Dr. J.B. Haddow for his outstanding supervision during this research. Without his guidance and insight, much of this research would not have been possible. The author is also indebted to Dr. A. Mioduchowski for his constructive advice, suggestions and words of encouragement.

This research has been funded in part by the Province of Alberta through a Province of Alberta fellowship.

Special thanks to April for her understanding and support.

Contents

Abstract iv

Acknowledgements v

Chapter 1

Introduction 1

1.1 Scope of Thesis 1

1.2 Previous Related Research 2

1.3 Thermodynamic Considerations 4

1.4 Numerical Methods for Finite Elasticity Problems 4

Chapter 2

Constitutive Relations 7

2.1 Fundamental Equations 7

2.2 Isothermal Strain Energy Functions 10

2.2.1 Strain Energy Functions for Incompressible Materials 10

2.2.2 Gaussian and Modified Gaussian Strain Energy Functions . . 11

2.2.3 Blatz and Ko Strain Energy Function 14

2.2.4 Blatz Strain Energy Function 15

2.3 Justification for Isothermal Stress-Deformation Relation 18

2.3.1 Static Simple Tension of a Solid Cylinder 18

2.3.2 Dynamic Deformation of a Cylinder 24

Chapter 3

Governing Equations 28

3.1 Spherically Symmetric Deformation 28

3.1.1 Linear Elasticity 28

3.1.2 Finite Dynamic Deformation 32

3.1.3 Equilibrium Finite Deformation 36

3.1.4 Initial and Boundary Conditions 39

3.1.5 Jump Conditions 41

3.2 Cylindrically Symmetric Deformation 42

3.2.1 Linear Elasticity 42

3.2.2 Finite Dynamic Deformation 45

3.2.3 Equilibrium Finite Deformation 47

3.2.4 Initial and Boundary Conditions 50

3.2.5 Jump Conditions 51

3.3 Plane Stress of Uniformly Prestressed Sheets 52

3.3.1 Finite Dynamic Deformation 52

3.3.2 Initial and Boundary Conditions for Prestressed Sheets 54

3.3.3 Constitutive Relation : Mooney Rivlin sef 55

3.4 Concentric Cylinders 57

3.4.1 Finite Dynamic Deformation 57

3.4.2 Initial and Boundary Conditions 58

3.4.3 Jump Conditions 60

Chapter 4

Numerical Methods 62

4.1 Method of Characteristics 62

4.1.1 Solutions for Linear Elasticity 64

4.2 MacCormack's Method 69

4.2.1 Gottlieb-Turkel Scheme for Boundary Conditions 70

4.2.2 MacCormack's Method for the Unbounded Medium Problem . 71

4.2.3 MacCormack's Method with Gottlieb-Turkel Scheme 72

4.3 Hybrid Numerical Scheme 75

4.3.1 Boundary Condition Relations 75

4.3.2 Comparison with Linear Elasticity Solution 78

4.3.3 Verification of Jump Conditions 78

4.3.4 Comparison with a Previous Nonlinear Elasticity Solution . . 83

4.3.5 Interface Conditions for Concentric Cylinders 84

4.3.6 Limitations of the Hybrid Method 89

Chapter 5

Numerical Solutions **94**

5.1 Spherically Symmetric Deformation 94

5.1.1 Incompressible Spherical Shell 95

5.1.2 Equilibrium Solution : Spherical Cavity in an Unbounded Medium 97

5.1.3 Sudden Application of Pressure : Unbounded Medium 97

5.1.4 Sudden Application of Pressure : Spherical Shell 107

5.1.5 Sinusoidal Pulse : Unbounded Medium 107

5.1.6 Comparison of Gaussian Strain Energy Functions 111

5.1.7 Solutions for Blatz Strain Energy Function 113

5.2 Cylindrically Symmetric Deformation 115

5.2.1 Incompressible Cylindrical Tube 115

5.2.2 Sudden Application of Pressure 117

5.3 Plane Stress of Uniformly Prestressed Sheets 119

5.3.1 Comparison with Method of Characteristics 119

5.3.2 Prestressed Finite Sheets 120

5.3.3 Elastic Stability of Prestressed Finite Sheets 128

5.4 Concentric Cylinders 131

Chapter 6

Concluding Remarks **137**

References 139

Appendix A
Spherically Symmetric Deformation in Incompressible Materials 143

Appendix B
Finite Elasticity Terminology 149

List of Tables

4.1 Jump Discontinuities at Shock Fronts : Spherical Shell 83

5.1 Jump Discontinuities at Shock Fronts : Unbounded Medium 106

List of Figures

2.1 Pure Dilatation
Strain Energy Function Based on Hydrostatic Compression Data . . . 13

2.2 Pure Dilatation
Blatz and Ko Strain Energy Function 16

2.3 Simple Tension of a Solid Cylinder 19

2.4 Simple Tension of a Solid Cylinder
Isentropic/Isothermal Stress-Deformation Relations
$\beta = 9.35 \times 10^{-4}, \gamma = 880.39, \nu = 0.49989$ 23

2.5 Cylindrical Tube, $R_o/R_i = 2$
Isentropic/Isothermal Stress-Deformation Relations
modified Gaussian sef, $\nu = 0.495$
$p(\tau) = H(\tau)$ 27

4.1 Spherical Cavity in an Unbounded Medium
Response at $R = 1$
Method of Characteristics, Linear Elasticity, $\nu = 0.25$
$p(\tau) = 0.01\, H(\tau)$ 66

4.2 Spherical Shell, $R_o/R_i = 2$
Response Before Reflection, $\tau = 0.5$
Method of Characteristics, Linear Elasticity, $\nu = 0.25$
$p(\tau) = 0.01\, H(\tau)$ 67

4.3 Spherical Shell, $R_o/R_i = 2$
Response After Reflection, $\tau = 1.5$
Method of Characteristics, Linear Elasticity, $\nu = 0.25$
$p(\tau) = 0.01\, H(\tau)$ 68

4.4 Spherical Cavity in an Unbounded Medium
Response at $R = 1$
MacCormack's Method with Gottlieb-Turkel Boundary Conditions
Linear Elasticity, $\nu = 0.25$
$p(\tau) = 0.01\, H(\tau)$ 73

4.5 Spherical Shell, $R_o/R_i = 2$
Response Before Reflection, $\tau = 0.5$
Hybrid Scheme, Blatz sef, $\nu = 0.25$
$p(\tau) = 0.01\,H(\tau)$ 79

4.6 Spherical Shell, $R_o/R_i = 2$
Response After Reflection, $\tau = 1.5$
Hybrid Scheme, Blatz sef, $\nu = 0.25$
$p(\tau) = 0.01\,H(\tau)$ 80

4.7 Spherical Shell, $R_o/R_i = 2$
P_r and v at $\tau = 0.05$ and $\tau = 0.10$
Hybrid Scheme, modified Gaussian sef, $\nu = 0.495$
$p(\tau) = H(\tau)$ 81

4.8 Spherical Shell, $R_o/R_i = 2$
λ_r at $\tau = 0.05$ and $\tau = 0.10$
Hybrid Scheme, modified Gaussian sef, $\nu = 0.495$
$p(\tau) = H(\tau)$ 82

4.9 Spherical Shell, $R_o/R_i = 2$
Hybrid Scheme and Method of Characteristics
Blatz and Ko sef, $\nu = 0.3$
$p(\tau) = 0.25\,H(\tau)$ 85

4.10 Concentric Cylinders, $\nu_1 = 0.48$, $\nu_2 = 0.495$, $\zeta = \rho_{02}/\rho_{01} = 2$, $\psi = \mu_2/\mu_1 = 7$, $R_i = 1$, $R_* = 1.25$, $R_o = 1.5$.
Hybrid Method with Gottlieb-Turkel Boundary Conditions
Response at $\tau = 0.025$ and $\tau = 0.05$
Modified Gaussian sef, $\nu = 0.495$, $p(\tau) = H(\tau)$ 87

4.11 Spherical Cavity in an Unbounded Medium, Linear Elasticity
Hybrid Scheme, Effect of Spacial Step Size, $\Delta R = 0.0025$
Response at $\tau = 0.25$, $\tau = 0.50$, $\tau = 0.75$,
$p(\tau) = 0.01\,H(\tau)$ 90

4.12 Spherical Cavity in an Unbounded Medium, Linear Elasticity
Hybrid Scheme, Effect of Spacial Step Size, $\Delta R = 0.0001$
Response at $\tau = 0.25$, $\tau = 0.50$, $\tau = 0.75$,
$p(\tau) = 0.01\,H(\tau)$ 92

5.1 Phase Plane Solution, Motion of the Inner Cavity Wall
Incompressible Spherical Shell, neo-Hookean sef, $R_o/R_i = 2$
$p(\tau) = q\,H(\tau)$ 96

5.2 Spherical Cavity in an Unbounded Medium
Steady State Solution
Modified Gaussian sef, $\nu = 0.495$
$p(\tau) = H(\tau)$ 98

5.3 Spherical Cavity in an Unbounded Medium
Velocity at $\tau = 0.2$, 0.4 and 0.6
Modified Gaussian sef, $\nu = 0.495$
$p(\tau) = 10\,H(\tau)$ 99

5.4 Spherical Cavity in an Unbounded Medium
Radial Stretch at $\tau = 0.2$, 0.4 and 0.6
Modified Gaussian sef, $\nu = 0.495$
$p(\tau) = 10\,H(\tau)$ 101

5.5 Spherical Cavity in an Unbounded Medium
Nominal Radial Stress at $\tau = 0.2$, 0.4 and 0.6
Modified Gaussian sef, $\nu = 0.495$
$p(\tau) = 10\,H(\tau)$ 102

5.6 Spherical Cavity in an Unbounded Medium
Velocity, Stretch and Dilation at $R = R_i$
Modified Gaussian sef, $\nu = 0.495$
$p(\tau) = 10\,H(\tau)$ 103

5.7 Spherical Cavity in an Unbounded Medium
Velocity and Stretch at $R = R_i$
neo-Hookean sef
$p(\tau) = 10\,H(\tau)$ 104

5.8 Spherical Cavity in an Unbounded Medium
Motion of the Cavity Wall
Modified Gaussian sef, $\nu = 0.495$ and neo-Hookean sef
$p(\tau) = H(\tau)$ 105

5.9 Spherical Shell, $R_o/R_i = 2$
Motion of the Inner Cavity Wall
Modified Gaussian sef, $\nu = 0.495$, and neo-Hookean sef
$p(\tau) = H(\tau)$ 108

5.10 Phase Plane Solution for Spherical Shell, $R_o/R_i = 2$
Motion of the Inner Cavity Wall
Modified Gaussian sef, $\nu = 0.495$, and neo-Hookean sef
$p(\tau) = q\,H(\tau)$ 109

5.11 Spherical Cavity in an Unbounded Medium
Modified Gaussian sef, $\nu = 0.495$,
$p(\tau) = 10\,\sin(\pi\tau/0.1)H(\tau)\,H(0.1-\tau)$ 110

5.12 Spherical Cavity in an Unbounded Medium
Motion of the Inner Cavity Wall
Comparison of Gaussian Strain Energy Functions, $\nu = 0.463$
$p(\tau) = H(\tau)$ 112

5.13 Spherical Shell, $R_o/R_i = 2$
Motion of the Inner Cavity Wall
Blatz sef
$p(\tau) = 0.25\,H(\tau)$ 114

5.14 Phase Plane Solution for Cylindrical Tube
Motion of the Inner Cavity Wall
neo-Hookean sef, $R_o/R_i = 2$
$p(\tau) = q\,H(\tau)$ 116

5.15 Phase Plane Solution for Cylindrical Tube, $R_o/R_i = 2$
Motion of the Inner Cavity Wall
Modified Gaussian sef, $\nu = 0.495$ and neo-Hookean sef
$p(\tau) = 0.4\,H(\tau)$ 118

5.16 Plane Stress Deformation in an Unbounded Medium
Comparison of Hybrid Scheme with Method of Characteristics
Mooney-Rivlin sef, $\alpha = 0.75$, $\lambda_o = 1.2$, $\tau_* = 0.05$ 121

5.17 Plane Stress Deformation, $R_o/R_i = 6$, $v(6,\tau) = 0$
Solution Before Reflection, $\tau = 2$
Mooney-Rivlin sef, $\alpha = 0.6$, $\lambda_o = 1.2$, $\tau_* = 0.05$ 123

5.18 Plane Stress Deformation, $R_o/R_i = 6$, $v(6,\tau) = 0$
Solution After Reflection From Rigid Wall at $R = 6$, $\tau = 4$
Mooney-Rivlin sef, $\alpha = 0.6$, $\lambda_o = 1.2$, $\tau_* = 0.05$ 124

5.19 Plane Stress Deformation, $R_o/R_i = 6$, $v(6,\tau) = 0$
Solution After Reflection From Edge of Hole, $\tau = 6$
Mooney-Rivlin sef, $\alpha = 0.6$, $\lambda_o = 1.2$, $\tau_* = 0.05$ 125

5.20 Plane Stress Deformation, $R_o/R_i = 6$, $v(6,\tau) = 0$
Solution After Several Reflections, $\tau = 14.0$
Mooney-Rivlin sef, $\alpha = 0.6$, $\lambda_o = 1.2$, $\tau_* = 0.05$ 126

5.21 Plane Stress Deformation, $R_o/R_i = 6$, $v(6,\tau) = 0$
Formation of a Shock After Several Reflections, $\tau = 16.0$
Mooney-Rivlin sef, $\alpha = 0.6$, $\lambda_o = 1.2$, $\tau_* = 0.05$ 127

5.22 Plane Stress Deformation, $R_o/R_i = 2$, $v(2,\tau) = 0$
Solution Before Reflection, $\tau = 0.4$
Mooney-Rivlin sef, $\alpha = 0.6$, $\lambda_o = 1.2$, $\tau_* = 0.05$ 129

5.23 Plane Stress Deformation, $R_o/R_i = 2$, $v(2,\tau) = 0$
Solution After Reflection From Rigid Wall at $R = 2$, $\tau = 0.8$
Mooney-Rivlin sef, $\alpha = 0.6$, $\lambda_o = 1.2$, $\tau_* = 0.05$ 130

5.24 Concentric Cylinders, $\nu_1 = 0.48$, $\nu_2 = 0.495$, $\zeta = \rho_{02}/\rho_{01} = 2$, $\psi = \mu_2/\mu_1 = 7$, $R_i = 1$, $R_* = 1.25$, $R_o = 1.5$, $q = 1$.
Velocity at $\tau = 0.025$ and $\tau = 0.05$
Modified Gaussian sef 132

5.25 Concentric Cylinders, $\nu_1 = 0.48$, $\nu_2 = 0.495$, $\zeta = \rho_{02}/\rho_{01} = 2$, $\psi = \mu_2/\mu_1 = 7$, $R_i = 1$, $R_* = 1.25$, $R_o = 1.5$, $q = 1$.
Nominal Radial Stress at $\tau = 0.025$ and $\tau = 0.05$
Modified Gaussian sef 133

5.26 Concentric Cylinders, $\nu_1 = 0.48$, $\nu_2 = 0.495$, $\zeta = \rho_{02}/\rho_{01} = 2$, $\psi = \mu_2/\mu_1 = 7$, $R_i = 1$, $R_* = 1.25$, $R_o = 1.5$, $q = 1$.
Radial Stretch at $\tau = 0.025$ and $\tau = 0.05$
Modified Gaussian sef 134

5.27 Concentric Cylinders, $\nu_1 = 0.48$, $\nu_2 = 0.495$, $\zeta = \rho_{02}/\rho_{01} = 1$, $\psi = \mu_2/\mu_1 = 3$, $R_i = 1$, $R_* = 1.25$, $R_o = 1.5$, $q = 1$.
Radial Stretch at $\tau = 0.025$ and $\tau = 0.05$
Modified Gaussian sef 136

Chapter 1

Introduction

1.1 Scope of Thesis

Propagation of spherically and cylindrically symmetric finite amplitude waves in compressible isotropic hyperelastic solids is considered in this thesis. As a preliminary, the constitutive behaviour of solid rubberlike materials is considered in Chapter 2, including thermodynamic aspects of the deformation.

Governing equations for both spherically and cylindrically symmetric finite elasticity are presented in conservation form in Chapter 3. When a realistic constitutive relation is utilized, a hyperbolic system of first order quasi-linear partial differential equations is obtained. This system, together with appropriate boundary and initial conditions, defines a boundary-initial-value problem for which an exact analytical solution can not, in general, be obtained.

Numerical methods are considered in Chapter 4. Limitations and stability problems of existing techniques are discussed and a hybrid numerical scheme is introduced. The hybrid scheme is attractive due to its relative ease of implementation, despite complexities of shock formation and reflection at material boundaries. Confidence in the validity of the hybrid scheme is based on comparison of various numerical results with limiting cases for which exact solutions are available and on comparison with published nonlinear finite deformation solutions which have been obtained independently.

Numerical results for several important problems of spherically and cylindrically symmetric elastodynamic deformation are presented in Chapter 5. These include :

- finite elastic expansion of a spherical cavity in an unbounded medium and spherically symmetric deformation of a thick-walled shell.
- finite elastic expansion of a cylindrical cavity in an unbounded medium and cylindrically symmetric deformation of a thick-walled tube.
- finite amplitude plane stress unloading waves in prestressed sheets of both finite outer radius and unbounded extent.
- finite elastic deformation of concentric cylindrical tubes, each of which has distinct material properties.

1.2 Previous Related Research

Spherically and cylindrically symmetric elastodynamic deformation problems have been previously considered by several researchers. Analytical solutions have been obtained for the corresponding linear elasticity problem, and various numerical techniques have been used to obtain solutions for both linear and nonlinear deformation. A brief summary of the related previous research in this area is presented below.

Knowles (1960) solved the problem of the expansion of an incompressible cylindrical hyperelastic tube. A modification of this solution for a spherical shell is included in this thesis. The expansion of an incompressible tube or shell is a single-degree-of-freedom vibration problem rather than a wave propagation problem; the propagation velocity of longitudinal waves in an incompressible material is infinite. The governing equation for this problem is a second order nonlinear ODE which gives the position of a particular radius as a function of time. Although an exact solution to this ODE is unavailable (when a realistic strain energy function is considered), a numerical solution can be obtained using standard techniques.

Knowles and Jakub (1965) considered the finite dynamic deformation of an incompressible elastic medium containing a spherical cavity. Their solution gives the period and maximum amplitude of the motion of the cavity wall in terms of an improper integral. A complete expression for the periodic motion is not given.

Miklowitz (1960), used a Laplace Transform technique for the linear elasticity problem of plane stress unloading waves, in a prestressed sheet, due to a suddenly punched hole. For this particular case, analytical inversion of the Laplace transform was possible but in general, numerical methods are needed to evaluate the resulting inversion integrals. The Laplace Transform method is restricted to problems of linear elasticity.

Chou and Koenig (1966) applied the method of characteristics to solve linear elasticity problems of cylindrical tubes and spherical shells. The characteristic relations are integrated using a numerical finite difference scheme.

Haddow and Mioduchowski (1975, 1977) applied the method of characteristics to problems of nonlinear finite deformation. Implementation of this method for problems of this type is relatively difficult as is discussed in section 1.4 and Chapter 4. In addition, the method of characteristics does not seem applicable to almost-incompressible elastic solids for the cylindrical tube and spherical shell problems since the method becomes unstable as Poisson ratio increases. This is because the slopes dR/dt, of two of the families of characteristics [1] approach ∞ as $\nu \rightarrow 0.5$. The highest Poisson ratio for which results are obtained by Haddow and Mioduchowski (1978) is $\nu = 0.48$. The Poisson ratio of most solid rubbers is in the range

---

[1] For spherically symmetric and cylindrically symmetric deformation, there are three families of characteristics, one of which is parallel to the time axis in the space-time domain.

$0.463 \leq \nu \leq 0.499895$ as given by numerous references including Chadwick (1974a) and Beatty and Stalnaker (1986).

1.3 Thermodynamic Considerations

Most of the previous research and solutions for spherically and cylindrically symmetric elastodynamic problems ignores the thermodynamic aspects of the deformation and related constitutive material description. It is commonly assumed that the use of an isothermal stress-deformation relation is a suitable approximation.

An alternative approximation is to consider an adiabatic deformation. This is motivated by the low thermal conductivity of most solid rubbers (Baumeister et al., 1978). If it is further assumed that the effect of the entropy jump across a shock can be neglected (Bland, 1969), then the use of an isentropic stress-deformation relation is appropriate.

Chadwick (1974) and Chadwick and Creasy (1984) propose equations of state for strictly entropic and modified entropic elasticity, respectively. The model for strictly entropic elasticity is used in chapter 2 to evaluate the difference between isentropic and isothermal stress-deformation relations for the range of deformations considered in this thesis.

1.4 Numerical Methods for Finite Elasticity Problems

When a realistic constitutive relation is utilized, the governing equations for spherically and cylindrically symmetric deformation are a quasi-linear system of hyperbolic PDE's. The form of these equations and associated boundary and initial conditions necessitates implementation of a numerical method to obtain a solution.

Both the method of characteristics and various finite difference methods have been successfully used for various elastodynamic problems involving formation of a shock. Implementation of the method of characteristics for problems of nonlinear finite deformation is relatively complicated for several reasons :

- Since the propagation speed of the disturbance is not constant, the characteristics are not of constant slope and hence do not form straight lines in the space-time plane. Their position is not known apriori and must be determined as part of the solution.
- In general, the characteristic velocity and shock velocity do not coincide. The complexity of implementing the method of characteristics is compounded when wave reflection occurs and when partial transmission and reflection at an interface between dissimilar materials exists.

Numerous finite difference methods have been proposed, including the Lax-Wendroff, Godunov, MacCormack, Rusanov and Upwind schemes (Sod, 1978). Each of these is a first order scheme, except the MacCormack and Lax-Wendroff schemes which are of second order accuracy. A general form for second- and third-order difference schemes is given by Warming, et al. (1973). Successful application of some of these schemes for specific problems in elastodynamics has been demonstrated by various researchers including Haddow, et al. (1987a, 1987b).

The use of finite difference methods for elastodynamic problems is attractive due to the relative ease of implementation. This is primarily due to the implicit shock-capturing nature of these methods. Both the location and intensity of a discontinuity are obtained without explicit use of jump relations or shock fitting procedures.

When applied to the problems of spherically and cylindrically symmetric elasticity, the use of MacCormack's finite difference method with boundary conditions obtained from the Gottlieb-Turkel scheme (1978) does not yield plausible results. The scheme is numerically unstable; the solution for the dependent variables increases without bound. This stability limitation is illustrated and further discussed in Chapter 4.

A hybrid finite difference-characteristic scheme is proposed. This scheme is based on MacCormack's method with boundary conditions obtained using both the method of characteristics and the Gottlieb-Turkel scheme. The use of the characteristic relation is important to avoid numerical instability.

Chapter 2

Constitutive Relations

2.1 Fundamental Equations

A fundamental equation of state for an isotropic hyperelastic solid is given by the internal energy as a function of stretch and entropy,

$$U = \hat{U}\,(\lambda_i\,,\,s) \tag{2.1}$$

where s is the specific entropy and $\hat{U}$ is a symmetric function of the principal stretches $\lambda_i\,,\ i = 1,2,3$.

The nominal stress [1] P_i, corresponding to the principal stretches λ_i and the temperature T are given by

$$\begin{aligned} P_i(\lambda_i\,,s) &= \rho_o \frac{\partial \hat{U}}{\partial \lambda_i}, \\ T(\lambda_i\,,s) &= \frac{\partial \hat{U}}{\partial s}. \end{aligned} \tag{2.2}$$

where ρ_o is the density in the undeformed reference configuration. If heat conduction is neglected (so that the deformation is considered to be adiabatic) and if the effect on the constitutive relations of the entropy change across a shock is neglected, then an isentropic relation between stress and deformation is given by

$$P_i = \rho_o\,\frac{\partial \hat{U}(\lambda_i,\,0)}{\partial \lambda_i}, \tag{2.3}$$

where the entropy in the reference configuration is zero. The adiabatic approximation is reasonable since most solid rubbers have a low thermal conductivity (Baumeister et al., 1978).

---

[1] More precisely, the principal components of the Biot stress as discussed by Ogden (1984).

The jump in entropy at a shock depends on the magnitude of the shock (Whitham, 1974). As a result, the deformation behind a shock of changing strength can not be isentropic. However, neglect of the effect of the entropy jump across a shock on the constitutive relations is justified for shocks of moderate strength (Bland, 1969) as are considered in this thesis.

An alternative fundamental equation of state is given by the Helmholtz free energy per unit mass A, taken as a function of stretch and temperature

$$A = \hat{A}\,(\lambda_i, T), \tag{2.4}$$

where $\hat{A}$ is a symmetric function of the principal stretches λ_i. Equation (2.4) can be obtained from the internal energy using a Legendre transformation. It follows that

$$\begin{aligned} P_i\,(\lambda_i\,,T) &= \rho_o \frac{\partial \hat{A}}{\partial \lambda_i}, \\ s\,(\lambda_i\,,T) &= -\frac{\partial \hat{A}}{\partial T}. \end{aligned} \tag{2.5}$$

If an isothermal relation between stress and stretch at constant temperature T_o is considered, then

$$P_i(\lambda_i\,,T_o) = \rho_o \frac{\partial \hat{A}\,(\lambda_i\,,T_o)}{\partial \lambda_i}. \tag{2.6}$$

For a relation of this form, it is customary to express the strain energy function per unit volume of the natural reference state at temperature T_o as

$$W(\lambda_i) = \rho_o\,\hat{A}\,(\lambda_i\,,T_o). \tag{2.7}$$

It follows that

$$P_i = \frac{\partial W}{\partial \lambda_i} \tag{2.8}$$

for isothermal deformation from the reference state. The principal Cauchy stress components for isotropic materials are related to the corresponding nominal stress components by

$$\sigma_i = \frac{\lambda_i}{J} P_i, \tag{2.9}$$

where $J = \lambda_1\lambda_2\lambda_3$ and summation convention does not apply.

The compressible deformation of spherical shells and cylindrical tubes which are considered in this thesis, is based on strain energy functions for compressible isotropic elastic solids of the form

$$W(\lambda_i) = \mu\, f(\lambda_i) + \kappa\, g(J), \tag{2.10}$$

where μ and κ are the isothermal shear and bulk modulii, respectively, for infinitesimal deformation from the natural reference state at temperature T_o. The function $f(\lambda_i)$ is symmetric in λ_i and

$$f(\lambda_i) = 0 \tag{2.11}$$

for pure dilatation, that is when $\lambda_1 = \lambda_2 = \lambda_3$. The function $g(J)$ satisfies the conditions

$$\begin{aligned} g(1) &= g'(1) = 0, \\ g''(1) &= 1, \end{aligned} \tag{2.12}$$

where $J = 1$ for isochoric deformation. Justification of the form (2.10) for rubberlike materials, is given by Chadwick and Creasy (1984). Justification for the use of an isothermal relation between stress and deformation is presented in section 2.3.

2.2 Isothermal Strain Energy Functions

Three strain energy functions (sef) for compressible materials are considered in this thesis. The Gaussian, and Blatz and Ko strain energy functions, can be expressed in the form (2.10) and are compressible generalizations of the incompressible neo-Hookean form.

The Blatz sef is derived for the deformation of a polyurethane foam rubber. A brief discussion of limitations of this sef is presented in section 2.2.4.

2.2.1 Strain Energy Functions for Incompressible Materials

The discussion of incompressible materials considered in this thesis is based on either the neo-Hookean sef

$$\begin{aligned} W &= \frac{\mu}{2}(I_1 - 3), \\ I_1 &= {\lambda_1}^2 + {\lambda_2}^2 + {\lambda_3}^2, \end{aligned} \tag{2.13}$$

or the more general Mooney-Rivlin form

$$W = \frac{\mu}{2}\left\{(I_1 - 3)\alpha + (I_2 - 3)(1 - \alpha)\right\}, \tag{2.14}$$

where $0 \leq \alpha \leq 1$ and

$$I_2 = {\lambda_1}^2{\lambda_2}^2 + {\lambda_2}^2{\lambda_3}^2 + {\lambda_3}^2{\lambda_1}^2. \tag{2.15}$$

The parameter α can be adjusted in accordance with experimental data.

2.2.2 Gaussian and Modified Gaussian Strain Energy Functions

It is shown by Ogden (1982) that experimental data for hydrostatic compression of solid rubberlike materials can be described by

$$\frac{p}{\kappa} = \frac{1}{9}\{J^{-10} - J^{-1}\}, \tag{2.16}$$

where p is the hydrostatic pressure and κ is the bulk modulus for infinitesimal deformation from the natural state.

It follows from (2.8), (2.9), (2.10) and (2.11), for hydrostatic compression,

$$\frac{p}{\kappa} = -\frac{dg}{dJ}, \tag{2.17}$$

so that integration of (2.16) gives

$$g(J) = \frac{1}{9}\left(\frac{J^{-9}}{9} + \ln J - \frac{1}{9}\right) \tag{2.18}$$

where the constant of integration is specified by (2.12a). Using this relation for $g(J)$, a compressible generalization of the neo-Hookean sef based on (2.10) and (2.13) is

$$W = \frac{\mu}{2}\left\{\lambda_1{}^2 + \lambda_2{}^2 + \lambda_3{}^2 - 3\,J^{2/3}\right\} + \frac{\kappa}{9}\left\{\frac{J^{-9}}{9} + \ln J - \frac{1}{9}\right\}. \tag{2.19}$$

The second term of (2.19) can be expanded using a Taylor series

$$\frac{1}{2}\,\kappa\,(J-1)^2 + O\,(J-1)^3. \tag{2.20}$$

Use of this relation results in the Gaussian sef for compressible elastic deformation

$$W = \frac{\mu}{2}\left\{\lambda_1{}^2 + \lambda_2{}^2 + \lambda_3{}^2 - 3\,J^{2/3}\right\} + \frac{1}{2}\,\kappa\,(J-1)^2. \tag{2.21}$$

The sef (2.19) is an extension of the Gaussian sef (2.21), and it will be referred to as the modified Gaussian strain energy function throughout this thesis.

Equation (2.16) is based on experimental data for hydrostatic compression and is not experimentally verified for hydrostatic tension. For hydrostatic tension, there are problems associated with the formation of cavities and only relatively small volume increases have been achieved experimentally (Ogden, 1984). However, if the deformation is such that $|J-1| << 1$, the sef (2.19) reduces to the Gaussian sef (2.21) and is a reasonable expression for the material behaviour. This is supported in figure 2.1 which shows the relations for pure dilatation in which nondimensional pressure

$$p^* = \frac{-9p}{\kappa}, \tag{2.22}$$

is plotted against dilatation $(J-1)$. The discrete data points are from the experimental work by Adams and Gibson (1930) and Bridgman (1945) and are in excellent agreement with the curve given by (2.16). Extension of the curve for hydrostatic tension in which $(J-1) << 1$ is plausible.

For the deformation of solid rubberlike materials considered in this thesis, the dilatation is small due to the nearly incompressible nature of the material at high Poisson ratios. In addition, only positive pressures are applied at the inner cavity of the spherical and cylindrical shells under consideration.

For the special case of spherically symmetric deformation

$$\begin{aligned} \lambda_1 &= \lambda_r, \\ \lambda_2 &= \lambda_3 = \lambda_\phi, \\ J &= \lambda_r \lambda_\phi^2. \end{aligned} \tag{2.23}$$

The modified Gaussian sef (2.19) is of the form

$$W = \frac{\mu}{2}\left\{\lambda_r^2 + 2\lambda_\phi^2 - 3J^{2/3}\right\} + \frac{\kappa}{9}\left\{\frac{J^{-9}}{9} + \ln J - \frac{1}{9}\right\}, \tag{2.24}$$

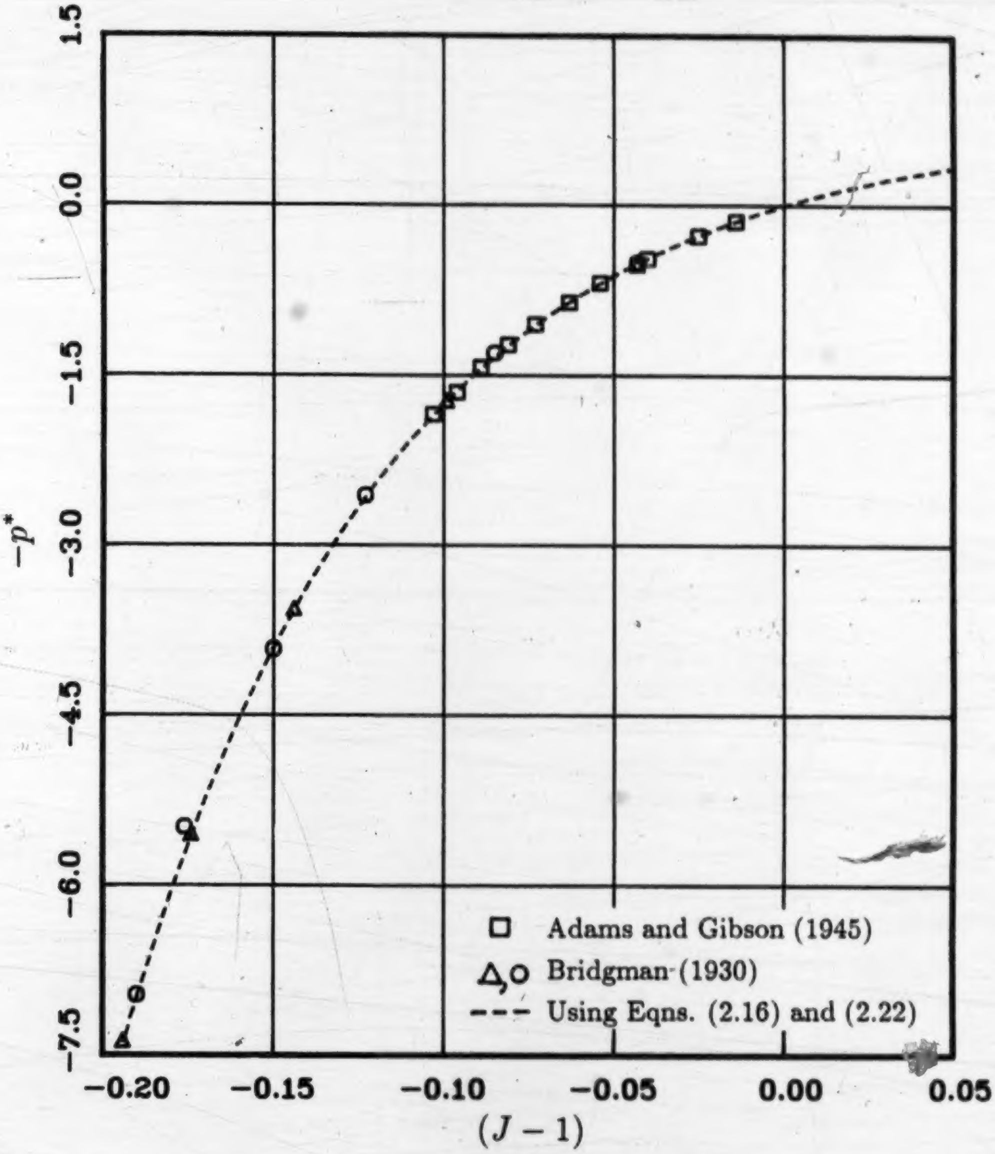

Figure 2.1: Pure Dilatation
Strain Energy Function Based on Hydrostatic Compression Data

and the Gaussian sef (2.21) is of the form

$$W = \frac{\mu}{2}\left\{\lambda_r{}^2 + 2\lambda_\phi{}^2 - 3J^{2/3}\right\} + \frac{1}{2}\,\kappa\,(J-1)^2. \tag{2.25}$$

For the special case of plane strain, cylindrically symmetric deformation

$$\begin{aligned}
\lambda_1 &= \lambda_r, \\
\lambda_2 &= \lambda_\theta, \\
\lambda_3 &= 1, \\
J &= \lambda_r\,\lambda_\theta,
\end{aligned} \tag{2.26}$$

and the Gaussian sef (2.21) is

$$W = \frac{\mu}{2}\left\{\lambda_r{}^2 + \lambda_\theta{}^2 + 1 - 3\,J^{\,2/3}\right\} + \frac{1}{2}\,\kappa\,(J-1)^2. \tag{2.27}$$

2.2.3 Blatz and Ko Strain Energy Function

The Blatz and Ko sef (1962) is also a compressible generalization of the neo-Hookean model and is usually expressed in the form

$$W = \frac{\mu}{2}\left\{(I_1 - 3) + \frac{(1-2\nu)}{\nu}\left(J^{2\nu/2\nu-1} - 1\right)\right\}, \tag{2.28}$$

where ν is Poisson's ratio for infinitesimal deformation from the natural undeformed state. This sef can also be written in the general form (2.10) with

$$\begin{aligned}
f(\lambda_i) &= \frac{1}{2}\,(I_1 - 3\,J^{2/3}), \\
g(J) &= \frac{3}{4}\,\frac{(1-2\nu)}{(1+\nu)}\left\{3\,(J^{2/3} - 1) + \frac{(1-2\nu)}{\nu}\left(J^{2\nu/2\nu-1} - 1\right)\right\}.
\end{aligned} \tag{2.29}$$

An important limitation of the Blatz and Ko sef is that, if a realistic value of ν is chosen for solid rubber, this sef predicts unrealistically high values of pressure for hydrostatic compression. This is illustrated in figure 2.2, which is similar to that presented by Ogden (1984), and shows nondimensional pressure

$$p^* = \frac{9p}{\kappa} \tag{2.30}$$

as a function of $(1 - J)$. For the Blatz and Ko sef, the nondimensional pressure term is

$$\frac{p}{\kappa} = \frac{3}{2}\left(\frac{1-2\nu}{1+\nu}\right)\left\{J^{1/(2\nu-1)} - J^{-1/3}\right\}. \tag{2.31}$$

which can be obtained using (2.17) and (2.29*b*). The discrete data points are experimental data from the research of Adams and Gibson (1930) and Bridgman (1945). The continuous curves are given by (2.31) and (2.30) for various values of Poisson's ratio.

The experimental data imply that the relation between p and $(1 - J)$ is independent of Poisson's ratio. This is not in agreement with the relation predicted by the Blatz and Ko relation (2.31). At high Poisson ratios, the predicted value of pressure at a particular dilatation is significantly in error.

Numerical results for spherically symmetric deformation using the Blatz and Ko sef are presented in this thesis primarily for comparison with the numerical results given by Haddow and Mioduchowski (1976). These authors use this sef and the method of characteristics to solve the problem of finite deformation of a spherical shell.

2.2.4 Blatz Strain Energy Function

Blatz (1969) proposed the following sef for polyurethane foam rubber

$$W = \frac{\mu}{2}\left\{\frac{1}{{\lambda_1}^2} + \frac{1}{{\lambda_2}^2} + \frac{1}{{\lambda_3}^2} + 2J - 5\right\}, \tag{2.32}$$

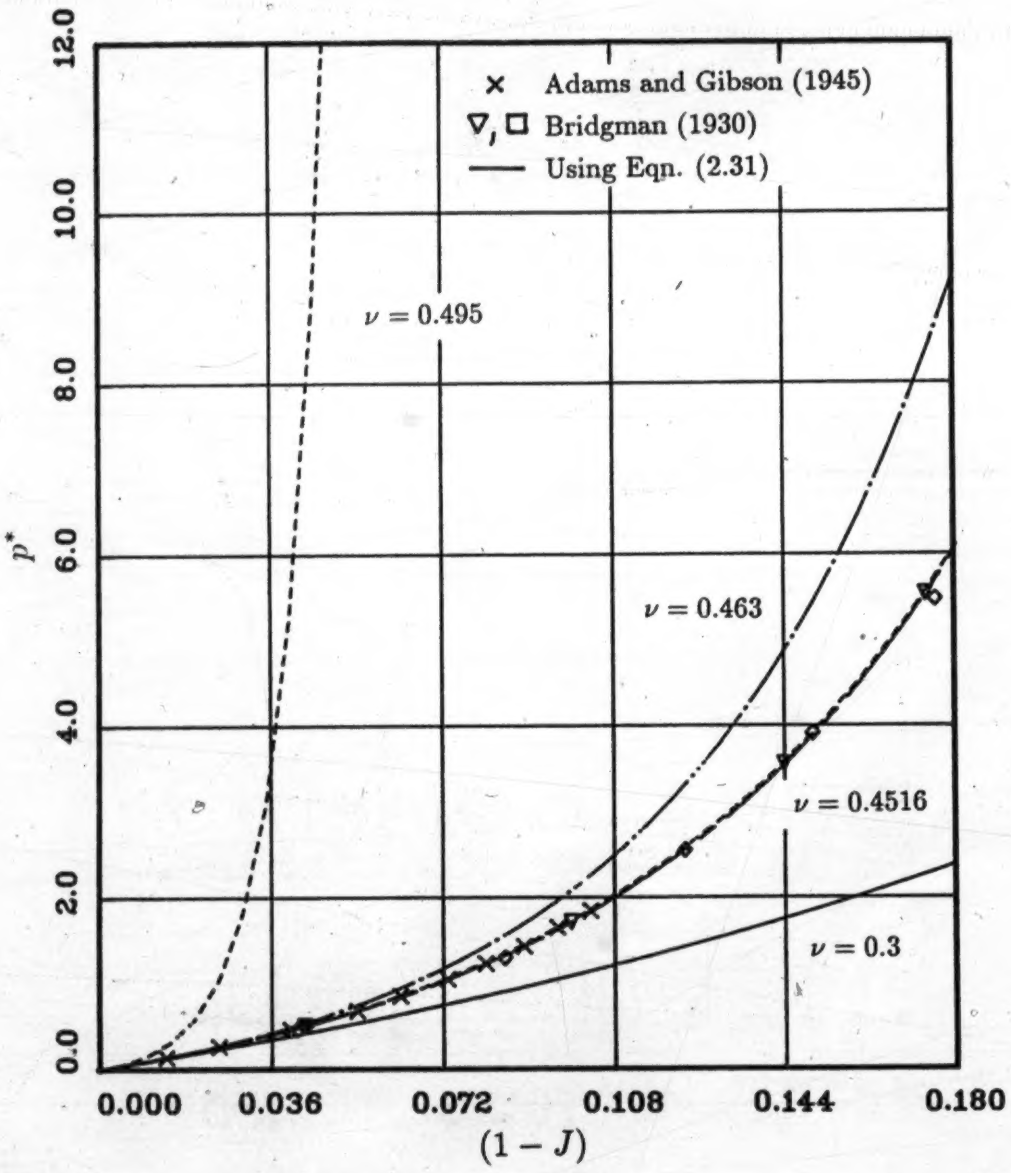

Figure 2.2: Pure Dilatation
Blatz and Ko Strain Energy Function

where $J = \lambda_1\lambda_2\lambda_3$ and a Poisson ratio of $\nu = 0.25$ is implied. The shear modulus μ and Poisson ratio ν are for infinitesimal deformation from the natural undeformed state.

The Blatz sef is based on experimental data in which samples of polyurethane foam rubber were subjected to simple and strip-biaxial tension. Measurements were made under equilibrium conditions. The particular foam rubber which was tested had a 47% void space and the effect of this void space on the dynamic deformation of the foam material is not well understood. If the scattering effect of the voids can be neglected, and if the static properties are adequate for the solution of dynamic deformation problems, then the use of the Blatz sef is justified. It is not the intention of this thesis to explore this uncertainty.

Numerical results for deformation of spherical and cylindrical shells using the Blatz sef are included in this thesis, based on the assumption that the use of the Blatz relation is justified for dynamic deformation. This is in accordance with the work of other researchers (Davison, 1966) who have also made this assumption. However, the results should be treated with some caution.

2.3 Justification for Isothermal Stress-Deformation Relation

An estimate of the error involved in using an isothermal relation between stress and stretch, rather than an isentropic relation, is presented in this section. This is demonstrated by two examples which illustrate the difference between the numerical solutions obtained for isothermal and isentropic stress-deformation relations.

Although in principle, there is no difficulty in using the isentropic relation instead of the isothermal relation, the error involved is negligible for the deformations considered in this thesis. The numerical solutions presented in chapter 5 are primarily for isothermal strain energy functions.

2.3.1 Static Simple Tension of a Solid Cylinder

Consider the simple extension of a cylindrical test-piece of arbitrary simply connected cross section. The test-piece is subjected to simple tension as shown in figure 2.3 and is deformed statically.

Chadwick (1974a) considers a similar problem but introduces several approximations to obtain closed form solutions for the temperature T, dilatation term J and nominal axial stress P_1. The solution presented here is obtained numerically and does not require the use of approximations to simplify the formulation. Chadwick also considers a superimposed atmospheric pressure which is easily included but has a minimal effect on the deformation. The atmospheric pressure is not included here for clarity.

Following Chadwick, the Helmholtz free energy per unit mass is given by the form

$$A = \frac{W}{\rho_o}\left(\frac{T}{T_o}\right) - \frac{\alpha\kappa\, h(J)\,(T - T_o)}{\rho_o} + c(T - T_o) - cT\ \ln\left(\frac{T}{T_o}\right), \qquad (2.33)$$

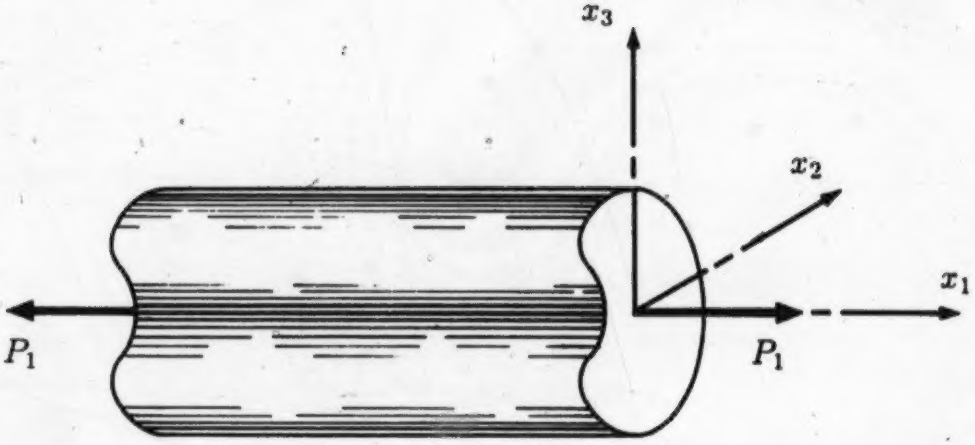
x_3
x_2
x_1
P_1
P_1

Figure 2.3: Simple Tension of a Solid Cylinder

for a solid which exhibits strictly entropic elasticity for isochoric deformation. The density in the natural reference configuration at temperature T_o is ρ_o, c is the specific heat at constant deformation and α is the volume coefficient of thermal expansion.

A solid is said to exhibit strictly entropic elasticity for isochoric deformation if the stress arises entirely from changes in entropy (no contribution from the change in internal energy). For such a material, the internal energy $U(J,T)$, can be expressed as the sum

$$U(J,T) = U_1(J) + U_2(T). \tag{2.34}$$

For isochoric deformation, $U_1(1) = 0$ and the internal energy is a function of T alone. The specific heat at constant deformation is a function of T alone for all deformations.

In obtaining (2.33), the specific heat is taken as constant and this is a reasonable approximation since $(T - T_o)/T_o << 1$. The function W is taken to be the modified Gaussian sef (2.19) and $h(J)$ is an empirically derived response function given by

$$\begin{aligned} h(J) &= 2(J^{5/2} - 1)/5, \\ &= (J-1) + O(J-1)^2. \end{aligned} \tag{2.35}$$

Equation (2.35b) can be derived from (2.35a) using a Taylor expansion and is a valid approximation provided $|J - 1| << 1$.

The model given by (2.33) is a limiting case of a model for modified entropic elasticity, later proposed by Chadwick and Creasy (1984). The strictly entropic elasticity model is used in this analysis, rather than the modified form, to estimate the maximum difference between an isothermal stress-deformation relation and an isentropic relation. Most solid rubbers are approximately 80% entropic (Chadwick and Creasy, 1984).

The principal Biot stress components P_i, and entropy s, are given by (2.5a)

and (2.5b). Using the Helmholtz free energy given by (2.33), these terms are

$$P_i = \left(\frac{T}{T_o}\right)\frac{\partial W(\lambda_i)}{\partial \lambda_i} - \alpha\kappa(T-T_o)\frac{J^{5/2}}{\lambda_i},$$

$$s = -\frac{W}{\rho_o T_o} + \frac{\alpha\kappa h(J)}{\rho_o} + c\ \ln\left(\frac{T}{T_o}\right). \tag{2.36}$$

where (2.35a) gives $h(J)$. Using the nondimensional quantities

$$\overline{P}_i = \frac{P_i}{\mu}, \qquad \overline{s} = \frac{s}{c},$$

$$\beta = \frac{\mu}{\rho_o c T_o}, \quad \gamma = \frac{\alpha\kappa T_o}{\mu}, \quad \overline{W} = \frac{W}{\mu}, \tag{2.37}$$

the nondimensional nominal stress and entropy are

$$\overline{P}_i = \left\{\left(\frac{T}{T_o}\right)\frac{\partial \overline{W}}{\partial \lambda_i} - \frac{\gamma(T-T_o)}{T_o}\frac{J^{5/2}}{\lambda_i}\right\},$$

$$\overline{s} = \beta\left\{-\overline{W} + \gamma h(J)\right\} + \ln\left(\frac{T}{T_o}\right). \tag{2.38}$$

Henceforth nondimensional qualities are used but the overbar notation is omitted.

For the special case of simple tension considered in figure 2.3,

$$\lambda_2 = \lambda_3 = \sqrt{\frac{J}{\lambda_1}},$$

$$P_2 = P_3 = 0. \tag{2.39}$$

Using the modified Gaussian sef W given by (2.19), isentropic deformation from the natural reference state is governed by

$$\begin{aligned}
\frac{T}{T_o}\left\{\left(\lambda_1 - \frac{J^{2/3}}{\lambda_1}\right) + \frac{\Gamma}{9\,\lambda_1}\left(1 - J^{-9}\right)\right\} - \frac{\gamma\,(T - T_o)}{T_o}\frac{J^{5/2}}{\lambda_1} &= P_1, \\
\frac{T}{T_o}\left\{\left(\lambda_2 - \frac{J^{2/3}}{\lambda_2}\right) + \frac{\Gamma}{9\,\lambda_2}\left(1 - J^{-9}\right)\right\} - \frac{\gamma\,(T - T_o)}{T_o}\frac{J^{5/2}}{\lambda_2} &= 0, \\
-\beta\left\{W - \gamma\, h(J)\right\} + \ln\left(\frac{T}{T_o}\right) &= 0. \qquad (2.40)
\end{aligned}$$

where $\Gamma = \kappa/\mu$. It is noted that the entropy is zero in the natural undeformed state. Equations (2.40) are a coupled system of nonlinear equations which can be solved for the dependent variables (J, T, P_1) using a Newton-Raphson scheme.

Consider formulation of the same uniaxial problem using isothermal stretch-deformation relations. Using the modified Gaussian set, the deformation is described by

$$\begin{aligned}
\left(\lambda_1 - \frac{J^{2/3}}{\lambda_1}\right) + \frac{\Gamma}{9\,\lambda_1}\left(1 - J^{-9}\right) &= P_1, \\
\left(\lambda_2 - \frac{J^{2/3}}{\lambda_2}\right) + \frac{\Gamma}{9\,\lambda_2}\left(1 - J^{-9}\right) &= 0, \qquad (2.41)
\end{aligned}$$

which can also be solved for the dependent variables (J, P_1) using a Newton Raphson scheme.

The solutions shown in figure 2.4, compare the dependent variables P_1 and J using the two formulations of isentropic and isothermal stress-deformation relations. The temperature curve for the isentropic stress-deformation formulation is included and shows the thermal inversion behaviour typical of solid rubber.

The solutions shown are for particular values of β, γ, μ and T_o, chosen in accordance with the properties of a vulcanized natural rubber as described by Wood and Martin (1964). The pertinent material properties of the rubber are

$$\alpha = 6.36 \times 10^{-4}\ m \qquad {}^{o}K^{-1}$$

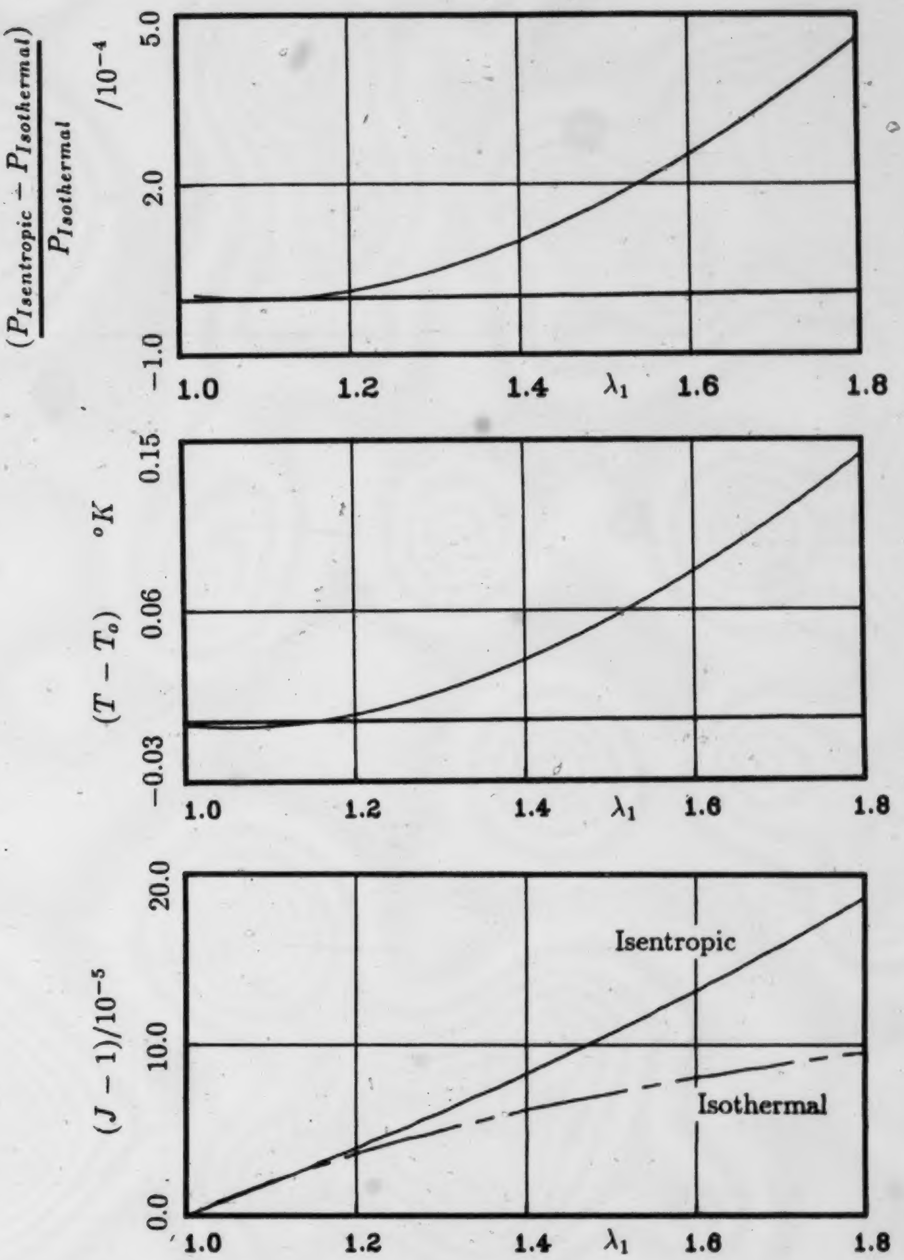

Figure 2.4: Simple Tension of a Solid Cylinder
Isentropic/Isothermal Stress-Deformation Relations
$\beta = 9.35 \times 10^{-4}, \gamma = 880.39, \nu = 0.49989$

$$\begin{aligned}
\kappa &= 1.95 \times 10^{6} && kPa \\
\mu &= 4.2 \times 10^{2} && kPa \\
c &= 1662 && J\,kg^{-1}\,K^{-1} \\
\rho_o &= 906.5 && kg\,m^{-3} \\
T_o &= 298.15 && {}^{o}K
\end{aligned} \tag{2.42}$$

which result in the nondimensional quantities

$$\begin{aligned}
\beta &= 9.35 \times 10^{-4} \\
\gamma &= 880.39 \\
\nu &= 0.49989
\end{aligned} \tag{2.43}$$

For simple tension up to a stretch of 1.8, the difference in the nominal axial stress component (P_1) for isothermal and isentropic deformation is indistinguishable for the scales plotted. The dilatation J, differs for stretches greater than approximately $\lambda_1 = 1.2$, the difference is most apparent when the term $(J-1)$ is compared. However, the effect on the principal stretches λ_2, λ_3 is small. This is evident since

$$\lambda_2 = \lambda_3 = \sqrt{\frac{J}{\lambda_1}}. \tag{2.44}$$

Although there is a significant difference in the magnitude of the term $(J-1)$ for the deformation considered, the maximum difference in the principal stretches is negligible. For example, for a stretch of $\lambda_1 = 1.8$ the stretch $\lambda_2 = \lambda_3$ differs by less than 0.005% between the two formulations.

2.3.2 Dynamic Deformation of a Cylinder

The second example which illustrates the magnitude of the difference between an isothermal stress-deformation relation and an isentropic relation, is to consider the dynamic deformation of a cylindrical shell. The analysis for a spherical shell is similar and results in the same conclusions. A complete discussion of the governing equations and numerical solution technique for the isothermal stress-deformation formulation is given in chapters 3 and 4. Only the significant differences for the isentropic stress-deformation formulation are presented here.

For cylindrically symmetric deformation, the governing equations are given in nondimensional form

$$\begin{aligned} \frac{\partial v}{\partial \tau} - \frac{\partial P_r}{\partial R} - \frac{(P_r - P_\theta)}{R} &= 0, \\ \frac{\partial \lambda_r}{\partial \tau} - \frac{\partial v}{\partial R} &= 0, \\ \frac{\partial \lambda_\theta}{\partial \tau} - \frac{v}{R} &= 0, \end{aligned} \tag{2.45}$$

where P_r and P_θ are the nominal stress in the radial and tangential directions respectively, λ_r and λ_θ are the stretch in the radial and tangential directions, v is velocity, R is the radius in the natural reference state and τ is time. The nondimensionalization scheme given by (2.37) has been used with

$$\overline{v} = v\sqrt{\frac{\rho_o}{\mu}}, \qquad \overline{\tau} = \frac{t}{R_i}\sqrt{\frac{\mu}{\rho_o}}, \qquad \overline{R} = \frac{R}{R_i}, \tag{2.46}$$

where R_i is the radius of the cavity wall in the reference state.

An isentropic relation between stress and deformation can be obtained from the internal energy

$$P_i(\lambda_i, s_o) = \rho_o \frac{\partial U(\lambda_i, s_o)}{\partial \lambda_i}, \tag{2.47}$$

where the entropy in the reference configuration is $s_o = 0$. Using the Helmholtz free energy (2.33) and a Legendre transformation, the nondimensional nominal stress can thus be written

$$P_r = \frac{\gamma(\lambda_r\lambda_\theta)^{5/2}}{\lambda_r}\Big\{1 - \exp\,(W - \gamma h(J))\Big\} + \frac{\partial W}{\partial \lambda_r}\Big\{\exp\,\beta(W - \gamma h(J))\Big\},$$

$$P_\theta = \frac{\gamma(\lambda_r\lambda_\theta)^{5/2}}{\lambda_\theta}\Big\{1-\exp\,(W-\gamma h(J))\Big\} + \frac{\partial W}{\partial\lambda_\theta}\Big\{\exp\,\beta\,(W-\gamma h(J))\Big\},$$

$$J = \lambda_r\,\lambda_\theta,$$

$$h(J) = 2\,(J^{5/2}-1)/5, \tag{2.48}$$

where W is the isothermal sef, taken to be the modified Gaussian sef (2.19) for the purpose of this example. These relations, in combination with the governing equations (2.45) specify the isentropic stress-deformation formulation.

The isothermal stress-deformation formulation is presented in detail in Chapter 3 and is only briefly discussed here. The nominal stresses P_r and P_θ, using the modified Gaussian sef, are

$$\begin{aligned} P_r &= \frac{\partial W}{\partial\lambda_r} = \Big(\lambda_r - \lambda_\theta(\lambda_r\lambda_\theta)^{-1/3}\Big) + \frac{\Gamma}{9}\Big(\frac{1}{\lambda_r} - \lambda_r{}^{-10}\lambda_\theta{}^{-9}\Big), \\ P_\theta &= \frac{\partial W}{\partial\lambda_\theta} = \Big(\lambda_\theta - \lambda_r(\lambda_r\lambda_\theta)^{-1/3}\Big) + \frac{\Gamma}{9}\Big(\frac{1}{\lambda_\theta} - \lambda_r{}^{-9}\lambda_\theta{}^{-10}\Big), \end{aligned} \tag{2.49}$$

and these relations, in combination with the governing equations (2.45) specify the isothermal stress-deformation formulation.

Both the isentropic and isothermal formulations can be solved using the numerical techniques described in chapter 4. The solution shown in figure 2.5 is for a particular choice of material properties which are typical of solid rubbers as given by (2.42) and (2.43). The figure shows the time dependence of λ_r, λ_θ and v at the inside wall of the cylindrical tube for the isentropic formulation. The isothermal formulation yields similar results and cannot be distinguished from the isentropic solution at the scales plotted.

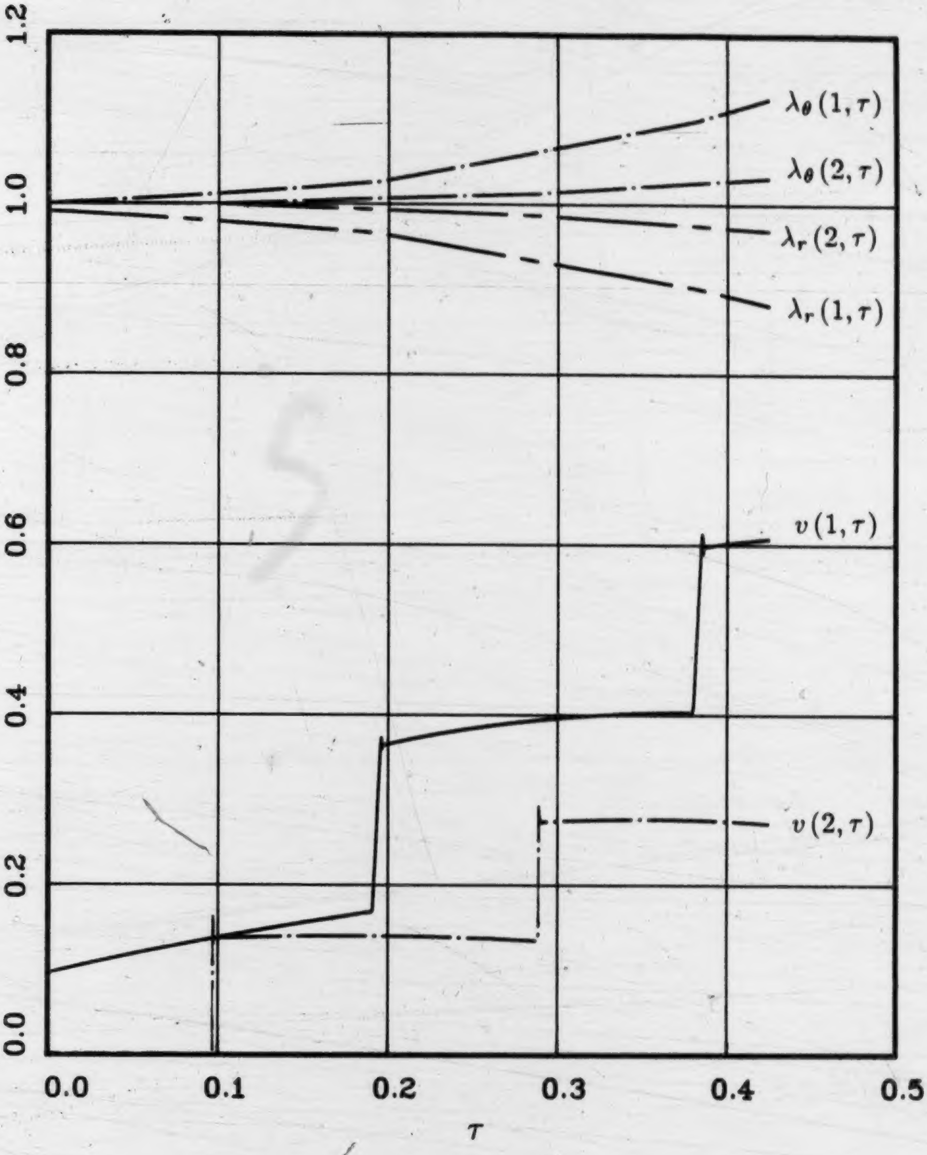

Figure 2.5: Cylindrical Tube, $R_o/R_i = 2$
Isentropic/Isothermal Stress-Deformation Relations
modified Gaussian sef, $\nu = 0.495$
$p(\tau) = H(\tau)$

Chapter 3

Governing Equations

3.1 Spherically Symmetric Deformation

3.1.1 Linear Elasticity

The governing equations for linearly elastic spherically symmetric deformation are derived in detail in a number of references (Graff 1975, Chou and Koenig, 1966). The equations presented here are in a slightly different form which is convenient for the implementation of the numerical scheme used in this thesis.

Consider a spherical coordinate system where r is the radial coordinate, ϕ is the colatitude angle and θ is the azimuthal angle as defined in the usual notation. For the special case of spherically symmetric deformation in which body forces are neglected, the nontrivial equation of motion is

$$\frac{\partial \sigma_r}{\partial r} + \frac{2\left(\sigma_r - \sigma_\theta\right)}{r} = \rho \frac{\partial v}{\partial t}, \tag{3.1}$$

where ρ is the density, σ_r and σ_θ are stresses is in the radial and tangential directions respectively and the velocity in the radial direction is given by v. The equality $\sigma_\phi = \sigma_\theta$ is due to the spherical symmetry.

Consider the following nondimensional quantities

$$\overline{\sigma_r} = \frac{\sigma_r}{\mu}, \qquad \overline{\tau} = \frac{t}{r_o}\sqrt{\frac{\mu}{\rho}},$$

$$\overline{v} = v\sqrt{\frac{\rho}{\mu}}, \qquad \overline{\sigma_\phi} = \frac{\sigma_\phi}{\mu}, \qquad \overline{\sigma_\theta} = \frac{\sigma_\theta}{\mu}, \tag{3.2}$$

where μ is the shear modulus and r_o is the inner radius of the spherical cavity. All further references to these variables is with respect to the nondimensional form but the overbar notation is omitted.

The nontrivial infinitesimal strain components are given by

$$\begin{aligned} e_{rr} &= \frac{\partial u_r}{\partial r}, \\ e_{\phi\phi} &= \frac{u_r}{r}, \end{aligned} \tag{3.3}$$

where spherical symmetry has been used to eliminate terms. A system of governing equations for dynamic, spherically symmetric, linearly elastic deformation is

$$\begin{aligned} \frac{\partial v}{\partial \tau} - \frac{\partial \sigma_r}{\partial r} - \frac{2\,(\sigma_r - \sigma_\phi)}{r} &= 0, \\ \frac{\partial\, e_{rr}}{\partial \tau} - \frac{\partial v}{\partial r} &= 0, \\ \frac{\partial\, e_{\phi\phi}}{\partial \tau} - \frac{v}{r} &= 0, \end{aligned} \tag{3.4}$$

where (3.4b) and (3.4c) result from differentiation of (3.3a) and (3.3b) with respect to time.

Hooke's law for isotropic, isothermal deformation is given in suffix notation

$$\sigma_{ij} = \left(\frac{2\,\nu}{1-2\nu}\right) e_{kk}\,\delta_{ij} + 2\,e_{ij}\,, \tag{3.5}$$

where σ_{ij} is nondimensionalized by dividing by the shear modulus μ. Substitution of the nontrivial stresses σ_r and σ_ϕ obtained from (3.5), into the governing equations (3.4) results in the matrix form

$$\frac{\partial}{\partial \tau}\left\{\begin{matrix} v \\ e_{rr} \\ e_{\phi\phi} \end{matrix}\right\} + \left\{\begin{matrix} 0 & -\beta_1 & -1 \\ -1 & 0 & 0 \\ 0 & 0 & 0 \end{matrix}\right\} \frac{\partial}{\partial r}\left\{\begin{matrix} v \\ e_{rr} \\ e_{\phi\phi} \end{matrix}\right\} + \left\{\begin{matrix} -2\,(\,2\,e_{rr} - \beta_2\,e_{\phi\phi}\,)/r \\ 0 \\ -v/r \end{matrix}\right\} = 0 \tag{3.6}$$

where

$$\begin{aligned} \beta_1 &= \frac{2(1-\nu)}{(1-2\nu)}, \\ \beta_2 &= \frac{4\nu}{(1-2\nu)}, \end{aligned} \tag{3.7}$$

The eigenvalues of the square matrix are

$$\begin{aligned} c_1 &= 0, \\ c_2 &= +\sqrt{\frac{2(1-\nu)}{(1-2\nu)}}, \\ c_3 &= -\sqrt{\frac{2(1-\nu)}{(1-2\nu)}}, \end{aligned} \tag{3.8}$$

which give the nondimensional speed of propagation of longitudinal waves.

An alternate, and equally useful form for application of the numerical scheme used in this thesis, is to express the governing equations in terms of the nontrivial stress components instead of the nontrivial strain components. This is accomplished by expressing Hooke's law in nondimensional form as

$$e_{ij} = \frac{1}{2}\left\{\sigma_{ij} - \frac{\nu}{(1+\nu)}\sigma_{kk}\,\delta_{ij}\right\}, \tag{3.9}$$

and considering time differentiation of the nontrivial strains e_{rr} and $e_{\phi\phi}$. The resulting system of equations can be written in matrix form as

$$\begin{aligned} &\left\{\begin{matrix} 0 & 0 & -1 \\ 1 & -2\nu & 0 \\ 1 & (\nu-1)/\nu & 0 \end{matrix}\right\}\frac{\partial}{\partial\tau}\left\{\begin{matrix}\sigma_r \\ \sigma_\phi \\ v\end{matrix}\right\} + \left\{\begin{matrix} 1 & 0 & 0 \\ 0 & 0 & -2(1+\nu) \\ 0 & 0 & 0 \end{matrix}\right\}\frac{\partial}{\partial r}\left\{\begin{matrix}\sigma_r \\ \sigma_\phi \\ v\end{matrix}\right\} \\ &\qquad + \left\{\begin{matrix} 2/r & -2/r & 0 \\ 0 & 0 & 0 \\ 0 & 0 & 2(1+\nu)/\nu r \end{matrix}\right\}\left\{\begin{matrix}\sigma_r \\ \sigma_\phi \\ v\end{matrix}\right\} = 0. \end{aligned} \tag{3.10}$$

Pre-multiplication of the inverse of the matrix which precedes the time differentiated term yields the system of equations given by

$$\frac{\partial}{\partial \tau}\left\{\begin{matrix} \sigma_r \\ \sigma_\phi \\ v \end{matrix}\right\} + \left\{\begin{matrix} 0 & 0 & A_{13} \\ 0 & 0 & A_{23} \\ -1 & 0 & 0 \end{matrix}\right\} \frac{\partial}{\partial r}\left\{\begin{matrix} \sigma_r \\ \sigma_\phi \\ v \end{matrix}\right\} + \left\{\begin{matrix} b_1\, v \\ b_2\, v \\ 2\,(\sigma_\phi - \sigma_r)/r \end{matrix}\right\} = 0, \qquad (3.11)$$

where

$$\begin{aligned} A_{13} &= 2\,(\nu - 1)/(1 - 2\,\nu), \\ A_{23} &= -2\,\nu/(1 - 2\,\nu), \\ b_1 &= -4\,\nu/\left\{r\,(1 - 2\,\nu)\right\}, \\ b_2 &= -2/\left\{r\,(1 - 2\,\nu)\right\}, \end{aligned} \qquad (3.12)$$

The governing equations, given by either (3.6) or (3.11) are a system of hyperbolic equations with real eigenvalues given by (3.8).

Chou and Koenig (1966) use the method of characteristics to solve a system similar to (3.11), expressed in terms of the dependent variables of stress and velocity. Relations along characteristics can be determined using the techniques described in Whitham (1974) and are as follows.

On $dr/d\tau = +\sqrt{2\,(1-\nu)/(1-2\nu)}$, the characteristic relation is

$$d\sigma_r - \sqrt{\frac{2\,(1-\nu)}{(1-2\nu)}}\, dv = \left\{-2\,(\sigma_r - \sigma_\phi) + 2\nu\sqrt{\frac{2}{(1-\nu)(1-2\nu)}}\, v\right\}\frac{dr}{r}. \qquad (3.13)$$

On $dr/d\tau = -\sqrt{2\,(1-\nu)/(1-2\nu)}$, the characteristic relation is

$$d\sigma_r + \sqrt{\frac{2\,(1-\nu)}{(1-2\nu)}}\, dv = \left\{-2\,(\sigma_r - \sigma_\phi) - 2\nu\sqrt{\frac{2}{(1-\nu)(1-2\nu)}}\, v\right\}\frac{dr}{r}. \qquad (3.14)$$

On $dr/d\tau = 0$,

$$d\sigma_\phi = \frac{\nu}{(1-\nu)}\, d\sigma_r + 2\,\frac{(1+\nu)}{(1-\nu)}\,\frac{v}{r}\, d\tau. \tag{3.15}$$

The problem of solving the system of hyperbolic PDE's given by (3.11) has been reduced to solving a system of ODE's given by (3.13) - (3.15), along the characteristic directions which are constant for linear elasticity.

The jump relations across the characteristics can be derived from the characteristic relations following the procedure given by Chou and Koenig (1966). These relations are summarized as

$$\begin{aligned} [\,\sigma_r\,] &= K\,r^{-1}, \\ [\,\sigma_\phi\,] &= \left(\frac{\nu}{1-\nu}\right) K\,r^{-1}, \\ [\,v\,] &= \mp\sqrt{\frac{(1-2\nu)}{2\,(1-\nu)}}\,K\,r^{-1}, \end{aligned} \tag{3.16}$$

where the upper sign is for the family of characteristics of positive slope and the lower sign is for the family of characteristics of negative slope. The square brackets denote a jump defined by the difference between the quantity just behind and just ahead of the discontinuity and the constant K can be determined from the boundary conditions. These relations indicate that for spherically symmetric deformation, discontinuities vary as r^{-1}.

3.1.2 Finite Dynamic Deformation

The governing equations for finite dynamic expansion of a spherical cavity in an unbounded medium are derived in detail by several authors. See for example, Fung

(1965) or Graff (1975). The Lagrangian equations of motion are written in symbolic notation as

$$Div\,\mathbf{P} + \rho_o\,\mathbf{b} = \rho_o \frac{\partial \mathbf{v}}{\partial t}, \tag{3.17}$$

where $\mathbf{P}$ is the first Piola-Kirchhoff stress tensor, [1] ρ_o is the density in the reference configuration, $\mathbf{b}$ is the body force per unit mass, $\mathbf{v}$ is velocity and t is time. The notation Div denotes the divergence with respect to the reference configuration. For spherical symmetry, $\mathbf{P}$ is given by

$$\mathbf{P} = diag\,\{P_r, P_\phi, P_\phi\}. \tag{3.18}$$

Three scalar equations of motion are implied by (3.17). For the special case of spherically symmetric deformation, two of the three equations of motion are trivially satisfied. If body forces are neglected, the non-trivial equation of motion, in Lagrangian form, is

$$\frac{\partial v}{\partial t} - \frac{\partial}{\partial R}\left(\frac{P_r}{\rho_o}\right) - \frac{2\,(P_r - P_\phi)}{\rho_o R} = 0, \tag{3.19}$$

where the nominal stress is defined in terms of the area of the undeformed configuration. The velocity in the radial direction is given by v and spherical symmetry has been used in the ϕ and θ directions.

For finite deformation, it is convenient to consider the two stretch terms which give the radial and tangential stretch in the r and ϕ directions. These are

$$\begin{aligned} \lambda_r &= \frac{\partial r}{\partial R}, \\ \lambda_\phi &= \frac{r}{R}, \end{aligned} \tag{3.20}$$

---

[1] **The nominal stress tensor is the transpose of the first Piola-Kirchhoff stress tensor, but for spherically symmetric deformation, the distinction disappears.**

where lower case letters refer to the deformed configuration and uppercase letters refer to the reference configuration. Due to the spherical symmetry of the deformation, the stretch in the azimuthal direction (λ_ϕ) is equal to the stretch in the colatitude direction (λ_θ).

Consider the following nondimensional quantities

$$\overline{P_r} = \frac{P_r}{\mu}, \quad \overline{P_\phi} = \frac{P_\phi}{\mu}, \quad \overline{W} = \frac{W}{\mu},$$
$$\overline{R} = \frac{R}{R_i}, \quad \overline{\tau} = \frac{t}{R_i}\sqrt{\frac{\mu}{\rho_o}}, \quad \overline{v} = v\sqrt{\frac{\rho_o}{\mu}}, \tag{3.21}$$

where R_i is the inner radius of the spherical cavity, ρ_o is the density of the undeformed configuration and μ is the shear modulus for infinitesimal deformation from the ground state. All further references are with respect to these nondimensional quantities although the overbar notation is omitted.

Finite spherically symmetric elastic deformation is given in nondimensional form

$$\frac{\partial}{\partial \tau}\left\{\begin{array}{c} v \\ \lambda_r \\ \lambda_\phi \end{array}\right\} + \frac{\partial}{\partial R}\left\{\begin{array}{c} -P_r \\ -v \\ 0 \end{array}\right\} + \left\{\begin{array}{c} -2\,(P_r - P_\phi)/R \\ 0 \\ -v/R \end{array}\right\} = 0, \tag{3.22}$$

where time derivatives of the stretch terms given by (3.20) have been used for compatibility.

If the isentropic approximation is considered, substitution of the elastic constitutive relations

$$\begin{aligned} P_r &= P_r(\lambda_r, \lambda_\phi), \\ P_\phi &= P_\phi(\lambda_r, \lambda_\phi), \end{aligned} \tag{3.23}$$

in equation (3.22) results in a system of totally hyperbolic partial differential equations in conservation form provided that

$$\frac{\partial P_r}{\partial \lambda_r} > 0. \tag{3.24}$$

The hyperbolic nature of the governing equations and the resulting restriction on the convexity of P_r is further discussed in section 4.1.

The modified Gaussian sef can be written in nondimensional form for spherically symmetric deformation

$$W(\lambda_r, \lambda_\phi) = \frac{1}{2}\left\{\lambda_r{}^2 + 2\lambda_\phi{}^2 - 3(\lambda_r\lambda_\phi{}^2)^{2/3} + \frac{\Gamma}{9}\left\{\frac{(\lambda_r\lambda_\phi{}^2)^{-9}}{9} + \ln\,(\lambda_r\lambda_\phi{}^2) - \frac{1}{9}\right\}\right\}. \tag{3.25}$$

Using this sef, the nominal stresses for spherically symmetric deformation are

$$P_r = \frac{\partial W}{\partial \lambda_r} = \left\{\lambda_r - \lambda_\phi{}^2(\lambda_r\lambda_\phi{}^2)^{-1/3}\right\} + \frac{\Gamma}{9}\left\{\frac{1}{\lambda_r} - \lambda_r{}^{-10}\lambda_\phi{}^{-18}\right\},$$

$$P_\phi = \frac{1}{2}\frac{\partial W}{\partial \lambda_\phi} = \left\{\lambda_\phi - \lambda_r\lambda_\phi(\lambda_r\lambda_\phi{}^2)^{-1/3}\right\} + \frac{\Gamma}{9}\left\{\frac{1}{\lambda_\phi} - \lambda_r{}^{-9}\lambda_\phi{}^{-19}\right\}, \tag{3.26}$$

where $\Gamma = \kappa/\mu$.

The Blatz and Ko sef is discussed in section 2.2.3 and is given in nondimensional form, for spherically symmetric deformation,

$$W = \frac{1}{2}\left\{\left(\lambda_r{}^2 + 2\lambda_\phi{}^2 - 3\right) + \frac{1-2\nu}{\nu}\left\{\left(\lambda_r\lambda_\phi{}^2\right)^{2\nu/(2\nu-1)} - 1\right\}\right\}, \tag{3.27}$$

where ν is Poisson's ratio for infinitesimal deformation from the ground state. For the Blatz and Ko sef, the nondimensional nominal stresses for spherically symmetric deformation are

$$P_r = \frac{\partial W}{\partial \lambda_r} = \left\{\lambda_r - \lambda_\phi{}^2\left(\lambda_r\lambda_\phi{}^2\right)^{1/(2\nu-1)}\right\},$$

$$P_\phi = \frac{1}{2}\frac{\partial W}{\partial \lambda_\phi} = \left\{\lambda_\phi - \lambda_r\lambda_\phi\left(\lambda_r\lambda_\phi{}^2\right)^{1/(2\nu-1)}\right\}. \tag{3.28}$$

The Blatz sef is given in nondimensional form for spherically symmetric deformation as

$$W(\lambda_r, \lambda_\phi) = \frac{1}{2}\left\{\frac{1}{\lambda_r{}^2} + \frac{2}{\lambda_\phi{}^2} + 2\lambda_r\lambda_\phi{}^2 - 5\right\}. \tag{3.29}$$

This sef describes deformation in a sponge rubber for which the Poisson ratio is $\nu = 0.25$ for infinitesimal deformation from the ground state. The nondimensional nominal stresses are

$$P_r = \frac{\partial W}{\partial \lambda_r} = \frac{1}{2}\left\{-2\lambda_r{}^{-3} + 2\lambda_\phi{}^2\right\},$$

$$P_\phi = \frac{1}{2}\frac{\partial W}{\partial \lambda_\phi} = \frac{1}{2}\left\{-2\lambda_\phi{}^{-3} + 2\lambda_r\lambda_\phi\right\}. \tag{3.30}$$

3.1.3 Equilibrium Finite Deformation

The equation which governs spherically symmetric equilibrium deformation can be written as a single ordinary differential equation if the isentropic approximation is considered and equations (3.23) apply. For the problem in which a pressure is suddenly applied and held constant at the wall of a spherical cavity in an unbounded medium, the solution for the dynamic deformation problem approaches the solution of the corresponding equilibrium deformation problem as $\tau \to \infty$. This can be used to verify the numerical solution for the dynamic problem at large time.

The governing ODE for finite equilibrium deformation can be obtained by replacing the equation of motion (3.19) with the equilibrium equation

$$\frac{\partial P_r}{\partial R} + \frac{2\left(P_r - P_\phi\right)}{R} = 0, \tag{3.31}$$

The use of an isothermal sef $W(\lambda_r, \lambda_\phi)$, results in the nominal stress components

$$P_r \quad = \quad \frac{\partial W(\lambda_r, \lambda_\phi)}{\partial \lambda_r},$$

$$P_\phi = \frac{1}{2}\frac{\partial W(\lambda_r, \lambda_\phi)}{\partial \lambda_\phi}. \tag{3.32}$$

Substitution of (3.32) into (3.31) yields

$$\frac{\partial}{\partial R}\left(\frac{\partial W}{\partial \lambda_r}\right) + \frac{2}{R}\left(\frac{\partial W}{\partial \lambda_r} - \frac{1}{2}\frac{\partial W}{\partial \lambda_\phi}\right) = 0, \tag{3.33}$$

where

$$\frac{\partial}{\partial R}\left(\frac{\partial W}{\partial \lambda_r}\right) = \left(\frac{\partial^2 W}{\partial {\lambda_r}^2}\frac{d\lambda_r}{dR} + \frac{\partial^2 W}{\partial \lambda_r \partial \lambda_\phi}\frac{d\lambda_\phi}{dR}\right). \tag{3.34}$$

For the limiting case of equilibrium deformation, both the radial and tangential stretch are functions of R only. The dependence of λ_ϕ on R is given by

$$\lambda_\phi = \frac{r}{R} = f(R),$$

$$r = R\,f(R). \tag{3.35}$$

Differentiating (3.35) with respect to R defines $\lambda_r(R)$ in terms of $\lambda_\phi(R)$

$$\lambda_r = \frac{dr}{dR} = R\,f'(R) + f(R), \tag{3.36}$$

where $f'(R)$ denotes differentiation with respect to R. Substitution of relations (3.35a) and (3.36) into (3.33) results in the second order ODE

$$\left(\frac{\partial^2 W}{\partial {\lambda_r}^2}R\right) f'' + \left(2\frac{\partial^2 W}{\partial {\lambda_r}^2} + \frac{\partial^2 W}{\partial \lambda_r \partial \lambda_\phi}\right) f' + \frac{2}{R}\left(\frac{\partial W}{\partial \lambda_r} - \frac{1}{2}\frac{\partial W}{\partial \lambda_\phi}\right) = 0. \tag{3.37}$$

For the modified Gaussian sef, the pertinent terms are

$$W = \frac{1}{2}\left\{{\lambda_r}^2 + 2{\lambda_\phi}^2 - 3(\lambda_r {\lambda_\phi}^2)^{2/3}\right\} + \frac{\Gamma}{9}\left\{\frac{(\lambda_r {\lambda_\phi}^2)^{-9}}{9} + \ln(\lambda_r {\lambda_\phi}^2) - \frac{1}{9}\right\},$$

$$
\begin{aligned}
\frac{\partial W}{\partial \lambda_r} &= \lambda_r - \lambda_\phi{}^2(\lambda_r\lambda_\phi{}^2)^{-1/3} + \frac{\Gamma}{9}\left\{\frac{1}{\lambda_r} - \lambda_r{}^{-10}\lambda_\phi{}^{-18}\right\}, \\
\frac{1}{2}\frac{\partial W}{\partial \lambda_\phi} &= \lambda_\phi - \lambda_r\lambda_\phi(\lambda_r\lambda_\phi{}^2)^{-1/3} + \frac{\Gamma}{9}\left\{\frac{1}{\lambda_\phi} - \lambda_r{}^{-9}\lambda_\phi{}^{-19}\right\}, \\
\frac{\partial^2 W}{\partial \lambda_r{}^2} &= 1 + \frac{1}{3}\lambda_\phi{}^4(\lambda_r\lambda_\phi{}^2)^{-4/3} + \frac{\Gamma}{9}\left\{-\frac{1}{\lambda_r{}^2} + 10\lambda_r{}^{-11}\lambda_\phi{}^{-18}\right\}, \\
\frac{\partial^2 W}{\partial \lambda_r \partial \lambda_\phi} &= -\frac{4}{3}(\lambda_r\lambda_\phi{}^2)^{-1/3} + 2\,\Gamma\left\{\lambda_r{}^{-10}\lambda_\phi{}^{-19}\right\}.
\end{aligned}
\tag{3.38}
$$

Similar relations can be obtained for other strain energy functions such as the Blatz and Blatz and Ko relations.

The boundary conditions for static deformation are similar to the boundary conditions for the dynamic case. For deformation of a cavity in an unbounded medium, the material is in the initial state at R_∞. If the Cauchy radial stress is specified at the cavity wall ($R = 1$), then a relation between λ_r and λ_ϕ is specified since

$$\sigma_r = \sigma_r(\lambda_r, \lambda_\phi). \tag{3.39}$$

If λ_ϕ is known at $R = 1$, this relation can be used to define $f'(R = 1)$ by solving for λ_r and using $\lambda_r = (Rf' + f)$. In general (3.39) is a nonlinear equation.

Implementation of the Runge-Kutta technique for the problem of the expansion of a spherical cavity in an unbounded medium involves an iterative procedure.

- Assume a value for $f(R = 1)$

- Determine λ_r using the boundary condition at $R = 1$ and thus determine $f'(R = 1)$.

- Use the Runge Kutta method to solve the ODE for the solution at a radius $R = R_{max}$, numerically representative of R_∞.
- Adjust the assumed value of $f(R = 1)$ until the boundary condition $\lambda_r = \lambda_\phi = 1$ is satisfied at $R = R_{max}$.

The choice of R_{max} as the value of R which is numerically representative of R_∞, is a limitation of this implementation of the ODE solution scheme. This limitation has an observed minimal effect on the solution since $f'(R)$ approaches zero as R approaches infinity.

3.1.4 Initial and Boundary Conditions

For a material which is undeformed and at rest in the reference state, the initial stretches and velocity are

$$\begin{aligned} \lambda_r(R,0) &= 1, \\ \lambda_\phi(R,0) &= 1, \\ v(R,0) &= 0. \end{aligned} \tag{3.40}$$

Relatively simple modifications are required to consider the deformation of a prestressed medium or to consider a cavity which is initially in spherically symmetric motion. [2]

Boundary conditions can be specified at a physical boundary of the spherically symmetric cavity - either the inner radius where $R = R_i$, or an outer radius where $R = R_o$ if the medium is not of infinite extent. Two physically realistic boundary conditions considered in this thesis are the specification of the velocity v, and the specification of the Cauchy radial stress σ_r.

---

[2] Cylindrically symmetric deformation of a prestressed sheet is considered in section 3.3.

If the pressure at the inner radius of a spherical cavity is specified, then the corresponding Cauchy radial stress, σ_r, is given at the inner cavity wall ($R = 1$). The nondimensional Cauchy stress, defined in terms of the deformed coordinate system, can be related to the nondimensional nominal radial stress P_r, using

$$\sigma_r = \frac{1}{{\lambda_\phi}^2} P_r. \tag{3.41}$$

For spherically symmetric deformation described by the modified Gaussian sef (3.25), the expression for the nondimensional nominal radial stress P_r is given by (3.26a). Using this relation and (3.41), the expression for the radial Cauchy stress σ_r is

$$\sigma_r = \frac{1}{{\lambda_\phi}^2}\left\{\lambda_r - {\lambda_\phi}^2(\lambda_r{\lambda_\phi}^2)^{-1/3}\right\} + \frac{\Gamma}{9}\left\{\frac{1}{\lambda_r} - {\lambda_r}^{-10}{\lambda_\phi}^{-18}\right\}. \tag{3.42}$$

If a Heaviside step function of pressure is applied at the inner radius of a spherical cavity, the Cauchy stress at $R = 1$ is

$$\sigma_r\,(1,\, \tau) = -q\, H(\tau), \tag{3.43}$$

where q is a constant and $H(\tau)$ is the Heaviside function. Substitution of (3.43) into (3.42), to eliminate σ_r yields an expression for the boundary condition at $R = 1$,

$$-\,q\, H(\tau) = \frac{1}{{\lambda_\phi}^2}\left\{\lambda_r - {\lambda_\phi}^2(\lambda_r{\lambda_\phi}^2)^{-1/3} + \frac{\Gamma}{9}\left\{\frac{1}{\lambda_r} - {\lambda_r}^{-10}{\lambda_\phi}^{-18}\right\}\right\}. \tag{3.44}$$

Specification of the radial stress is analogous to specification of the relation between λ_r and λ_ϕ. For the deformation of a thick-walled spherical shell, a relation similar to that given by (3.43) can be used to prescribe the applied radial stress at the outer surface.

If the spherical cavity is initially quiescent, then at a time just before the Heaviside step function of pressure is applied, ($\tau = 0^-$), $\lambda_r = \lambda_\phi = 1$. At time $\tau = 0^+$, the boundary condition (3.43) can only be satisfied if there is a jump in λ_r. There can not be a jump in λ_ϕ since the displacement is continuous and $\lambda_\phi = r/R$.

A similar analysis can be considered using the Blatz, and Blatz and Ko strain energy functions given by (3.29) and (3.27) respectively.

3.1.5 Jump Conditions

If a Heaviside step function of internal pressure is applied at the inner wall of a spherical cavity or if a wave breaks, the solution describing the elastic deformation will have discontinuities of the dependent variables v and λ_r (or v, P_r, P_ϕ). This weak solution will satisfy the system of equations (3.22), where the solution is continuously differentiable - i.e., everywhere except at the discontinuity itself.

At the discontinuity, the solution for spherically symmetric elastic deformation must satisfy the jump relations

$$\begin{aligned} V_S\,[\,v\,] &= -[\,P_r\,], \\ V_S\,[\,\lambda_r] &= -[\,v\,], \\ [\,\lambda_\phi] &= 0, \end{aligned} \tag{3.45}$$

where V_S is the shock velocity and the brackets indicate a jump defined by the difference between the quantity just behind and just ahead of the discontinuity. The stresses P_r and P_ϕ, and the radial stretch λ_r, are discontinuous across a shock front. The tangential stretch λ_ϕ is continuous since the radial displacement is continuous. It follows from (3.45a) and (3.45b) that

$$V_S = \pm\sqrt{\frac{[\,P_r\,]}{[\,\lambda_r\,]}}, \tag{3.46}$$

where the positive sign refers to a shock travelling radially outward and the negative sign refers to a shock travelling radially inward.

3.2 Cylindrically Symmetric Deformation

The governing equations for cylindrically symmetric deformation are similar to those of the spherically symmetric case presented in section 3.1. Because of this similarity, only a brief presentation of the governing equations for cylindrically symmetric deformation is given. Important differences between the cylindrically symmetric and spherically symmetric cases are noted.

3.2.1 Linear Elasticity

Consider a cylindrical polar coordinate system where r is the radial coordinate, θ is the polar angle and z is the axial coordinate defined in the usual manner. For the special case of cylindrically symmetric deformation in which body forces are neglected, the nontrivial equation of motion is

$$\frac{\partial \sigma_r}{\partial r} + \frac{(\sigma_r - \sigma_\theta)}{r} = \rho \frac{\partial v}{\partial t}, \tag{3.47}$$

where the nondimensional scheme given by (3.21) has been used.

If the length of the cylinder is large in comparison to the diameter, end effects can be neglected. In particular for plane strain, the nontrivial infinitesimal strain components are

$$\begin{aligned} e_{rr} &= \frac{\partial u_r}{\partial r}, \\ e_{\theta\theta} &= \frac{u_r}{r}. \end{aligned} \tag{3.48}$$

The governing equations for cylindrically symmetric linear elasticity are

$$\begin{aligned} \frac{\partial v}{\partial \tau} - \frac{\partial \sigma_r}{\partial r} - \frac{(\sigma_r - \sigma_\theta)}{r} &= 0, \\ \frac{\partial e_{rr}}{\partial \tau} - \frac{\partial v}{\partial r} &= 0, \\ \frac{\partial e_{\theta\theta}}{\partial \tau} - \frac{v}{r} &= 0, \end{aligned} \tag{3.49}$$

where (3.49*b*) and (3.49*c*) result from differentiation of (3.48*a*) and (3.48*b*) with respect to time. Using Hooke's law in the form given by (3.5) the governing equations can be written in matrix form as

$$\frac{\partial}{\partial \tau}\left\{\begin{array}{c} v \\ e_{rr} \\ e_{\theta\theta} \end{array}\right\} + \left\{\begin{array}{ccc} 0 & -\eta_1 & -\eta_2 \\ -1 & 0 & 0 \\ 0 & 0 & 0 \end{array}\right\} \frac{\partial}{\partial r}\left\{\begin{array}{c} v \\ e_{rr} \\ e_{\theta\theta} \end{array}\right\} + \left\{\begin{array}{c} 2\,(e_{\theta\theta} - e_{rr})/r \\ 0 \\ -v/r \end{array}\right\} = 0, \tag{3.50}$$

where

$$\begin{aligned} \eta_1 &= 2(1-\nu)/(1-2\nu), \\ \eta_2 &= 2\nu/(1-2\nu). \end{aligned} \tag{3.51}$$

The eigenvalues of the square coefficient matrix are the same as for the spherical deformation case and are given by (3.8).

An alternate form of the equations for cylindrically symmetric linear elasticity is obtained by expressing the governing equations in term of the nontrivial stress components instead of the nontrivial strain components. Using Hooke's law in the form (3.9), and after some manipulation, the system of equations can be written in matrix form

$$\frac{\partial}{\partial \tau}\left\{\begin{array}{c} \sigma_r \\ \sigma_\theta \\ v \end{array}\right\} + \left\{\begin{array}{ccc} 0 & 0 & A_{13} \\ 0 & 0 & A_{23} \\ -1 & 0 & 0 \end{array}\right\} \frac{\partial}{\partial r}\left\{\begin{array}{c} \sigma_r \\ \sigma_\theta \\ v \end{array}\right\} + \left\{\begin{array}{c} b_1 v \\ b_2 v \\ (\sigma_\theta - \sigma_r)/r \end{array}\right\} = 0, \tag{3.52}$$

where

$$\begin{aligned} A_{13} &= -2(1-3\nu)/(1-5\nu) \\ A_{23} &= -4\nu/(1-5\nu) \\ b_1 &= -4\nu/(1-5\nu)r \\ b_2 &= -2(1-3\nu)/(1-5\nu)r \end{aligned} \tag{3.53}$$

The governing equations, given by either (3.50) or (3.52) are a system of hyperbolic equations with real eigenvalues given by (3.8). On the family of characteristics for which $dr/d\tau = 0$, the characteristic relation is

$$\frac{d\,e_{\theta\theta}}{d\tau} - \frac{v}{R} = 0. \tag{3.54}$$

This relation and the relations along the other two characteristics can be determined using the techniques described in Whitham (1974).

The jump relations across the characteristics can be derived from the characteristic relations following the procedure given by Chou and Koenig (1966). These relations are summarized as

$$\begin{aligned} [\sigma_r] &= K\,r^{-1/2}, \\ [\sigma_\theta] &= \left(\frac{\nu}{1-\nu}\right) K\,r^{-1/2}, \\ [\,v\,] &= \mp\sqrt{\frac{(1-2\nu)}{2\,(1-\nu)}}\,K\,r^{-1/2}, \end{aligned} \tag{3.55}$$

where the upper sign is for the family of characteristics of positive slope and the lower sign is for the family of characteristics of negative slope. The constant K can be determined from the boundary conditions. For cylindrically symmetric deformation, discontinuities vary as $r^{-1/2}$.

3.2.2 Finite Dynamic Deformation

If the length of a cylinder is large in comparison to the diameter, end effects can be neglected and the non-trivial equation of motion is given in Lagrangian form as

$$\frac{\partial v}{\partial \tau} - \frac{\partial}{\partial R}\left(\frac{P_r}{\rho_o}\right) - \frac{(P_r - P_\theta)}{R} = 0, \tag{3.56}$$

where the nondimensional scheme (3.21) and the symmetry of the θ direction has been used. The nominal stress in the r direction is P_r and is defined in terms of the area of the undeformed configuration and the velocity in the radial direction is given by v.

For cylindrically symmetric deformation, it is convenient to express the radial, tangential, and axial stretch as

$$\lambda_r = \frac{\partial r}{\partial R}, \qquad \lambda_\theta = \frac{r}{R}, \qquad \lambda_z = \frac{z}{Z}, \tag{3.57}$$

where (r, θ, z) are the coordinates in the deformed state and (R, Θ, Z) are the coordinates in the undeformed reference state. In this discussion, plane strain is assumed so that $\lambda_z = 1$. Finite dynamic cylindrically symmetric elastic deformation is governed by

$$\frac{\partial}{\partial \tau}\begin{Bmatrix} v \\ \lambda_r \\ \lambda_\theta \end{Bmatrix} + \frac{\partial}{\partial R}\begin{Bmatrix} -P_r \\ -v \\ 0 \end{Bmatrix} + \begin{Bmatrix} -(P_r - P_\theta)/R \\ 0 \\ -v/R \end{Bmatrix} = 0, \tag{3.58}$$

where time derivatives of the stretch terms given by $(3.57a)$ and $(3.57b)$have been used for compatibility.

If an isentropic approximation is considered, substitution of the elastic constitutive relations given by

$$\begin{aligned} P_r &= P_r(\lambda_r, \lambda_\theta), \\ P_\theta &= P_\theta(\lambda_r, \lambda_\theta), \end{aligned} \tag{3.59}$$

in equation (3.58) results in a system of strictly hyperbolic partial differential equations in conservation form if a realistic sef is considered.

For cylindrically symmetric deformation, the modified Gaussian sef (2.19), can be written in nondimensional form.

$$W(\lambda_r, \lambda_\theta) = \frac{1}{2}\left\{\lambda_r^{\,2} + \lambda_\theta^{\,2} + 1 - 3(\lambda_r\lambda_\theta)^{2/3} + \frac{\Gamma}{9}\left\{\frac{(\lambda_r\lambda_\theta)^{-9}}{9} + \ln\,(\lambda_r\lambda_\theta) - \frac{1}{9}\right\}\right\}. \tag{3.60}$$

The nominal stress in the r and θ directions are

$$\begin{aligned} P_r = \frac{\partial W}{\partial \lambda_r} &= \left\{\lambda_r - \lambda_\theta(\lambda_r\lambda_\theta)^{-1/3}\right\} + \frac{\Gamma}{9}\left\{\frac{1}{\lambda_r} - \lambda_r^{\,-10}\lambda_\theta^{\,-9}\right\}, \\ P_\theta = \frac{\partial W}{\partial \lambda_\theta} &= \left\{\lambda_\theta - \lambda_r(\lambda_r\lambda_\theta)^{-1/3}\right\} + \frac{\Gamma}{9}\left\{\frac{1}{\lambda_\theta} - \lambda_r^{\,-9}\lambda_\theta^{\,-10}\right\}, \end{aligned} \tag{3.61}$$

where $\Gamma = \kappa/\mu$.

The Blatz and Ko sef is given in nondimensional form for cylindrically symmetric deformation as

$$W = \frac{1}{2}\left\{\left(\lambda_r^{\,2} + \lambda_\theta^{\,2} - 2\right) + \frac{1-2\nu}{\nu}\left\{(\lambda_r\lambda_\theta)^{2\nu/(2\nu-1)} - 1\right\}\right\}, \tag{3.62}$$

where ν is Poisson's ratio for infinitesimal deformation from the ground state. For the Blatz and Ko sef, the nondimensional nominal stresses for cylindrically symmetric deformation are

$$P_r = \frac{\partial W}{\partial \lambda_r} = \left\{\lambda_r + (\lambda_r\lambda_\theta)^{1/(2\nu-1)}\right\},$$
$$P_\theta = \frac{\partial W}{\partial \lambda_\theta} = \left\{\lambda_\theta + (\lambda_r\lambda_\theta)^{1/(2\nu-1)}\right\}. \tag{3.63}$$

For the Blatz sef, the nondimensional form for cylindrically symmetric deformation is

$$W(\lambda_r, \lambda_\theta) = \frac{1}{2}\left\{\frac{1}{\lambda_r{}^2} + \frac{1}{\lambda_\theta{}^2} + 2\lambda_r\lambda_\theta - 4\right\}, \tag{3.64}$$

and the nondimensional nominal stresses for cylindrically symmetric deformation are

$$P_r = \frac{\partial W}{\partial \lambda_r} = \left\{\lambda_\theta - \frac{1}{\lambda_r{}^3}\right\},$$
$$P_\theta = \frac{\partial W}{\partial \lambda_\theta} = \left\{\lambda_r - \frac{1}{\lambda_\theta{}^3}\right\}. \tag{3.65}$$

3.2.3 Equilibrium Finite Deformation

As is the case for spherically symmetric deformation, the equation which governs cylindrically symmetric equilibrium deformation can be written as a single ordinary differential equation if the isentropic approximation is considered and equations (3.59) apply. For the problem in which a pressure is suddenly applied and held constant at the wall of a cylindrical cavity in an unbounded medium, the solution for the dynamic deformation problem approaches the solution of the corresponding equilibrium deformation problem as $\tau \to \infty$.

The equilibrium equation for cylindrically symmetric deformation is

$$\frac{\partial P_r}{\partial R} + \frac{(P_r - P_\theta)}{R} = 0, \tag{3.66}$$

and can be obtained by omitting the inertia term of the equation of motion (3.56). The use of an isothermal stress-deformation relation $W(\lambda_r, \lambda_\theta)$ results in the nominal stress components

$$P_r = \frac{\partial W(\lambda_r, \lambda_\theta)}{\partial \lambda_r},$$

$$P_\theta = \frac{\partial W(\lambda_r, \lambda_\theta)}{\partial \lambda_\theta}, \tag{3.67}$$

Substitution of (3.67) into (3.66) yields

$$\frac{\partial}{\partial R}\left(\frac{\partial W}{\partial \lambda_r}\right) + \frac{1}{R}\left(\frac{\partial W}{\partial \lambda_r} - \frac{\partial W}{\partial \lambda_\theta}\right) = 0, \tag{3.68}$$

where

$$\frac{\partial}{\partial R}\left(\frac{\partial W}{\partial \lambda_r}\right) = \left(\frac{\partial^2 W}{\partial {\lambda_r}^2}\frac{d\lambda_r}{dR} + \frac{\partial^2 W}{\partial \lambda_r \partial \lambda_\theta}\frac{d\lambda_\theta}{dR}\right), \tag{3.69}$$

For cylindrically symmetric equilibrium deformation, both the radial and tangential stretch are functions of R only and the dependence of λ_θ on R is given by

$$\lambda_\theta = \frac{r}{R} = f(R),$$

$$r = R\,f(R). \tag{3.70}$$

Differentiating (3.70b) with respect to R defines $\lambda_r(R)$ in terms of $\lambda_\theta(R)$ and the use of this relation with (3.70a) results in the second order ODE

$$\left(\frac{\partial^2 W}{\partial {\lambda_r}^2}R\right) f'' + \left(2\,\frac{\partial^2 W}{\partial {\lambda_r}^2} + \frac{\partial^2 W}{\partial \lambda_r \partial \lambda_\theta}\right) f' + \frac{1}{R}\left(\frac{\partial W}{\partial \lambda_r} - \frac{\partial W}{\partial \lambda_\theta}\right) = 0. \tag{3.71}$$

For the modified Gaussian sef, the pertinent terms are

$$W = \frac{1}{2}\left\{{\lambda_r}^2 + {\lambda_\theta}^2 + 1 - 3(\lambda_r\lambda_\theta)^{2/3}\right\} + \frac{\Gamma}{9}\left\{\frac{(\lambda_r\lambda_\theta)^{-9}}{9} + \ln(\lambda_r\lambda_\theta) - \frac{1}{9}\right\},$$

$$\begin{aligned}
\frac{\partial W}{\partial \lambda_r} &= \lambda_r - \lambda_\theta(\lambda_r\lambda_\theta)^{-1/3} + \frac{\Gamma}{9}\left\{\frac{1}{\lambda_r} - {\lambda_r}^{-10}{\lambda_\theta}^{-9}\right\}, \\
\frac{\partial W}{\partial \lambda_\theta} &= \lambda_\theta - \lambda_r(\lambda_r\lambda_\theta)^{-1/3} + \frac{\Gamma}{9}\left\{\frac{1}{\lambda_\theta} - {\lambda_r}^{-9}{\lambda_\theta}^{-10}\right\}, \\
\frac{\partial^2 W}{\partial {\lambda_r}^2} &= 1 + \frac{1}{3}{\lambda_\theta}^2(\lambda_r\lambda_\theta)^{-4/3} + \frac{\Gamma}{9}\left\{-\frac{1}{{\lambda_r}^2} + 10{\lambda_r}^{-11}{\lambda_\theta}^{-9}\right\}, \\
\frac{\partial^2 W}{\partial \lambda_r \partial \lambda_\theta} &= -\frac{2}{3}(\lambda_r\lambda_\theta)^{-1/3} + \Gamma\left\{{\lambda_r}^{-10}{\lambda_\theta}^{-10}\right\}. \qquad (3.72)
\end{aligned}$$

Similar relations can be obtained for other strain energy functions such as the Blatz and Blatz and Ko relations.

For expansion of a cavity in an unbounded medium, the material remains in the initial state as $R \to \infty$. If the Cauchy radial stress is specified at the cavity wall ($R = 1$), then a relation between λ_r and λ_θ is given. This relation can be solved for λ_r in terms of λ_θ and can thus be used to define $f'(1)$ for a given $f(1)$ using $\lambda_r = (Rf' + f)$.

Implementation of the Runge-Kutta technique for solution of the governing ODE for the expansion of a cylindrical cavity in an unbounded medium, involves the assumption of a value for $f(1)$ and iteration of this value until the boundary condition that $f(R_{max}) = 1$ is satisfied. The choice of a finite value of R_{max}, as the value of R which is numerically representative of R_∞, is a limitation of this implementation of the solution scheme. This has an observed minimal effect on the solution since $f'(R)$ approaches zero as R approaches infinity.

3.2.4 Initial and Boundary Conditions

For a material which is undeformed and at rest in the reference state, the initial stretch and initial velocity are

$$\begin{aligned} \lambda_r(R,0) &= 1, \\ \lambda_\theta(R,0) &= 1, \\ v(R,0) &= 0. \end{aligned} \tag{3.73}$$

For the plane strain, cylindrically symmetric deformations considered in this thesis, only the case of a cylinder which is initially undeformed and at rest is considered. Relatively minor modifications are required to consider other initial conditions such as a prestressed state or initial motion. Plane stress deformation of a sheet which is initially loaded by a uniform radial stress, is considered in section 3.3.

Two physically realistic boundary conditions considered for the plane strain deformation of a cylinder are the specification of the velocity v, and the specification of the Cauchy radial stress σ_r.

For cylindrically symmetric deformation of a material described by the modified Gaussian sef function (3.60), the expression for the nondimensional nominal radial stress P_r is given by (3.61a). The Cauchy stress, defined in terms of the deformed coordinate system, can be related to the nondimensional nominal radial stress P_r, using

$$\sigma_r = \frac{1}{\lambda_\theta} P_r. \tag{3.74}$$

If the pressure at the inner radius of a cylindrical cavity is specified, then the corresponding Cauchy radial stress is given at $R = 1$ since the boundary condition specifying $\sigma_r(1,\tau)$ defines a relation between λ_r and λ_θ. A similar relation can be used to prescribe the applied radial stress at the outer surface of a thick-walled cylindrical tube.

If the medium is initially quiescent, at a time just before a Heaviside step function of pressure is applied, ($\tau = 0^-$), the stretch components are $\lambda_r = \lambda_\theta = 1$. Just after a Heaviside step function is applied, ($\tau = 0^+$), the boundary condition on $\sigma_r(\lambda_r, \lambda_\theta)$ can only be satisfied if there is a jump in λ_r. There can not be a jump in λ_θ since the displacement is continuous and $\lambda_\theta = r/R$.

3.2.5 Jump Conditions

If a Heaviside step function of internal pressure is applied at the inner wall of a cylindrical cavity, or if a wave breaks during the propagation of the disturbance, the solution describing the elastic deformation will have discontinuities of the dependent variables v and λ_r. This weak solution will satisfy the system of equations (3.58), where the solution is continuously differentiable.

At the discontinuity, the solution for cylindrically symmetric elastic deformation must satisfy the jump relations

$$\begin{aligned} V_S\,[v] &= -[P_r], \\ V_S\,[\lambda_r] &= -[v], \\ [\lambda_\theta] &= 0, \end{aligned} \tag{3.75}$$

where V_S is the shock velocity. The radial stretch λ_r, is discontinuous across a shock but the tangential stretch λ_θ, is continuous since the radial displacement is continuous. It follows from (3.75a) and (3.75b) that

$$V_S = \pm\sqrt{\frac{[P_r]}{[\lambda_r]}}, \tag{3.76}$$

where the positive sign refers to a shock travelling radially outward and the negative sign refers to a shock travelling radially inward.

3.3 Plane Stress of Uniformly Prestressed Sheets

Consider a thin uniform sheet of rubberlike material which is prestressed by a finite, isotropic biaxial stretch. A circular hole is suddenly punched in the sheet, resulting in plane stress unloading waves. The radius of the hole is assumed to be large compared with the thickness of the sheet and the state of stress after the hole is punched is a state of generalized plane stress.

This problem has been considered by Miklowitz (1960) for linear plane stress and by Mioduchowski et al. (1978) for nonlinear plane stress. These authors use the method of characteristics to solve for the nonlinear deformation in an unbounded medium.

The presentation given here is also for nonlinear deformation but uses the hybrid numerical scheme to simplify the problem solution. In addition, the numerical results are extended to consider the deformation of a sheet of finite dimensions. As in the work by Mioduchowski et al. (1978), numerical solutions are for the incompressible Mooney-Rivlin sef, chosen to facilitate comparison with the method of characteristics solution. Minimal modifications are required to extend the analysis for a compressible material as is briefly discussed in the next section.

3.3.1 Finite Dynamic Deformation

For the deformation of a prestressed sheet, consider the radial, tangential and axial stretch terms as given by (3.57). The coordinates given by (R, Θ, Z) are for the reference state, which is taken to be the unstressed state, and the coordinates given by (r, θ, z) are for the stressed state which exists before and after the circular hole is punched in the sheet.

If the thickness of the sheet is small compared to the radius of the punched hole, then a plane stress approximation can be used. For plane stress

$$\begin{aligned}\sigma_z(\pm h,\tau) &= 0,\\ \frac{\partial \sigma_z}{\partial z}(\pm h,\tau) &= 0,\end{aligned} \tag{3.77}$$

where σ_z is the Cauchy stress perpendicular to the surface of the sheet and $-h < z < h$. Equations (3.77) suggest that σ_z and hence the nominal stress P_z, are approximately zero throughout the thickness of the sheet.

The governing equations for cylindrically symmetric deformation are given in section 3.2.2 and are repeated here,

$$\begin{aligned}\frac{\partial v}{\partial \tau} - \frac{\partial P_r}{\partial R} - \frac{(P_r - P_\theta)}{R} &= 0,\\ \frac{\partial \lambda_r}{\partial \tau} - \frac{\partial v}{\partial R} &= 0,\\ \frac{\partial \lambda_\theta}{\partial \tau} - \frac{v}{R} &= 0.\end{aligned} \tag{3.78}$$

The first of these is the nontrivial equation of motion and the remaining equations are compatibility relations. The nondimensional scheme given by (3.21) has been used.

If W is a sef for an incompressible material, then the relation

$$\lambda_z = \frac{1}{\lambda_r \lambda_\theta}. \tag{3.79}$$

can be used to obtain

$$\hat{W}(\lambda_r,\lambda_\theta) = W(\lambda_r,\lambda_\theta,1/\lambda_r\lambda_\theta), \tag{3.80}$$

and the nominal radial and tangential stresses are given by

$$P_r = \frac{\partial \hat{W}(\lambda_r,\lambda_\theta)}{\partial \lambda_r},$$

$$P_\theta = \frac{\partial \hat{W}(\lambda_r, \lambda_\theta)}{\partial \lambda_\theta}. \tag{3.81}$$

respectively. For a compressible material with sef $W(\lambda_r, \lambda_\theta, \lambda_z)$, the nominal radial and tangential stretches are respectively given by

$$\begin{aligned} P_r &= \frac{\partial W(\lambda_r, \lambda_\theta, \lambda_z)}{\partial \lambda_r}, \\ P_\theta &= \frac{\partial W(\lambda_r, \lambda_\theta, \lambda_z)}{\partial \lambda_\theta}, \end{aligned} \tag{3.82}$$

and the plane stress approximation that $P_z = 0$, can be used to obtain $\lambda_z = \lambda_z(\lambda_r, \lambda_\theta)$ using

$$P_z = \frac{\partial W(\lambda_r, \lambda_\theta, \lambda_z)}{\partial \lambda_z} = 0. \tag{3.83}$$

If a realistic sef is considered, the use of (3.81) or (3.82) with (3.78) results in a system of strictly hyperbolic equations with dependent variables v, λ_r, and λ_θ.

3.3.2 Initial and Boundary Conditions for Prestressed Sheets

Consider a prestressed sheet which is initially at rest and loaded by a uniform radial stress $(P_r)_o$ corresponding to a uniform biaxial stretch λ_o. A circular hole, which is suddenly punched in the sheet, is of current radius $a(\tau)$ in the deformed coordinate system and radius A in the reference state so that the initial stretch is

$$\lambda_o = \frac{a(0)}{A}. \tag{3.84}$$

Consider the transition between the prestressed state, before the circular punch impacts ($\tau = 0^-$), and the state which exists at a time τ_* later at which the radial stress at the circular hole is zero,

$$P_r(R_i, \tau_*) = 0. \tag{3.85}$$

It is reasonable to assume that there is a linear transition from $(P_r)_o$ to the radially unstressed state at $R = R_i$ during the time τ_*, so that the boundary condition is

$$P_r(R_i,\tau) = (P_r)_o\left\{1 - \frac{\tau}{\tau_*}H(\tau)\right\}H(\tau_* - \tau), \tag{3.86}$$

where $H(\tau)$ is the Heaviside step function. [3] A limiting case of (3.86) is

$$P_r(R_i,\tau) = (P_r)_o\left\{1 - H(\tau)\right\}. \tag{3.87}$$

which corresponds to instantaneous punching. The unloading wave moves radially outward and reflects from the outer boundary if the sheet is of finite extent. Material ahead of the shock front is in the initial prestressed state unless a reflection occurs.

For deformation of a finite prestressed sheet for which the outer boundary at $R = R_o$ is rigidly fixed, the appropriate boundary condition is

$$v\,(R_o,\tau) = 0. \tag{3.88}$$

3.3.3 Constitutive Relation : Mooney Rivlin sef

For the deformation of prestressed sheets considered here, the isothermal stretch-deformation relation for an incompressible material is given by the Mooney-Rivlin sef (2.14) which is expressed in terms of the strain invariants I_1 and I_2 as given in section 2.2.1. For cylindrically symmetric generalized plane stress

$$\begin{aligned} I_1 &= {\lambda_r}^2 + {\lambda_\theta}^2 + \frac{1}{{\lambda_r}^2{\lambda_\theta}^2}, \\ I_2 &= {\lambda_r}^2{\lambda_\theta}^2 + \frac{1}{{\lambda_r}^2} + \frac{1}{{\lambda_\theta}^2}, \end{aligned} \tag{3.89}$$

---

[3] A suitable value for τ_* is $\tau_* = h/(2V_P)$ where h is the thickness of the sheet and V_P is the punch velocity (Miklowitz, 1960).

where the incompressibility condition has been used to define λ_z. This results in

$$\begin{aligned} P_r &= \frac{\partial W}{\partial \lambda_r} = \Big\{(\lambda_r - \lambda_r^{-3}\lambda_\theta^{-2})\alpha + (\lambda_r\lambda_\theta^{2} - \lambda_r^{-3})(1-\alpha)\Big\}, \\ P_\theta &= \frac{\partial W}{\partial \lambda_\theta} = \Big\{(\lambda_\theta - \lambda_r^{-2}\lambda_\theta^{-3})\alpha + (\lambda_r^{2}\lambda_\theta - \lambda_\theta^{-3})(1-\alpha)\Big\}. \end{aligned} \qquad (3.90)$$

Using (3.90*a*), the initial radial stress $(P_r)_o$ which corresponds to an initial stretch λ_o, is

$$(P_r)_o = \Big(\lambda_o - \frac{1}{\lambda_o^5}\Big)(1-\alpha+\alpha\lambda_o^2). \qquad (3.91)$$

The relation between λ_r and λ_θ at $R = R_i$ is given by

$$\Big\{(\lambda_r - \lambda_r^{-3}\lambda_\theta^{-2})\alpha + (\lambda_r\lambda_\theta^{2} - \lambda_r^{-3})(1-\alpha)\Big\} = P_r(R_i, \tau). \qquad (3.92)$$

3.4 Concentric Cylinders

Plane strain deformation of concentric cylinders is considered in this section. The cylinders are assumed to be a perfect fit in the unstressed, undeformed reference configuration and are composed of different hyperelastic materials. The analysis presented here is for the deformation of two uniform cylinders with different shear modulii, Poisson ratios and densities in the undeformed reference configuration. The inner cylinder occupies the region $R_i \leq R \leq R_*$ and the outer cylinder occupies the region $R_* \leq R \leq R_o$ where R_* is the radius at which the two cylinders are in contact.

With some modification and additional complexity of the numerical solution scheme, the analysis could be extended to consider several concentric cylinders.

3.4.1 Finite Dynamic Deformation

A nondimensionalization scheme based on the material properties of the inner cylinder of a two concentric cylinder pair is adopted. Using the subscript 1 to denote the inner cylinder and 2 to denote the outer cylinder, the nondimensional quantities are

$$\overline{P_r} = \frac{P_r}{\mu_1}, \qquad \overline{P_\theta} = \frac{P_\theta}{\mu_1}, \qquad \overline{W} = \frac{W}{\mu_1},$$
$$\overline{R} = \frac{R}{R_i}, \qquad \overline{\tau} = \frac{t}{R_i}\sqrt{\frac{\mu_1}{\rho_{o1}}}, \qquad \overline{v} = v\sqrt{\frac{\rho_{o1}}{\mu_1}}. \tag{3.93}$$

The governing equations for finite cylindrically symmetric deformation are presented in section 3.2. For the inner cylinder, the governing equations are given by (3.58) and are repeated below

$$\frac{\partial}{\partial \tau}\begin{Bmatrix} v \\ \lambda_r \\ \lambda_\theta \end{Bmatrix} + \frac{\partial}{\partial R}\begin{Bmatrix} -P_r \\ -v \\ 0 \end{Bmatrix} + \begin{Bmatrix} -(P_r - P_\theta)/R \\ 0 \\ -v/R \end{Bmatrix} = 0. \tag{3.94}$$

The nondimensional governing equations for the outer cylinder are given by

$$\frac{\partial}{\partial \tau}\left\{\begin{array}{c} v \\ \lambda_r \\ \lambda_\theta \end{array}\right\} + \frac{\partial}{\partial R}\left\{\begin{array}{c} -P_r/\zeta \\ -v \\ 0 \end{array}\right\} + \left\{\begin{array}{c} -(P_r - P_\theta)/(R\zeta) \\ 0 \\ -v/R \end{array}\right\} = 0, \tag{3.95}$$

where

$$\zeta = \frac{\rho_{o2}}{\rho_{o1}}. \tag{3.96}$$

3.4.2 Initial and Boundary Conditions

If both concentric cylinders are at rest and in their natural undeformed state, the initial conditions are

$$\begin{aligned} \lambda_r(R,0) &= 1 \\ \lambda_\theta(R,0) &= 1 \\ v(R,0) &= 0 \end{aligned} \tag{3.97}$$

where λ_r and λ_θ are the radial and tangential stretches respectively and v is the radial velocity.

Consider a deformation for which an isentropic approximation is valid and for which the use of an isothermal stress-deformation relation is applicable. If the deformation is caused by the application of a spatially uniform internal pressure at $R = R_i$, then a relation between λ_r and λ_θ is given at $R = R_i$.

For the specific case for which the modified Gaussian sef (3.60) governs the material properties of both the inner and outer cylinders, the nondimensional radial stress is given by

$$\begin{aligned}
\sigma_r &= \frac{1}{\lambda_\theta}\left\{\lambda_r - \lambda_\theta(\lambda_r\lambda_\theta)^{-1/3} + \frac{\Gamma_1}{9}\left(\frac{1}{\lambda_r} - \lambda_r{}^{-10}\lambda_\theta{}^{-9}\right)\right\} \qquad R_i \le R \le R_*, \\
\sigma_r &= \frac{\psi}{\lambda_\theta}\left\{\lambda_r - \lambda_\theta(\lambda_r\lambda_\theta)^{-1/3} + \frac{\Gamma_2}{9}\left(\frac{1}{\lambda_r} - \lambda_r{}^{-10}\lambda_\theta{}^{-9}\right)\right\} \qquad R_* \le R \le R_o,
\end{aligned} \tag{3.98}$$

where

$$\begin{aligned}
\Gamma_1 &= \frac{\kappa_1}{\mu_1} = \frac{2\,(1+\nu_1)}{3\,(1-2\nu_1)}, \\
\Gamma_2 &= \frac{\kappa_2}{\mu_2} = \frac{2\,(1+\nu_2)}{3\,(1-2\nu_2)}, \\
\psi &= \frac{\mu_1}{\mu_2}.
\end{aligned} \tag{3.99}$$

If a Heaviside step function of pressure is applied at the inner radius of the inner cylinder, then the boundary condition relating λ_r and λ_θ is

$$\sigma_r(1,\tau) = -q\,H(\tau), \tag{3.100}$$

where q is the magnitude of the suddenly applied pressure. The nonlinear equation given by (3.98a) can be used to obtain $\lambda_r(1,\tau)$ if $\lambda_\theta(1,\tau)$ is known.

At the boundary between the inner cylinder and the outer cylinder ($R = R_*$), the tangential stretch, velocity, and radial stress are continuous. These transition conditions are founded on the assumption that the cylinders remain in contact during the deformation and that a gap does not exist at the boundary between the cylinders.

Using equations (3.98a) and (3.98b), continuity of the radial stress at $R = R_*$ can be written

$$
\begin{aligned}
&\left\{\lambda_r^- - \lambda_\theta\left(\lambda_r^-\lambda_\theta\right)^{-1/3}\right\} + \frac{\Gamma_1}{9}\left\{\frac{1}{\lambda_r^-} - (\lambda_r^-)^{-10}\lambda_\theta{}^{-9}\right\},\\
&= \psi\left(\left\{\lambda_r^+ - \lambda_\theta\left(\lambda_r^+\lambda_\theta\right)^{-1/3}\right\} + \frac{\Gamma_2}{9}\left\{\frac{1}{\lambda_r^+} - (\lambda_r^+)^{-10}\lambda_\theta{}^{-9}\right\}\right), \qquad (3.101)
\end{aligned}
$$

where λ_r^+ and λ_r^- are the values of λ_r at $R = R_*^+$ and $R = R_*^-$ respectively and continuity of the tangential stretch $\lambda_\theta^- = \lambda_\theta^+ = \lambda_\theta$ has been used. Equation (3.101) may be solved for λ_r^+ for known values of λ_r^- and λ_θ.

At the outer radius of the outer cylinder, $R = R_o$ and a boundary condition similar to that which is applied at $R = 1$ can be specified. For the presentation considered in this thesis, the outer boundary is stress free ($\sigma_r = 0$). Minor modifications are required to specify other physically realistic boundary conditions such as a non-zero external pressure or a velocity boundary condition.

3.4.3 Jump Conditions

As is the case for the cylindrically symmetric deformation considered in section 3.2, if a wave breaks during the propagation of the disturbance, the solution describing the elastic deformation will have discontinuities of the dependent variables v and λ_r. This weak solution will satisfy the governing equations (3.94) and (3.95), where the solution is continuously differentiable.

At the location of the discontinuities, the solution for cylindrically symmetric elastic deformation must satisfy the jump relations

$$
\begin{aligned}
V_S\,[\,v\,] &= -[\,P_r\,],\\
V_S\,[\,\lambda_r] &= -[\,v\,] \qquad (R_i \leq R \leq R_*),\\
[\,\lambda_\theta] &= 0, \qquad (3.102)
\end{aligned}
$$

$$\begin{aligned} V_S\,[v] &= -[P_r]/\zeta, \\ V_S\,[\lambda_r] &= -[v] \qquad (R_* \le R \le R_o), \\ [\lambda_\theta] &= 0, \end{aligned} \tag{3.103}$$

for the inner and outer cylinder respectively and where V_S is the shock velocity. The quantity ζ appears due to the consideration that the nondimensional scheme is based on the properties of the inner cylinder.

It follows from (3.102) that the nondimensional shock velocity for the inner cylinder is

$$V_S = \pm\sqrt{\frac{[P_r]}{[\lambda_r]}}, \tag{3.104}$$

where the positive sign refers to a shock travelling radially outward and the negative sign refers to a shock travelling radially inward. The nondimensional shock velocity for the outer cylinder is

$$V_S = \pm\sqrt{\frac{1}{\zeta}\left(\frac{[P_r]}{[\lambda_r]}\right)}. \tag{3.105}$$

Chapter 4

Numerical Methods

4.1 Method of Characteristics

The method of characteristics can be used to solve the quasi-linear hyperbolic system of equations which result when elastic constitutive relations (3.23) are used in conjunction with (3.22) to describe spherically symmetric deformation. A similar hyperbolic system results when the elastic constitutive relations (3.59) are used in conjunction with (3.58) to describe cylindrically symmetric deformation. The analysis given in this section is for the spherically symmetric case; the cylindrical case differs only by minor modifications.

To determine the characteristic relations for spherically symmetric deformation, the system (3.22) must be written in nonconservation form

$$\frac{\partial}{\partial \tau}\left\{\begin{matrix} v \\ \lambda_r \\ \lambda_\phi \end{matrix}\right\} + \mathbf{A}\,\frac{\partial}{\partial R}\left\{\begin{matrix} v \\ \lambda_r \\ \lambda_\phi \end{matrix}\right\} + \mathbf{b} = 0, \tag{4.1}$$

where **A** is the matrix

$$\mathbf{A} = \left\{\begin{matrix} 0 & -\partial P_r/\partial\lambda_r & -\partial P_r/\partial\lambda_\phi \\ -1 & 0 & 0 \\ 0 & 0 & 0 \end{matrix}\right\}, \tag{4.2}$$

and **b** is the vector

$$\mathbf{b} = \left\{\begin{matrix} -2(P_r - P_\phi)/R \\ 0 \\ -v/R \end{matrix}\right\}. \tag{4.3}$$

Since the isentropic approximation is adopted, P_r and P_ϕ are functions of λ_r and λ_ϕ only. The method of characteristics can be applied to (4.1) to obtain the characteristic relations as is described in various references on characteristic theory (Whitham 1974, Hildebrand, 1976). The eigenvalues of the matrix **A** are

$$\begin{aligned} c_1 &= 0, \\ c_2 &= +\sqrt{\frac{\partial P_r}{\partial \lambda_r}}, \\ c_3 &= -\sqrt{\frac{\partial P_r}{\partial \lambda_r}}. \end{aligned} \tag{4.4}$$

Consequently, the system of equations (4.1) is strictly hyperbolic if $\partial P_r / \partial \lambda_r > 0$. Each eigenvalue represents the slope of a family of characteristics in the space-time or $R - \tau$ plane and the family of characteristics corresponding to $c_1 = 0$ are parallel to the τ axis.

On $dR/d\tau = +\sqrt{\partial P_r / \partial \lambda_r}$, the characteristic relation is

$$-\left\{\sqrt{\frac{\partial P_r}{\partial \lambda_r}}\right\}\frac{dv}{d\tau} + \left\{\frac{\partial P_r}{\partial \lambda_r}\right\}\frac{d\lambda_r}{d\tau} + \left\{\frac{\partial P_r}{\partial \lambda_\phi}\right\}\frac{d\lambda_\phi}{d\tau} = +\left\{\sqrt{\frac{\partial P_r}{\partial \lambda_r}}\right\}b_1 + \left\{\frac{\partial P_r}{\partial \lambda_\phi}\right\}\frac{v}{R}, \tag{4.5}$$

where

$$b_1 = \frac{-2}{R}\left(P_r - P_\phi\right). \tag{4.6}$$

On $dR/d\tau = -\sqrt{\partial P_r / \partial \lambda_r}$, the characteristic relation is

$$-\left\{\sqrt{\frac{\partial P_r}{\partial \lambda_r}}\right\}\frac{dv}{d\tau} + \left\{\frac{\partial P_r}{\partial \lambda_r}\right\}\frac{d\lambda_r}{d\tau} + \left\{\frac{\partial P_r}{\partial \lambda_\phi}\right\}\frac{d\lambda_\phi}{d\tau} = -\left\{\sqrt{\frac{\partial P_r}{\partial \lambda_r}}\right\}b_1 + \left\{\frac{\partial P_r}{\partial \lambda_\phi}\right\}\frac{v}{R}. \tag{4.7}$$

On $dR/d\tau = 0$, the characteristic relation is

$$\frac{d\lambda_\phi}{d\tau} = \frac{v}{R}, \tag{4.8}$$

which can easily be obtained by observing that the third equation of the governing system of equations (3.22) is in characteristic form.

For moderate deformation, the use of an isothermal stress-deformation relation results in negligible error and strain energy functions such as the modified Gaussian sef (3.25) can be used to express the characteristic relations in terms of the principal deformation components. [1] For this sef, the appropriate terms for use with the characteristic relations are

$$\begin{aligned}
\frac{\partial P_r}{\partial \lambda_r} &= 1+\frac{1}{3}\lambda_\phi{}^4\left\{(\lambda_r\lambda_\phi{}^2)^{-4/3}\right\}-\frac{\Gamma}{9}\left\{\frac{1}{\lambda_r{}^2}-10\lambda_r{}^{-11}\lambda_\phi{}^{-18}\right\},\\
\frac{\partial P_r}{\partial \lambda_\phi} &= 2\,\lambda_\phi+\frac{1}{3}\lambda_\phi{}^2\left\{(\lambda_r\lambda_\phi{}^2)^{-4/3}\right\}+\left\{(\lambda_r\lambda_\phi{}^2)^{-1/3}\right\}+2\,\Gamma\lambda_r{}^{-10}\lambda_\phi{}^{-19},\\
(P_r-P_\phi) &= (\lambda_r-\lambda_\phi)\left\{1-\lambda_\phi(\lambda_r\lambda_\phi{}^2)^{-1/3}\right\}+\frac{\Gamma}{9}\left\{\frac{1}{\lambda_r}-\frac{1}{\lambda_\phi}\right\}\left\{1-\lambda_r{}^{-9}\lambda_\phi{}^{-18}\right\}.
\end{aligned} \tag{4.9}$$

Similar relations can be obtained for the Blatz and Ko and Blatz strain energy functions.

4.1.1 Solutions for Linear Elasticity

The solutions given in this section are for spherically symmetric linear elasticity and are presented primarily for the verification and analysis of the numerical methods which are later used for problems of nonlinear elasticity. The numerical solutions for cylindrically symmetric linear elasticity are qualitatively similar and are not included here.

---

[1] Thermodynamic relations and assumptions are considered in section 2.

Spherically symmetric linear elasticity has been investigated by a number of authors including Chou and Koenig (1966) and Haddow and Mioduchowski (1975). The numerical results given here are in agreement with those obtained by these authors.

Consider a spherical cavity in an initially quiescent, unbounded medium. The spherical cavity is subjected to a Heaviside step function application of pressure of nondimensional magnitude 0.01. The material has a Poisson ratio of $\nu = 0.25$. Figure 4.1 shows the time dependence of circumferential stress $\sigma_\phi(1,\tau)$ and velocity $v(1,\tau)$, at the wall of the cavity as obtained using the method of characteristics. The steady state value, as $\tau \rightarrow \infty$, of the circumferential stress is $\sigma_\phi = 0.005$ and is in agreement with the equilibrium solution (Sokolnikoff, 1956). The solution shown in figure 4.1 was obtained using a discrete time step of nondimensional magnitude 0.04; the solution obtained with a smaller time step can not be distinguished at the scales used in this figure.

Figures 4.2 and 4.3 show the method of characteristics solution for linearly elastic deformation of a spherical shell for which $R_i = 1$, $R_o = 2$ and $\nu = 0.25$. This deformation is similar to that of the previous example but involves the additional complexity of reflections from the inner and outer shell surfaces. The outer shell surface is stress free, the inner surface is subjected to a spatially uniform, suddenly applied pressure of magnitude 0.01. The plots show the distribution of stress (σ_r and σ_ϕ) at two distinct times, $\tau = 0.5$ and $\tau = 1.5$. For $\nu = 0.25$, the nondimensional shock velocity is $c = 1.732$ and the travel time for the shock to traverse the spherical shell wall is thus $1/1.732 = 0.577$. The shock front of figure 4.2 is moving to the right, the shock front of figure 4.3 is also moving to the right after reflection from both the outer and inner cavity walls.

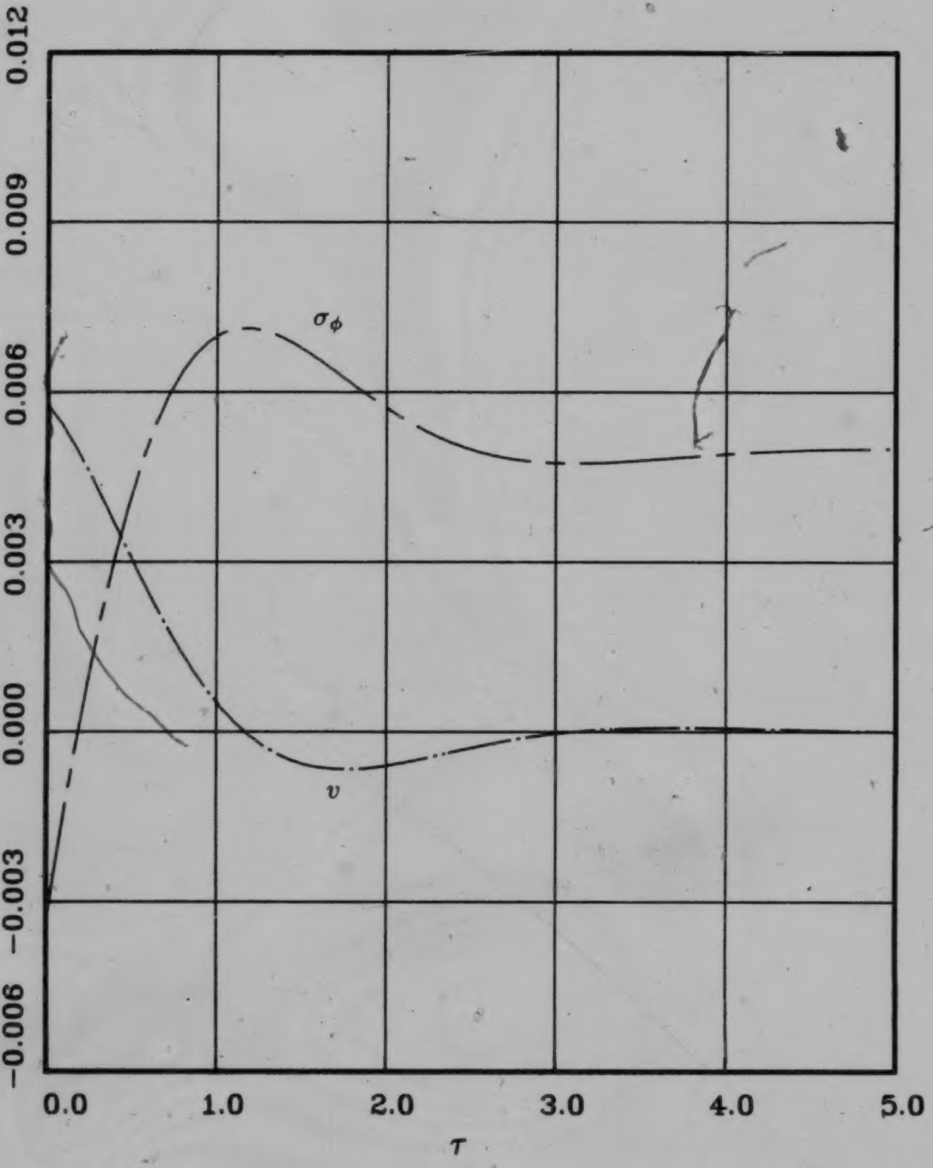

Figure 4.1: Spherical Cavity in an Unbounded Medium
Response at $R = 1$
Method of Characteristics, Linear Elasticity, $\nu = 0.25$
$p(\tau) = 0.01\,H(\tau)$

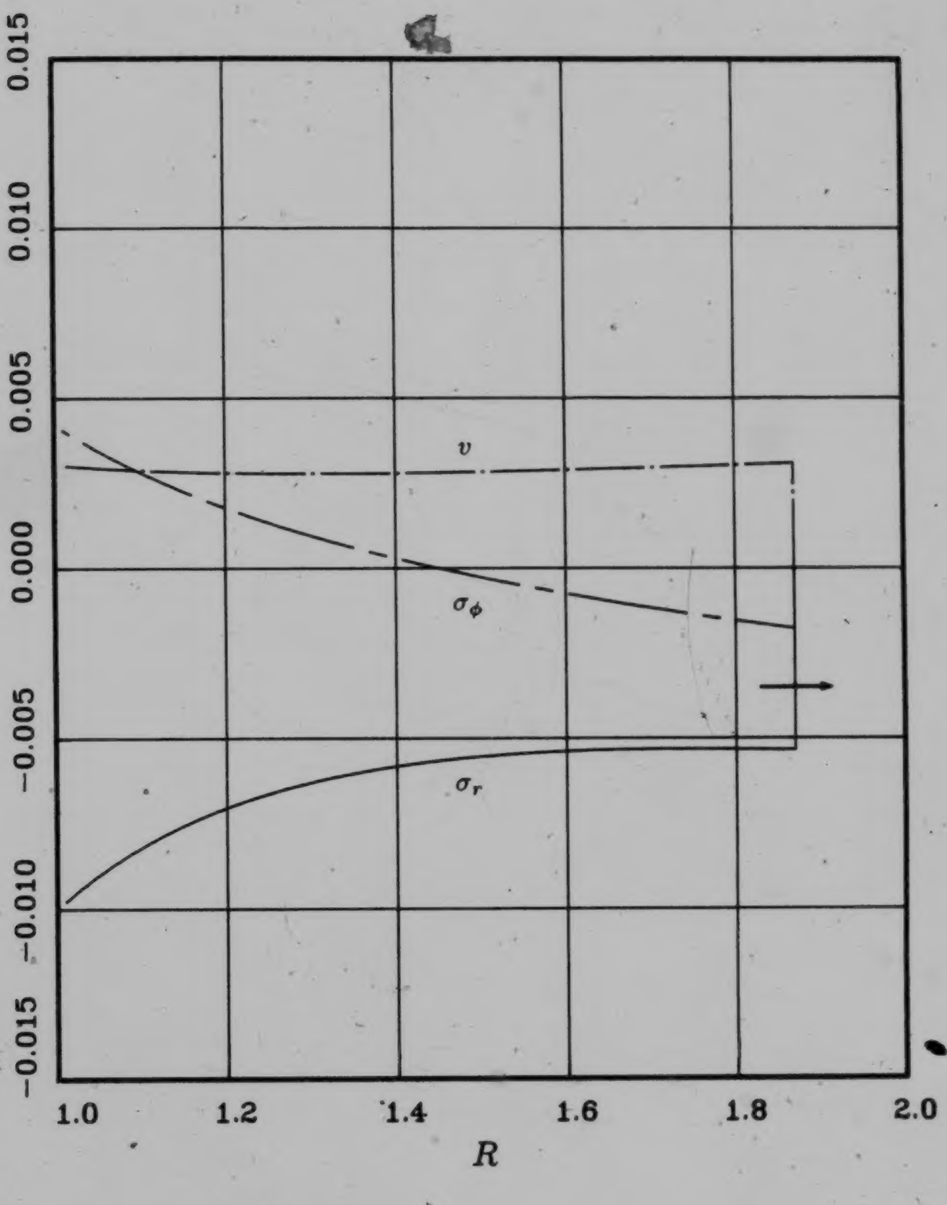

Figure 4.2: Spherical Shell, $R_o/R_i = 2$
Response Before Reflection, $\tau = 0.5$
Method of Characteristics, Linear Elasticity, $\nu = 0.25$
$p(\tau) = 0.01\,H(\tau)$

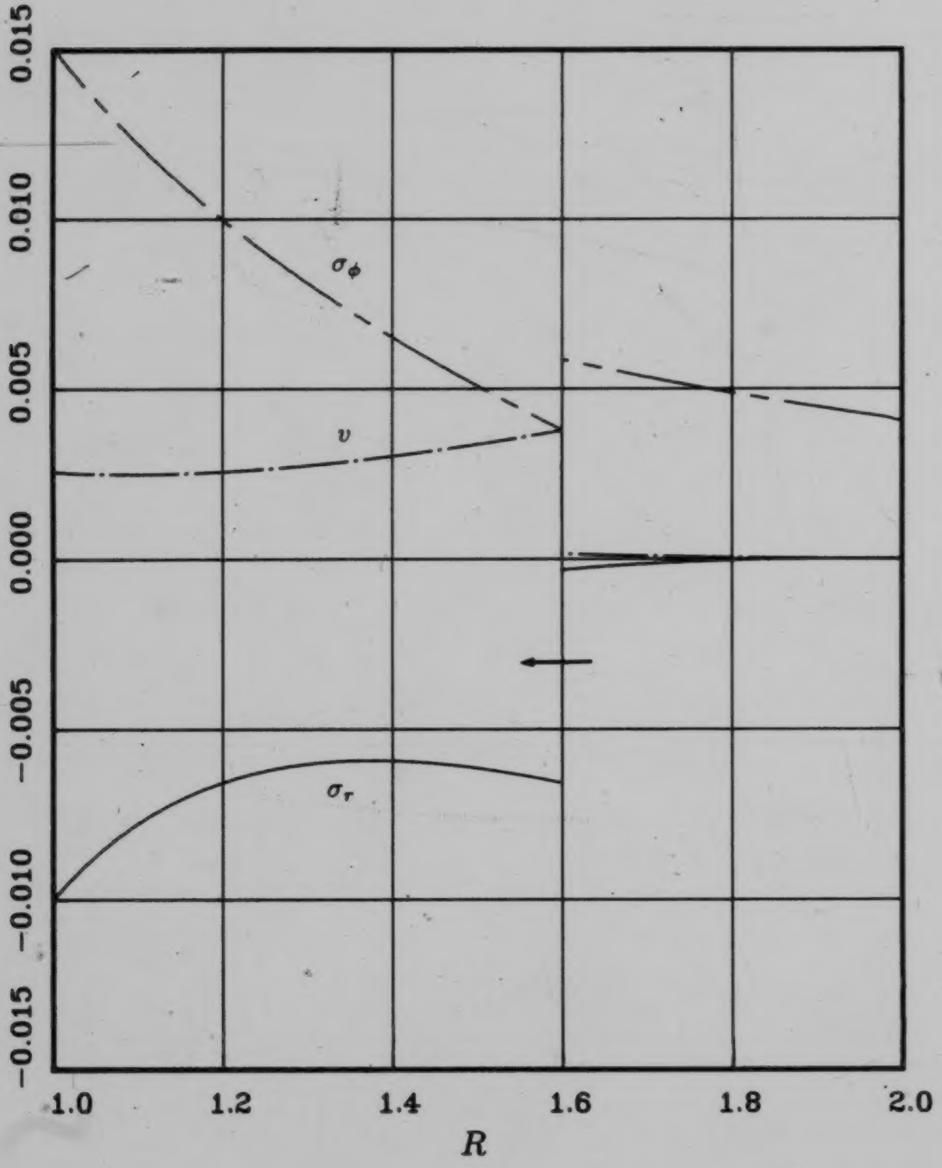

Figure 4.3: Spherical Shell, $R_o/R_i = 2$
Response After Reflection, $\tau = 1.5$
Method of Characteristics, Linear Elasticity, $\nu = 0.25$
$p(\tau) = 0.01\,H(\tau)$

4.2 MacCormack's Method

An alternative numerical method for solving hyperbolic systems of partial differential equations was proposed by MacCormack (1969). MacCormack's method is a finite difference predictor-corrector scheme which is based on the Runge-Kutta technique for ordinary differential equations (Warming et al., 1973). The method is appealing due to it's relative ease of implementation and implicit shock-capturing nature.

Consider the partial differential equations, given in conservation form

$$\frac{\partial \mathbf{u}}{\partial \tau} + \frac{\partial}{\partial R}\Big\{\mathbf{H}(\mathbf{u})\Big\} + \mathbf{b}(\mathbf{u}) = 0, \tag{4.10}$$

where $\mathbf{u}$ is a vector of dependent variables, and $\mathbf{H}(\mathbf{u})$ and $\mathbf{b}(\mathbf{u})$ are functions of $\mathbf{u}$. For this system, the predictor-corrector implementation of MacCormack's method is

$$\begin{aligned} \mathbf{u}_j^{\overline{(n+1)}} &= \mathbf{u}_j^n - \frac{\Delta\tau}{\Delta R}\Big\{\mathbf{H}(\mathbf{u}_{j+1}^n) - \mathbf{H}(\mathbf{u}_j^n)\Big\} - \Delta\tau\, b(\mathbf{u}_j^n), \\ \mathbf{u}_j^{(n+1)} &= \frac{1}{2}\Big\{\mathbf{u}_j^n + \mathbf{u}_j^{\overline{(n+1)}} - \frac{\Delta\tau}{\Delta R}\{\mathbf{H}(\mathbf{u}_j^{\overline{(n+1)}}) - \mathbf{H}(\mathbf{u}_{j-1}^{\overline{(n+1)}})\} - \Delta\tau\, b(\mathbf{u}_j^{\overline{(n+1)}})\Big\}. \end{aligned} \tag{4.11}$$

The superscript refers to an index of discrete time steps $\Delta\tau$, and the subscript refers to an index of discrete space steps ΔR. The term $\mathbf{u}_j^n$ is the finite difference approximation for $\mathbf{u}$ at grid point $(1 + j\Delta R,\ n\Delta\tau)$. Overbar notation indicates the predictor components, no overbar indicates the corrector components.

For spherically symmetric deformation, the vector $\mathbf{u}$ is given by $\{v, \lambda_r, \lambda_\phi\}^T$ and for cylindrically symmetric deformation $\mathbf{u}$ is given by $\{v, \lambda_r, \lambda_\theta\}^T$. If an adiabatic approximation is considered and the elastic constitutive relations (3.23) are used, then for the spherical case,

$$\mathbf{H}(\mathbf{u}) = \left\{\begin{array}{c} -P_r(\lambda_r, \lambda_\phi) \\ -v \\ 0 \end{array}\right\},$$

$$\mathbf{b} = \begin{Bmatrix} -2\left\{P_r(\lambda_r, \lambda_\phi) - P_\phi(\lambda_r, \lambda_\phi)\right\}/R \\ 0 \\ -v/R \end{Bmatrix}, \tag{4.12}$$

and for the cylindrical case,

$$\mathbf{b} = \begin{Bmatrix} -\left\{P_r(\lambda_r, \lambda_\theta) - P_\theta(\lambda_r, \lambda_\theta)\right\}/R \\ 0 \\ -v/R \end{Bmatrix}. \tag{4.13}$$

Some authors (Warming et al., 1973) suggest that the difference operator of the spatial derivative term of MacCormack's predictor-corrector scheme be reversed at alternating time steps. This is proposed in an attempt to average the effect of the differences between the predictor and corrector relations. An alternative to this is to specify the difference operator of the spatial derivative in terms of the direction of wave propagation. For the finite deformations considered in this thesis, neither of these two modifications improve the numerical results.

4.2.1 Gottlieb-Turkel Scheme for Boundary Conditions

As presented in section 3.1.4, two physically realistic boundary conditions considered in this thesis are the specification of velocity and the specification of Cauchy radial stress. If the velocity is specified, then the two remaining dependent variables (which are the stretch components), must be obtained by two boundary condition relations. If the Cauchy radial stress is specified, then a relation between the two principal stretches is specified and two additional boundary conditions are needed to complete the specification of the three dependent variables.

Gottlieb and Turkel (1978) consider various methods for obtaining the additional boundary conditions which are required for implementation of finite difference schemes. These authors propose that the difference operator of the space derivative term in MacCormack's scheme be reversed to facilitate implementation of the method at a boundary. For deformation of a spherical shell or cylindrical tube, this modification is required at both the inner and outer boundaries where $R = R_i$ and $R = R_o$ respectively.

At the inner radius of a spherical or cylindrical cavity, the forward-difference predictor formulation (4.11a) can be applied without modification but the backward-difference corrector formulation (4.11b) is not applicable. In order to obtain the corrector value of ξ at $R = 1$, where ξ is the appropriate element of $\mathbf{u}$, a forward-difference corrector equation

$$\xi_j^{(n+1)} = \frac{1}{2}\Big\{\xi_j^n + \xi_j^{\overline{(n+1)}} - \frac{\Delta\tau}{\Delta R}\{H(\xi_{j+1}^{\overline{(n+1)}}) - H(\xi_j^{\overline{(n+1)}})\} - \Delta\tau\, b(\xi_j^{\overline{(n+1)}})\Big\} \qquad (4.14)$$

is used. Similarly, at the outer radius of a spherical shell or cylindrical tube, the additional boundary conditions are found by a backward-backward difference scheme.

4.2.2 MacCormack's Method for the Unbounded Medium Problem

For spherically or cylindrically symmetric deformation of an unbounded medium, a scheme to express the unbounded medium in finite terms is needed to facilitate implementation of a numerical algorithm. The scheme used in this thesis is based on the consideration that the medium ahead of the shock front is in the initial state and unaffected until the disturbance arrives. The problem of expressing the unbounded medium in finite terms thus reduces to the problem of obtaining the radius of the shock front (or an upper bound for this value) since application of the finite difference algorithm in the undisturbed medium does not affect the solution. This is accomplished as follows.

For the linear homogeneous form of (4.10), that is with $\mathbf{b} = \mathbf{0}$, a necessary condition for numerical stability of the linear problem is that the Courant number $\omega \leq 1$, where

$$\omega = c\,\frac{\Delta\tau}{\Delta R}, \tag{4.15}$$

and c is the numerically largest eigenvalue of the square matrix $\mathbf{A}$ of (4.1) at a given time step. This stability criteria is known as the Courant-Friedrich-Lewy (CFL) condition and is discussed by MacCormack (1969) and Anderson et al. (1984). [2] With a chosen value of ω and a fixed value of ΔR, equation (4.15) can be used to determine $\Delta\tau$ with c computed from the numerical solution at the previous time step. For the problems considered in this thesis, the value of $\omega = 0.99$ was used as it was found that numerical instability occurs when $\omega = 1$.

At each time step, the shock can advance at most, a distance ΔR since

$$V_S < \ c \ \leq \frac{\Delta R}{\Delta\tau}, \tag{4.16}$$

where V_S is the shock speed and $\Delta\tau$ has been chosen using the CFL stability criteria. After N time steps, the disturbance can advance at most by N space steps and $R = 1 + N\Delta R$ is an upper bound for the radius of the shock front. At the time corresponding to the N^{th} time step, the finite difference predictor-corrector scheme (4.11) must be applied at all radii between $R = 1$ and $R = 1 + N\Delta R$, although application of the scheme at grid points beyond this radius does not influence the numerical results.

4.2.3 MacCormack's Method with Gottlieb-Turkel Scheme

The solution of figure 4.4 is obtained using MacCormack's method with the

---

[2] The CFL stability criteria is actually for initial value problems and relies on the assumption that the boundary conditions have no effect on stability.

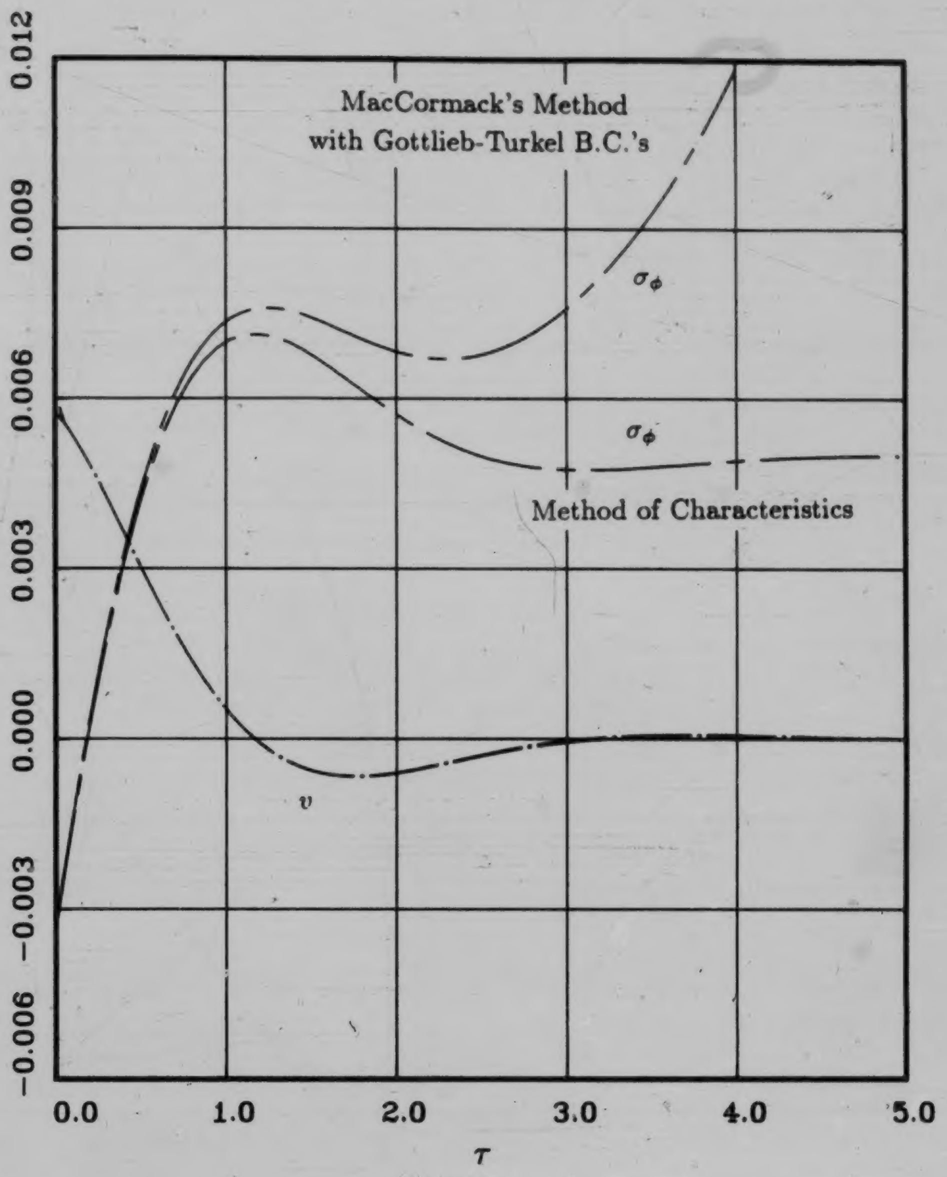

Figure 4.4: Spherical Cavity in an Unbounded Medium
Response at $R = 1$
MacCormack's Method with Gottlieb-Turkel Boundary Conditions
Linear Elasticity, $\nu = 0.25$
$p(\tau) = 0.01\, H(\tau)$

Gottlieb-Turkel scheme and is the same linear elasticity problem considered in section 4.1.1. The method of characteristics solution of figure 4.1 is superimposed for comparison. As is evident in this figure, MacCormack's method with the Gottlieb-Turkel scheme, yields results which diverge from the correct solution. For the particular deformation considered here, the method yields reasonable results up to nondimensional time of approximately 0.75; beyond this time the circumferential stress becomes unbounded. Note that the numerical solution for velocity does not exhibit instability even though the governing equations are coupled.

For the infinitesimal and finite deformation of spherical shells and cylindrical tubes considered in this thesis, MacCormack's method in combination with Gottlieb-Turkel scheme, is unstable and does not yield viable solutions. The instability seems to be related to the existence of the third family of characteristics which are parallel to the τ axis in the $R-\tau$ plane.

For the class of problems in which there are only two families of characteristics, MacCormack's method with Gottlieb-Turkel scheme yields satisfactory results. This has been demonstrated by Haddow et al. (1978a, 1978b), through several successful applications of MacCormack's method for elastodynamic deformation. In each of these successful applications, there are only two families of characteristics due to the form of the governing equations; there are no characteristics parallel to the τ axis. For the class of problems in which there are three families of characteristics, one of which is parallel to the τ axis in the $R-\tau$ plane, MacCormack's method with the Gottlieb-Turkel scheme is unstable and the scheme fails.

4.3 Hybrid Numerical Scheme

The instability of MacCormack's method, with the additional boundary conditions obtained from the Gottlieb-Turkel scheme, can be avoided by using a hybrid numerical scheme. This hybrid scheme, which is introduced in this section, is based on MacCormack's finite difference method with boundary conditions obtained from both the Gottlieb-Turkel procedure and the characteristic relation along the τ axis in the $R-\tau$ plane.

A significant advantage of this method, in comparison to other schemes such as the method of characteristics, is that the scheme is relatively easy to implement. The hybrid method is a shock capturing scheme for which the position and magnitude of a shock do not need to be specified to implement the solution. This is particularly significant for nonlinear problems.

The numerical solutions obtained using the hybrid scheme agree with the solutions for the limiting cases of infinitesimal deformation which have been obtained by other methods. This agreement is a check on the validity of the scheme. In addition, the hybrid method numerical solution is in agreement with the numerical solution for the special case of nonlinear finite deformation of a Blatz and Ko spherical shell, as independently determined by Haddow and Mioduchowski (1975). A comparison with their results, which are obtained using the method of characteristics, is presented in section 4.3.4.

4.3.1 Boundary Condition Relations

The hybrid method is essentially the MacCormack predictor-corrector scheme combined with some of the characteristic relations along characteristics which are parallel to the τ axis in the $R-\tau$ plane. The boundary conditions which are required to implement the scheme are obtained from the method of characteristics and the Gottlieb-Turkel scheme. The details of this method are presented for the spherically symmetric case only. The cylindrically symmetric case is similar and is not included here.

Two physically realistic boundary conditions are considered in this thesis and are first presented in chapter 3. A velocity boundary condition can be specified, for example, at a fixed boundary for which $v = 0$. Alternatively, the radial stress (σ_r) at the inner or outer radius can be specified by the application of a spatially uniform pressure.

If the velocity at the wall of a spherical cavity is specified, λ_r and λ_ϕ are required at the boundary in order to implement the finite difference scheme. When the velocity is specified, the hybrid method utilizes the Gottlieb-Turkel scheme to obtain λ_r using the predictor-corrector relations (4.11). For the specific case of spherically symmetric deformation, these relations are

$$\begin{aligned}(\lambda_r)_j^{\overline{n+1}} &= \left\{(\lambda_r)_j^{\,n} + \frac{\Delta\tau}{\Delta R}\left(v_{j+1}^{n} - v_j^{\,n}\right)\right\},\\ (\lambda_r)_j^{n+1} &= \frac{1}{2}\left\{(\lambda_r)_j^{\,n} + \lambda_{r_j}^{\overline{n+1}} + \frac{\Delta\tau}{\Delta R}\left(v_{j+1}^{\overline{n+1}} - v_j^{\overline{n+1}}\right)\right\},\end{aligned} \tag{4.17}$$

where $j = 1$ at the inner cavity wall. The hybrid method utilizes the characteristic relation along the τ axis of the $R - \tau$ plane given by (4.8) to obtain the boundary condition for λ_ϕ. In finite difference form, this characteristic relation is

$$\Delta\lambda_\phi = \frac{v}{R}\Delta\tau, \tag{4.18}$$

where $\Delta\lambda_\phi$ is the finite change in λ_ϕ for the finite time step $\Delta\tau$.

Alternatively, the Cauchy radial stress can be specified at a boundary. This is equivalent to specifying a relation between λ_r and λ_ϕ. In this case, two additional boundary conditions are also needed to implement the hybrid numerical method. The Gottlieb-Turkel procedure is used to obtain v and the characteristic relation (4.8) is used to obtain λ_ϕ.

For the specific case of spherically symmetric deformation, using (4.11) and (4.12), the predictor-corrector relations for v are

$$\begin{aligned} v^{\overline{n+1}} &= \left\{ v_j^n + \frac{\Delta\tau}{\Delta R}\Big((P_r)_{j+1}^{n+1} - (P_r)_j^{n+1} \Big) - \frac{2\,\Delta\tau}{R}\Big((P_\phi)_j^{n+1} - (P_r)_j^{n+1} \Big) \right\}, \\ v_j^{n+1} &= \frac{1}{2}\left\{ v_j^n + v_j^{\overline{n+1}} + \frac{\Delta\tau}{\Delta R}\Big((P_r)_{j+1}^{\overline{n+1}} - (P_r)_j^{\overline{n+1}} \Big) - \frac{2\,\Delta\tau}{R}\Big((P_\phi)_j^{\overline{n+1}} - (P_r)_j^{\overline{n+1}} \Big) \right\}, \end{aligned} \tag{4.19}$$

where $j = 1$ at the inner boundary. Using this value of v, the characteristic relation given by (4.18) is used to obtain λ_ϕ and the radial stretch λ_r is specified by the Cauchy radial stress boundary condition which relates λ_r and λ_ϕ. For a sudden application of pressure of magnitude q, which thereafter remains constant, the boundary condition relation can be written

$$\sigma_r\,(1,\tau) = -\,q\,H\,(\tau)\,,$$

or

$$\frac{P_r\,(1,\tau)}{\lambda_\phi} = -\,q\,H\,(\tau)\,. \tag{4.20}$$

A discontinuity of radial stress, that is a shock, is initiated at $R = 1$ and this discontinuity propagates radially outward. It follows that λ_r is discontinuous across a shock but λ_ϕ is continuous.

The use of characteristic relations along characteristics which are parallel to the τ axis is important in the implementation of the boundary conditions; if the Gottlieb - Turkel scheme is used for both additional boundary conditions, the numerical results are erroneous as has been previously shown. However, for the range of deformations considered in this thesis, there is no advantage in using the characteristic relations at all radii, although in principle there is no difficulty in doing so.

4.3.2 Comparison with Linear Elasticity Solution

The solution for the linearly elastic deformation considered in section 4.1.1 can also be obtained using the hybrid method. When compared with the method of characteristics solution or integral transform solution, the numerical results are in close agreement and are not included here as they can not be distinguished from those of figure 4.1 at the scales plotted.

The solutions for small amplitude finite deformation, shown in figures 4.5 and 4.6 can be compared with the solutions for infinitesimal deformation as determined by the method of characteristics given previously in figures 4.2 and 4.3. This finite deformation solution is for the Blatz sef [3] for which $\nu = 0.25$ as in the linear elasticity case. For a Heaviside application of pressure of magnitude $q = 0.01$, the finite deformation solution is in agreement with the infinitesimal deformation solution obtained using the method of characteristics.

4.3.3 Verification of Jump Conditions

The jump conditions presented in section 3.1.5 are used to check the results obtained from the numerical method. This is demonstrated by the example shown in figures 4.7 and 4.8 which show the relation between nominal stress, velocity, and radial stretch and R at various times. The results are for the deformation of a spherical

---

[3] The validity of the solutions is questionable since the Blatz sef models foam rubber and the static properties may not be applicable to the dynamic deformation problem.

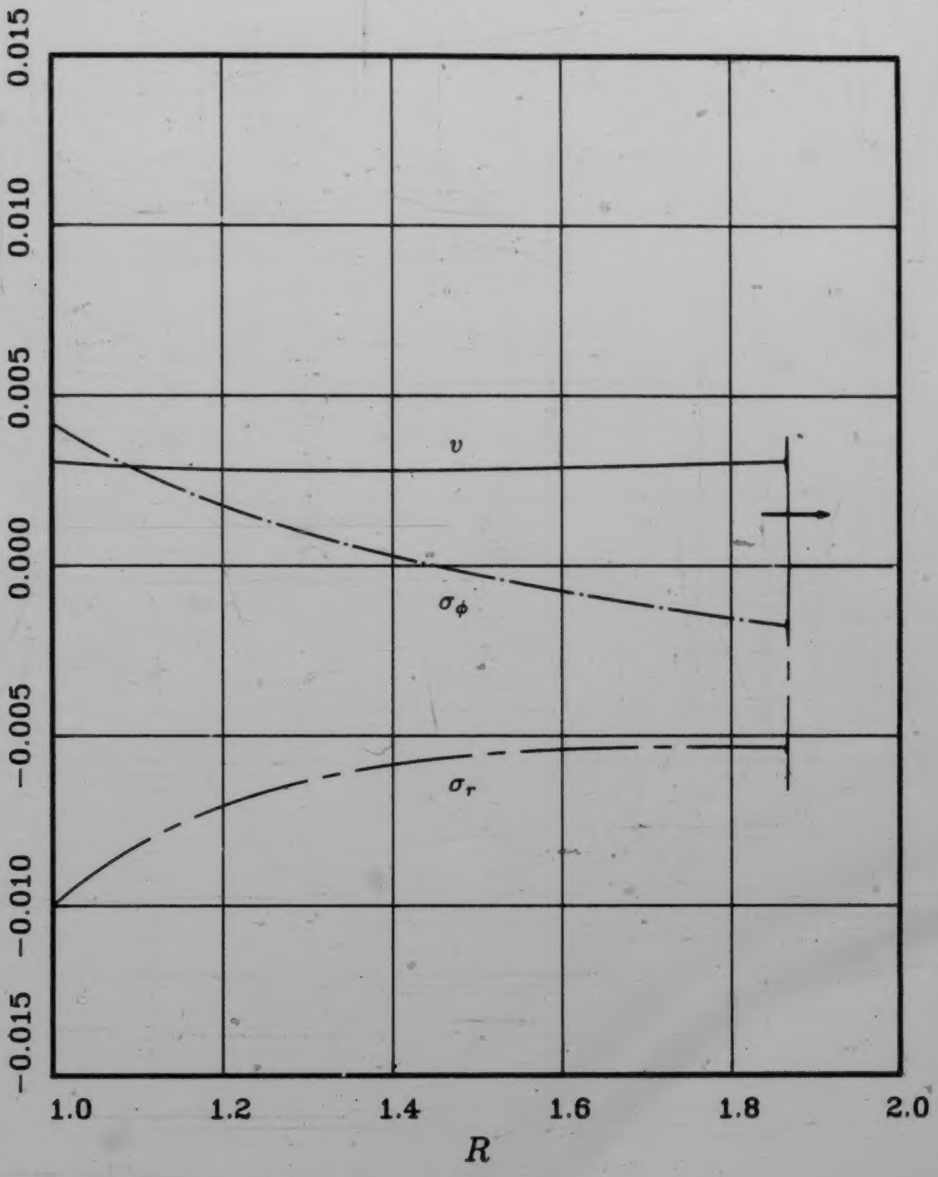

Figure 4.5: Spherical Shell, $R_o/R_i = 2$
Response Before Reflection, $\tau = 0.5$
Hybrid Scheme, Blatz sef, $\nu = 0.25$
$p(\tau) = 0.01\, H(\tau)$

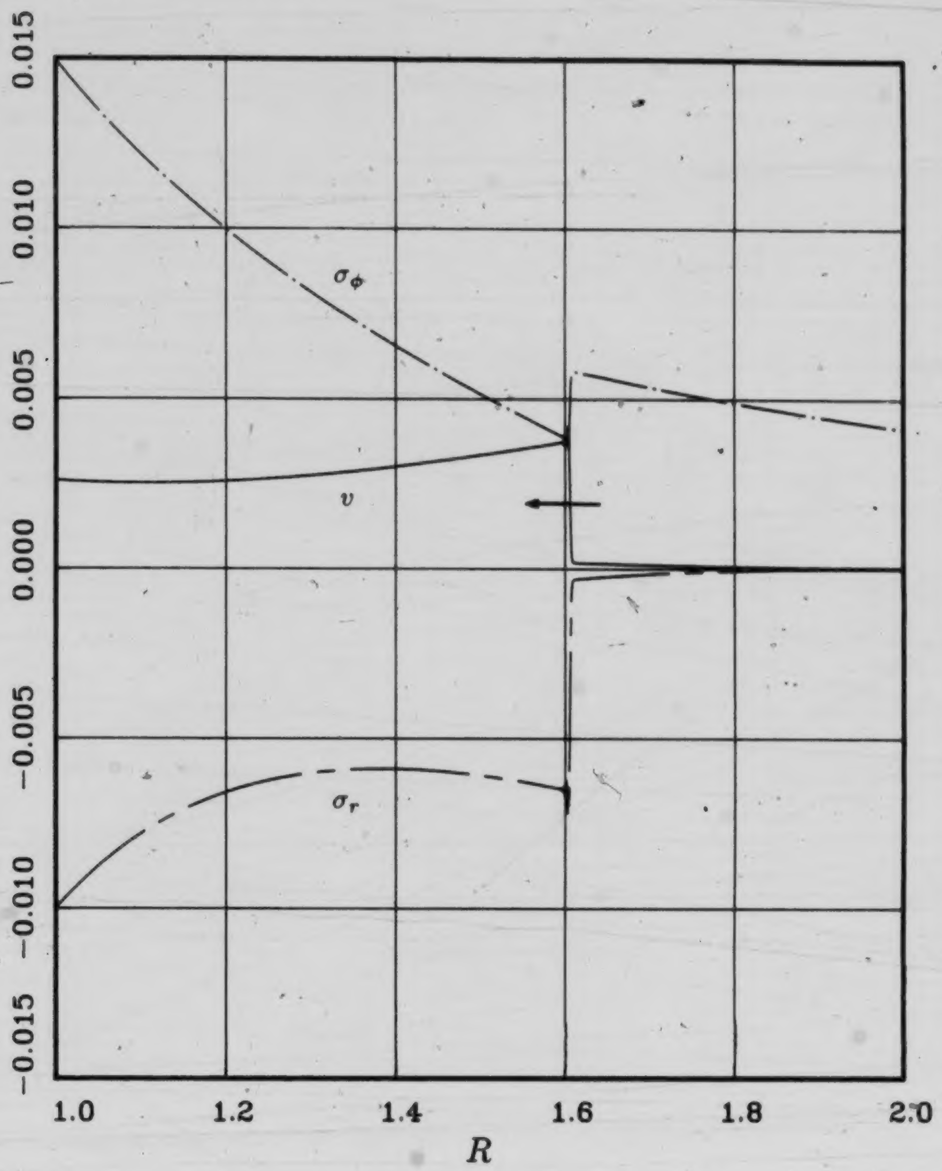

Figure 4.6: Spherical Shell, $R_o/R_i = 2$
Response After Reflection, $\tau = 1.5$
Hybrid Scheme, Blatz sef, $\nu = 0.25$
$p(\tau) = 0.01\, H(\tau)$

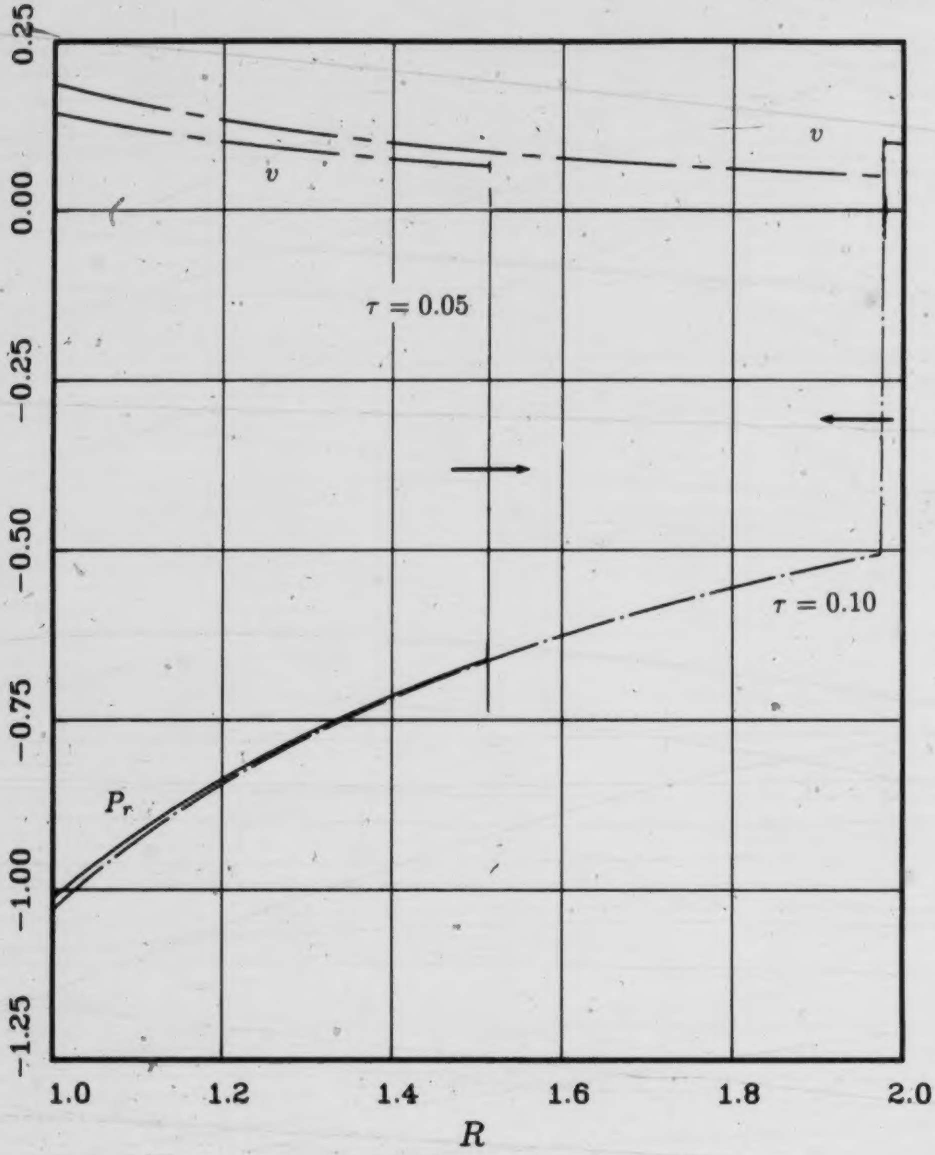

Figure 4.7: Spherical Shell, $R_o/R_i = 2$
P_r and v at $\tau = 0.05$ and $\tau = 0.10$
Hybrid Scheme, modified Gaussian sef, $\nu = 0.495$
$p(\tau) = H(\tau)$

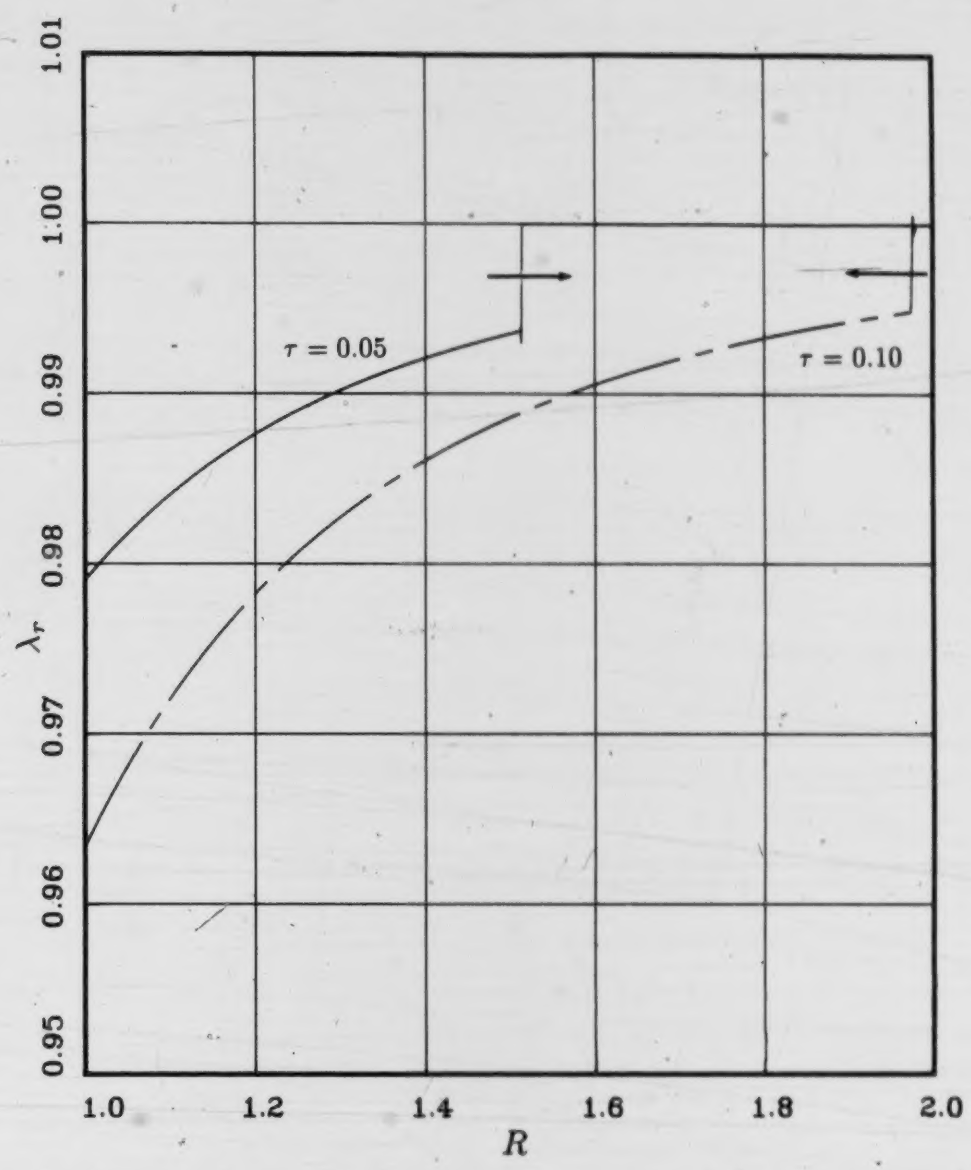

Figure 4.8: Spherical Shell, $R_o/R_i = 2$
λ_r at $\tau = 0.05$ and $\tau = 0.10$
Hybrid Scheme, modified Gaussian sef, $\nu = 0.495$
$p(\tau) = H(\tau)$

shell of modified Gaussian material with $R_o/R_i = 2$, $q = 1$, $\nu = 0.495$. Further examples of finite deformation are presented in Chapter 5.

The plots show the solution at time $\tau = 0.05$ (before reflection from the outer radius of the spherical shell) and at time $\tau = 0.10$, (after reflection from the outer radius). The magnitudes of the discontinuities at the shock fronts are presented in table 4.1 and the jump relations given by (3.45) are satisfied within an acceptable error.

		$\tau = 0.05$	$\tau = 0.10$
From Figures 4.7, 4.8	$[\lambda_r]$	0.00639	0.00496
	$[P_r]$	0.6625	0.50375
	$[v]$	0.0650	0.05000
Jump Relation Terms	$[v]^2$	0.004225	0.00250
	$[P_r]\,[\lambda_r]$	0.004233	0.002499

Table 4.1: Jump Discontinuities at Shock Fronts : Spherical Shell

4.3.4 Comparison with a Previous Nonlinear Elasticity Solution

Results from the hybrid method numerical solution for finite deformation of a Blatz and Ko spherical shell are compared with results from the method of characteristics solution given by Haddow and Mioduchowski (1975). As is discussed in chapter 2, the Blatz and Ko sef does not adequately represent the dilatation of solid rubberlike materials. The two solutions are presented here primarily for comparison of the two numerical methods.

Figure 4.9 shows the tangential stretch at the inner cavity wall (position of the inner cavity wall) as a function of nondimensional time. The Blatz and Ko material considered has a Poisson ratio $\nu = 0.3$ for infinitesimal deformation from the undeformed state. A step function application of pressure of magnitude $q = 0.25$, is applied at the inner radius; the outer radius is stress free.

The hybrid scheme solution is given by the continuous curve; the discrete points indicate results from the method of characteristics. There is excellent agreement between these two independent methods for this nonlinear, finite deformation problem.

Another example for finite deformation, comparing the hybrid scheme numerical solution with the method of characteristics solution, is given in section 5.3.1.

4.3.5 Interface Conditions for Concentric Cylinders

There are two difficulties which must be considered to implement the numerical scheme for the concentric cylinder problem. The first is that the spatial grid size can not be the same in both cylinders if the time step size and CFL stability criteria given by (4.15) are to be the same for both cylinders. This difficulty is overcome by choosing one of the spatial grid sizes and obtaining the other by equating the Courant number and time step of equation (4.15). If the spatial grid size for the outer cylinder, ΔR_o, is chosen, then ΔR_i is given by

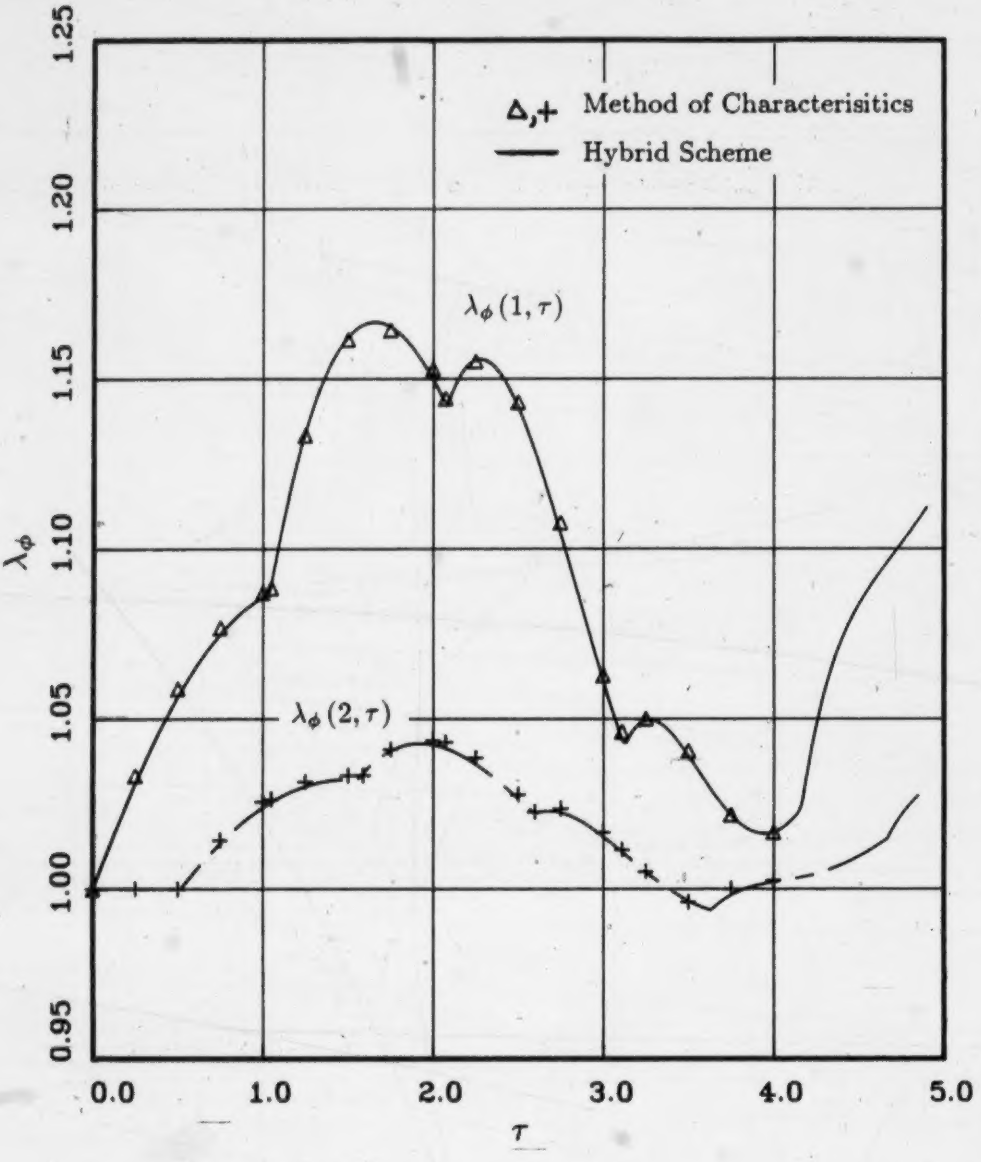

Figure 4.9: Spherical Shell, $R_o/R_i = 2$
Hybrid Scheme and Method of Characteristics
Blatz and Ko sef, $\nu = 0.3$
$p(\tau) = 0.25\,H(\tau)$

$$\Delta R_i = \Delta R_o \frac{\left(\sqrt{\partial P_r/\partial \lambda_r}\right)_i}{\left(\sqrt{\partial P_r/\partial \lambda_r}\right)_o}. \tag{4.21}$$

Equation (4.21) implies that ΔR_i must be adjusted at every time step since the ratio of eigenvalues changes due to the nonlinear nature of the problem. In principle, this can be implemented by a complicated interpolation scheme, although in practice, reasonable results can be obtained by setting the spatial grid sizes using (4.21) evaluated at the initial conditions. The penalty for this simplification is numerical dispersion.

The second difficulty in implementing a numerical scheme for concentric cylinders is to satisfy continuity of velocity, tangential stretch and Cauchy radial stress at the interface. The use of these three transition conditions and the relation along the characteristic which is parallel to the τ axis in the $R-\tau$ plane, leaves two remaining relations to be determined (since there are six dependent variables at $R = R_*$). This is similar to the need for the additional boundary conditions when the finite difference method is applied to a single cylindrical or spherical shell.[4]

In the case of the single shell, the use of a finite difference scheme with the Gottlieb-Turkel relations for both additional boundary conditions, does not yield a reasonable solution as is discussed in section 4.2.3 and shown in figure 4.4. A similar situation arises if the Gottlieb-Turkel relations are used for both interface conditions at the transition between the concentric cylinders. Figure 4.10 indicates this instability for concentric cylinders where $\zeta = 2$, $\psi = 7$, $\nu_1 = 0.48$, $\nu_2 = 0.495$, $R_i = 1$, $R_* = 1.25$ and $R_o = 1.5$. Note that these material properties are chosen to illustrate implementation of the interface conditions and may not describe a realistic material.

---

[4] For example, if v is specified at a boundary, two additional boundary condition relations are required to obtain λ_r and λ_θ.

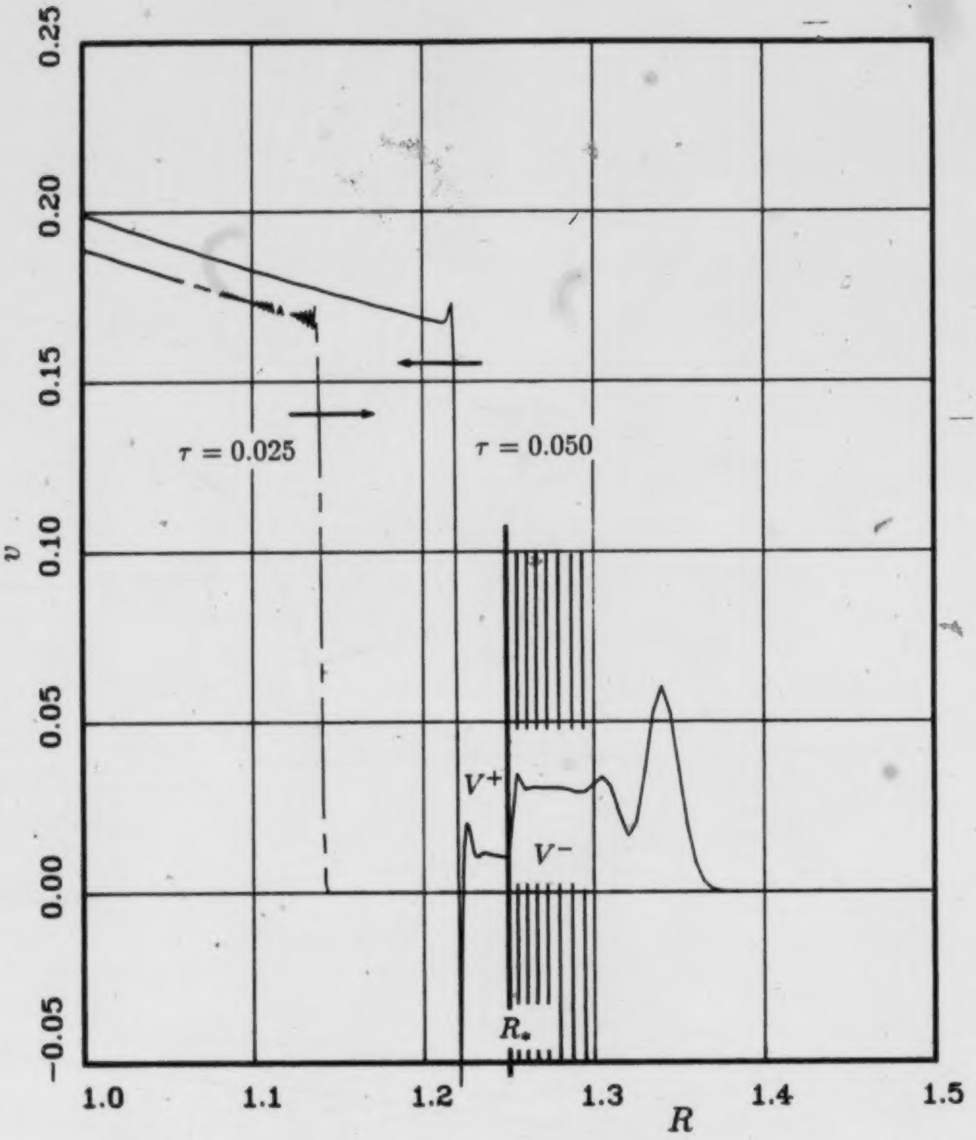

Figure 4.10: Concentric Cylinders, $\nu_1 = 0.48$, $\nu_2 = 0.495$, $\zeta = \rho_{02}/\rho_{01} = 2$, $\psi = \mu_2/\mu_1 = 7$, $R_i = 1$, $R_* = 1.25$, $R_o = 1.5$.
Hybrid Method with Gottlieb-Turkel Boundary Conditions
Response at $\tau = 0.025$ and $\tau = 0.05$
Modified Gaussian sef, $\nu = 0.495$, $p(\tau) = H(\tau)$

For this example, the modified Gaussian sef (3.25) is assumed to govern the response of both cylinders. The severe numerical dissipation and dispersion which is evident near the front of the disturbance, is a consequence of the crude grid step chosen to illustrate the instability phenomenon.

Note that the unsatisfactory results shown in figure 4.10 satisfy continuity of velocity, tangential stretch and Cauchy radial stress at the interface. For example, at $R = R_* = 1.25$, the velocity is continuous as required. However, a physically unrealistic change in velocity occurs just after the interface.

A modification to the hybrid numerical procedure is required to obtain a plausible solution. The modification involves three iterations at each time step to obtain the correct values of the dependent variables at the interface between the cylinders.

On the first iteration, the six required interface relations are obtained using two Gottlieb-Turkel relations, three relations obtained from continuity of velocity, tangential stretch and Cauchy radial stress, and the characteristic relation which is parallel to the τ axis at $R = R_*$,

$$\frac{d\lambda_\theta}{d\tau} = \frac{v}{R}. \tag{4.22}$$

The numerical solution obtained after this first iteration is in error. The magnitude of the error can be quantified by comparing the velocity of the inner cylinder at the interface (V^-), with the velocity of the outer cylinder at the interface (V^+). As is shown in figure 4.10, V^+ can be obtained by extrapolation of the solution in the outer cylinder in the spatial region beyond the interface. For continuity of velocity, the desired criteria is that $V^- = V^+$.

On the second iteration, the value of λ_r^- (λ_r for the inner cylinder at $R = R_*$), is perturbed by a small amount from its value which was used in the first iteration (given by the Gottlieb-Turkel scheme). The resulting error in velocity is again quantified by the difference between V^- and V^+ as described above. In general, this difference will still be non-zero, although the change in $(V^- - V^+)$ between the first and second iterations defines the dependence of this velocity difference on λ_r^-. Assuming that the correct value of λ_r^- is near that given by the Gottlieb-Turkel scheme, a linear extrapolation of the relation between the velocity error and the value of λ_r^-, with the objective that $(V^- - V^+) = 0$, specifies a corrected value of λ_r^-. For the numerical solutions presented in this thesis, this corrected value is then accepted and a third iteration, using this value, is used to advance the solution by one time step. Alternatively, an algorithm to further converge on the correct value of λ_r^- could be implemented, although this does not appear necessary for the numerical solutions considered in this thesis.

The hybrid numerical method, modified by this correction procedure, results in plausible solutions for the deformation of concentric cylinders which satisfy the required jump conditions given in section 3.4.3. In addition, the numerical results for the problem of two concentric cylinders reduce to the results for a single cylinder when the material properties of both cylinders are the same.

Solutions for finite deformation of concentric cylinders are presented in section 5.4.

4.3.6 Limitations of the Hybrid Method

Figure 4.11 shows the hybrid method solution for the deformation of an unbounded, linearly elastic medium. A Heaviside step function of pressure is applied at the wall of a spherical cavity with $q = 0.01$ and $\nu = 0.25$. The numerical dispersion and erroneous overshoot near the location of the discontinuity, is a limitation of

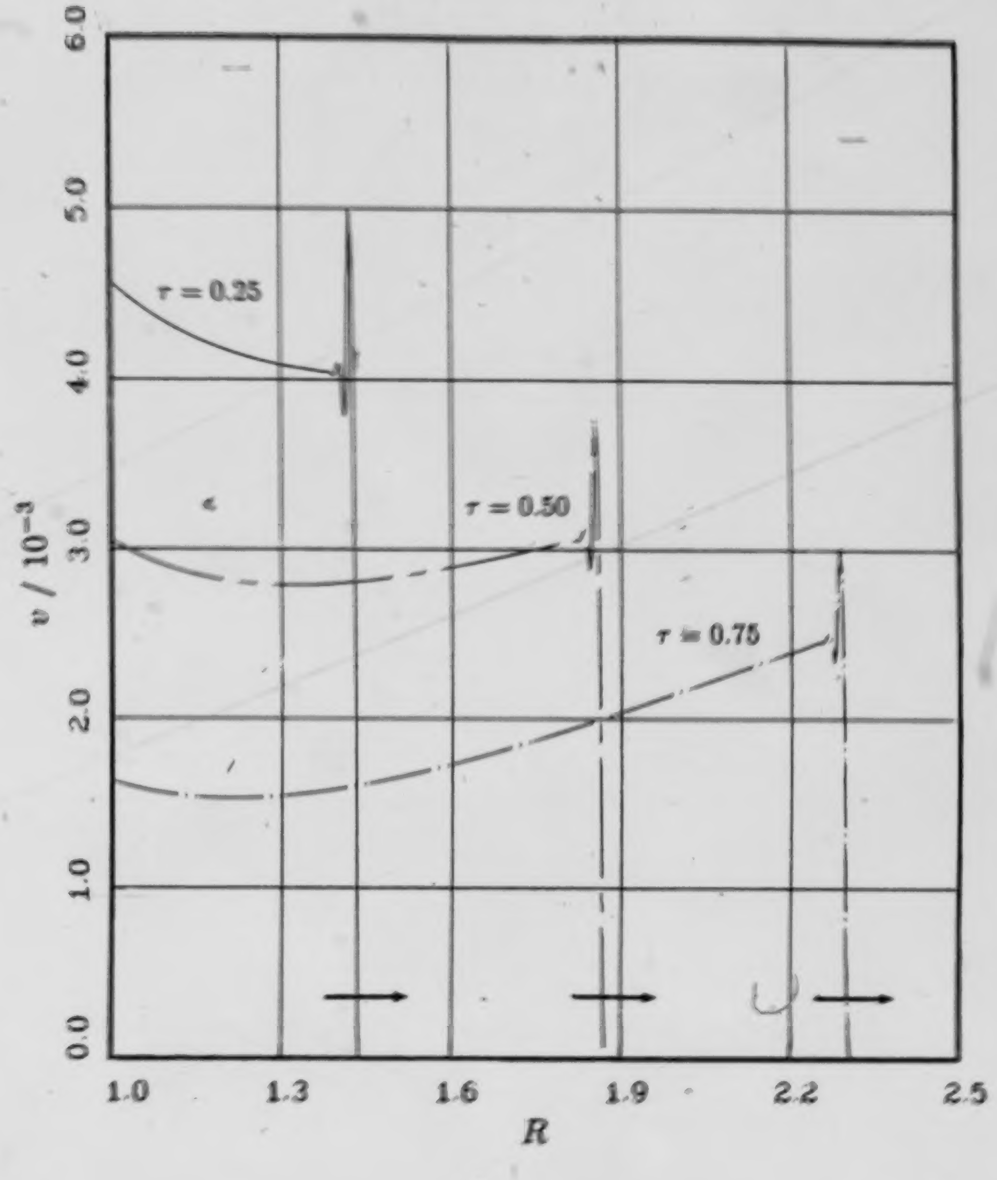

Figure 4.11: Spherical Cavity in an Unbounded Medium, Linear Elasticity Hybrid Scheme, Effect of Spacial Step Size, $\Delta R = 0.0025$ Response at $\tau = 0.25$, $\tau = 0.50$, $\tau = 0.75$, $p(\tau) = 0.01\,H(\tau)$

most shock capturing finite difference schemes. The severity of the dispersion and dissipation is particularly evident in this example due to the crude space step size of $\Delta R = 0.0025$, chosen to illustrate this limitation.

The plot shows the spatial distribution of velocity at three distinct times $\tau = 0.25$, $\tau = 0.50$ and $\tau = 0.75$ and is comparable to the solution of the same problem shown in figure 4.12 for a smaller grid size ($\Delta R = 0.0001$). As is evident, the numerical dispersion can be reduced by decreasing the spatial step size (and thus also the temporal grid size) although this is at the expense of increased computational time. Computation time is inversely related to the square of the spatial grid size since a change in the spatial grid size results in a change in the temporal grid size as given by (4.15).

For this linearly elastic deformation, the shock front propagates at the constant shock velocity given by (3.8) with $c = 1.732$ for $\nu = 0.25$. The positions of the shock front, which are similar for both the crude solution of figure 4.11 and the refined solution of figure 4.12, are in agreement with this shock velocity.

Comparison of the crude and refined solutions indicates that an extrapolation procedure, which is based on the solution in a region behind the shock, can be used to consider the effect of the overshoot at the shock front. For the refined solution shown in figure 4.12, such an extrapolation amounts to ignoring the overshoot. For crude solutions in which there is a significant amount of numerical dispersion and dissipation, the extrapolation procedure is more complex. This is further discussed and illustrated by an example in section 5.1.3.

If the overshoot shown in 4.12 is ignored, the jump conditions given by (3.45) are satisfied.

A second limitation of the finite difference scheme used in this thesis, is that the

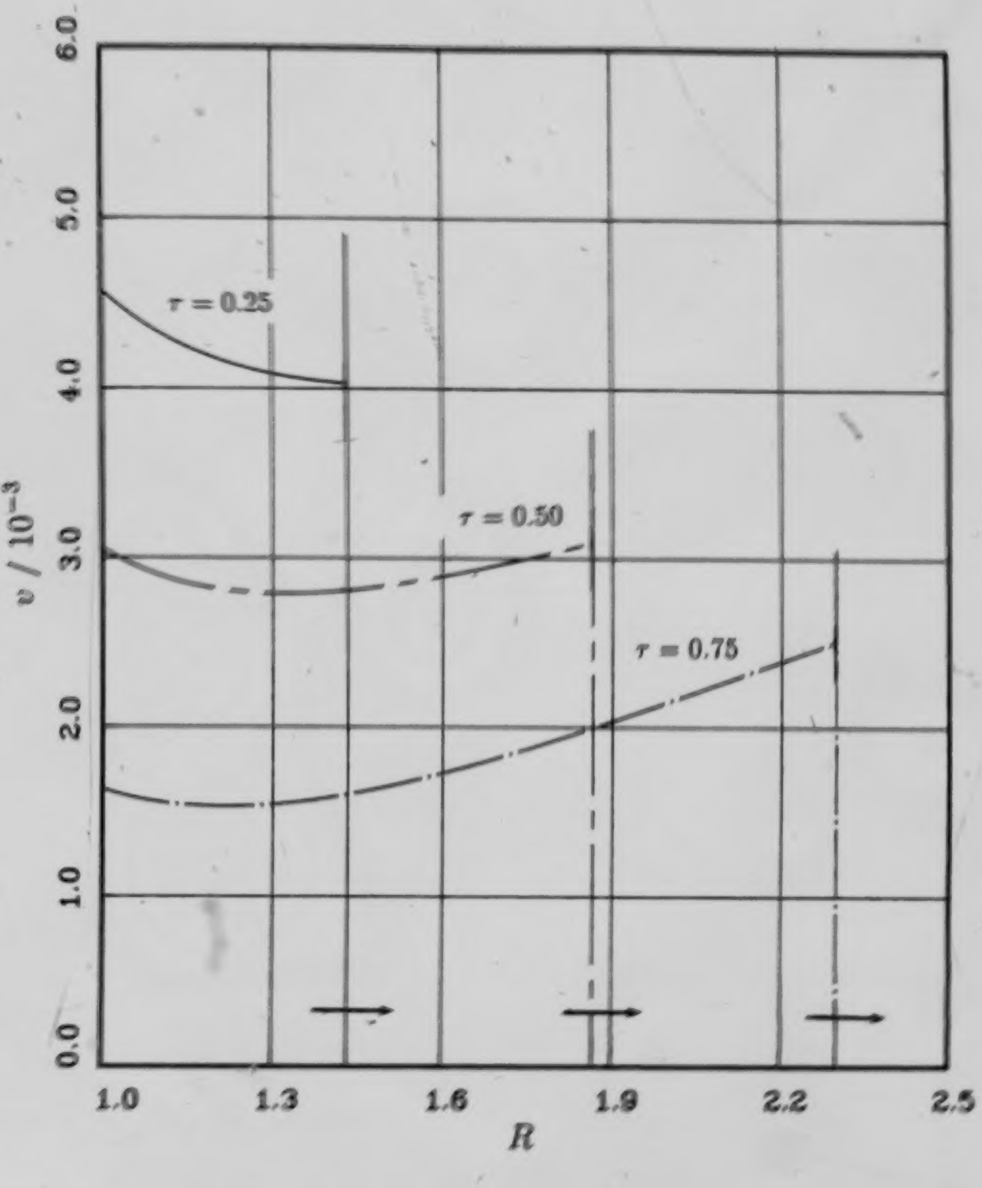

Figure 4.12: Spherical Cavity in an Unbounded Medium, Linear Elasticity Hybrid Scheme, Effect of Spacial Step Size, $\Delta R = 0.0001$ Response at $\tau = 0.25$, $\tau = 0.50$, $\tau = 0.75$, $p(\tau) = 0.01\, H(\tau)$

computation time for the problems of spherical and cylindrical deformation increases significantly as the material approaches incompressibility. This occurs because the relation between the spatial and time step size is dependent on the numerically largest eigenvalue of the **A** matrix in (4.1) and the eigenvalues increase in magnitude as the material approaches incompressibility. An estimate of this effect can be determined by considering the linear elasticity case in which the eigenvalues are constant and are related to the Poisson ratio as given by (3.8). Using $\nu = 0.463$ as the base case for which computation time is unity, the computation time increases by a factor of 2.6 for $\nu = 0.495$ and by a factor of 18.6 for $\nu = 0.4999$. Numerical solutions for Poisson ratios very near the incompressible limit, for which a reasonable grid size is maintained, likely require extensive use of a supercomputer. The largest Poisson ratio for which numerical results have been obtained by the author is $\nu = 0.4998$.

Chapter 5

Numerical Solutions

5.1 Spherically Symmetric Deformation

The numerical solutions presented in this section are for spherically symmetric elastodynamic problems, namely expansion of a spherical cavity in an unbounded medium and expansion of a thick-walled spherical shell.

If a spatially uniform, sudden application of pressure of magnitude q is applied at the cavity wall, the Cauchy radial stress at $R = 1$ is

$$\sigma_r(1,\tau) = -q\,H(\tau). \tag{5.1}$$

If the applied pressure is a sinusoidal pulse of magnitude q and duration τ_*, the Cauchy radial stress at $R = 1$ is

$$\sigma_r(1,\tau) = -q\,\sin\left(\frac{\pi\tau}{\tau_*}\right) H(\tau_* - \tau)\,H(\tau). \tag{5.2}$$

For the numerical solutions presented in this section, the boundary condition at $R = R_o$ is

$$\sigma_r(R_o,\tau) = 0, \tag{5.3}$$

although a non-zero stress or velocity boundary condition could also be implemented.

The radius ratio for thick-walled spherical shells considered here is $R_o/R_i = 2$. It is assumed that this ratio is sufficiently large that the shell remains spherically symmetric throughout the deformation.

The Gaussian sef (2.21) and the modified Gaussian sef (2.19) are in reasonable agreement with experimental data and are suitable for the moderate deformation of solid rubber considered in this thesis. [1] Experimental work by Bridgman (1947), Levinson and Burgess (1971), and Beatty and Stalnaker (1986), indicates that Poisson's ratio for most solid rubber is in the range

$$0.463 \leq \nu \leq 0.499895.$$

Numerical solutions for spherically symmetric deformation of a compressible solid rubber are obtained for the Gaussian sef (2.25), and the modified Gaussian sef (2.24), with $\nu = 0.495$. Numerical results for higher Poisson ratios can be obtained subject to the limitations of the hybrid numerical scheme as discussed in section 4.3.6.

Numerical solutions for deformation in incompressible, homogeneous elastic materials are obtained for the neo-Hookean sef, (2.13).

5.1.1 Incompressible Spherical Shell

The analysis of finite elastodynamic deformation of incompressible spherical shells is presented in Appendix A. A spatially uniform pressure of magnitude q is suddenly applied at the cavity wall and the boundary condition given by (5.1) applies.

Figure 5.1 shows the phase plane solution for the motion of the inner cavity wall of an incompressible spherical shell where $R_o/R_i = 2$. The phase plane closes; oscillation of the spherical shell is periodic provided that the magnitude of the suddenly applied pressure is less than the critical value, which is approximately $q_c = 0.7435$ for this configuration. [2] For $q < q_c$, the motion of the cavity wall is periodic and for $q > q_c$, the radial displacement increases monotonically until the shell bursts.

---

[1] **Isothermal strain energy functions are used to describe the stress-strain relations and are discussed in section 2.**

[2] **Nondimensional quantities as given by (3.93) are used exclusively in this section unless otherwise noted. As before, quantities with dimension of stress are nondimensional by dividing by the shear modulus μ.**

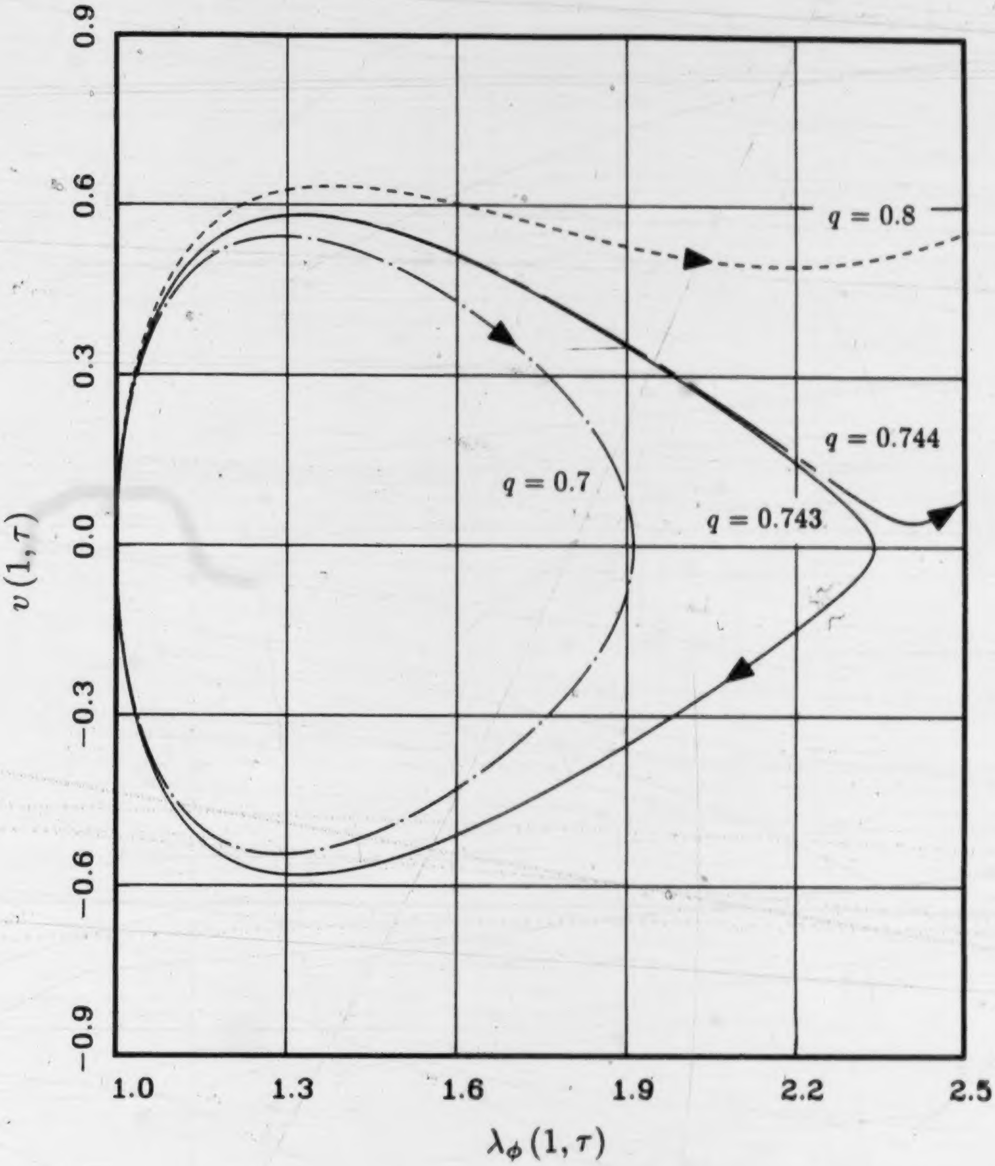

Figure 5.1: Phase Plane Solution, Motion of the Inner Cavity Wall Incompressible Spherical Shell, neo-Hookean sef, $R_o/R_i = 2$ $p(\tau) = q\,H(\tau)$

5.1.2 Equilibrium Solution : Spherical Cavity in an Unbounded Medium

Figure 5.2 shows the equilibrium solution for λ_r and λ_θ as a function of radius R for a spherical cavity in an unbounded medium. For this problem, a sudden change of pressure of magnitude $q = 1$ is applied at $R = 1$ and held constant. The constitutive behaviour is given by the modified Gaussian sef (2.25) with $\nu = 0.495$. The material is initially quiescent and in the unstressed natural state. The solution for the corresponding dynamic problem approaches the solution shown in this figure as $\tau \rightarrow \infty$.

A fourth-order Runge-Kutta technique with step size $\Delta R = 0.01$, was used to solve the governing ODE (3.37).

5.1.3 Sudden Application of Pressure : Unbounded Medium

Figures 5.3-5.7 show the hybrid scheme numerical solution for the expansion of a cavity in an unbounded medium due to a sudden application of pressure of magnitude $q = 10$. Solutions for compressible media are for the modified Gaussian sef given by (3.25) with $\nu = 0.495$. Solutions which are presented as a function of nondimensional radius are given at $\tau = 0.2, 0.4$ and 0.6, those which are presented as a function of nondimensional time are for $R = R_i$, i.e. the cavity wall.

Excessive numerical dissipation and smearing of the shock is evident at the shock fronts shown in figure 5.3. This is a consequence of the relatively crude step size of $\Delta R = 0.005$ used in this example. As is discussed in section 4.3.6, numerical dissipation and dispersion can be reduced by decreasing the grid size at the expense of increased computation time. Alternatively, an extrapolation procedure, such as that used by Haddow et al. (1986) can be used to obtain a solution. This procedure involves extrapolation of the relations between the various dependent variables and

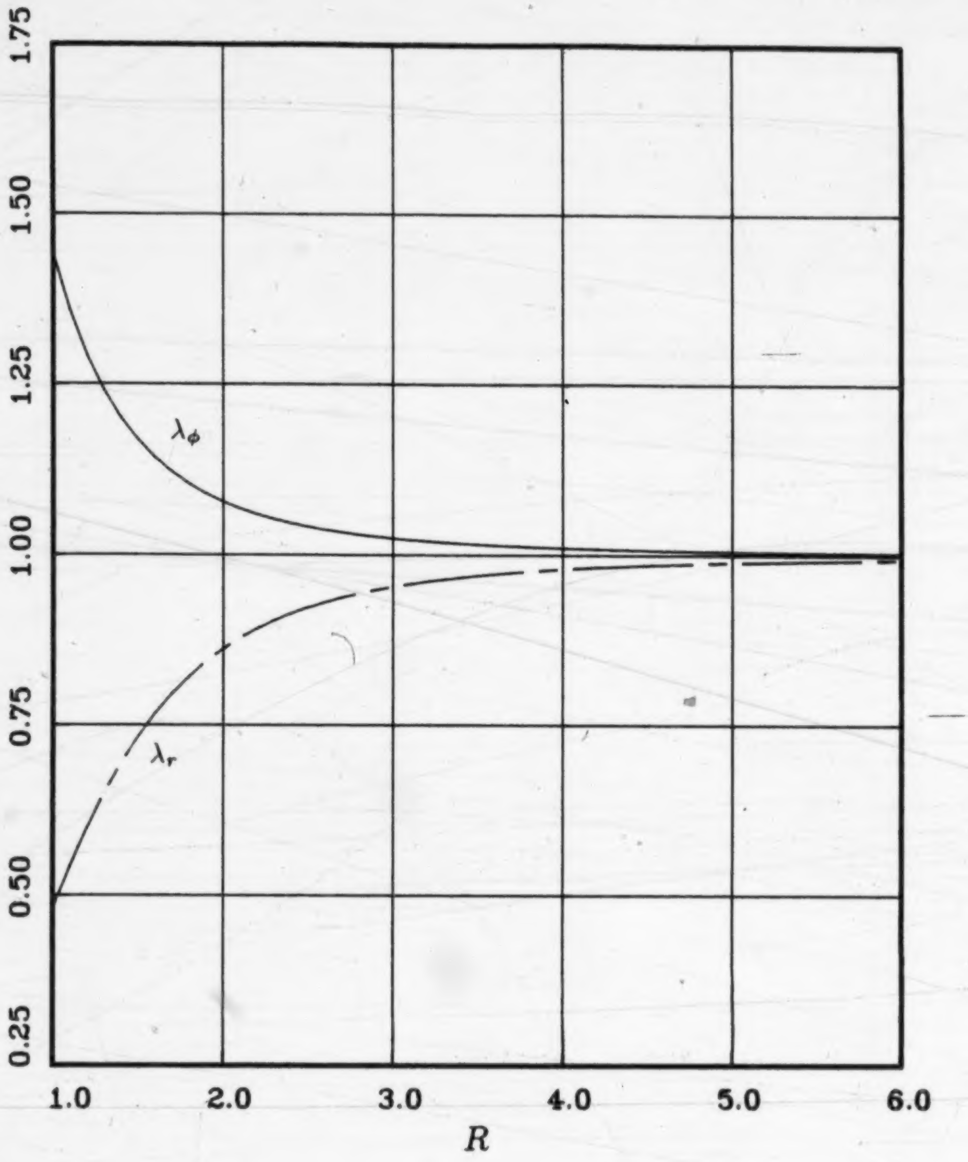

Figure 5.2: Spherical Cavity in an Unbounded Medium
Steady State Solution
Modified Gaussian sef, $\nu = 0.495$
$p(\tau) = H(\tau)$

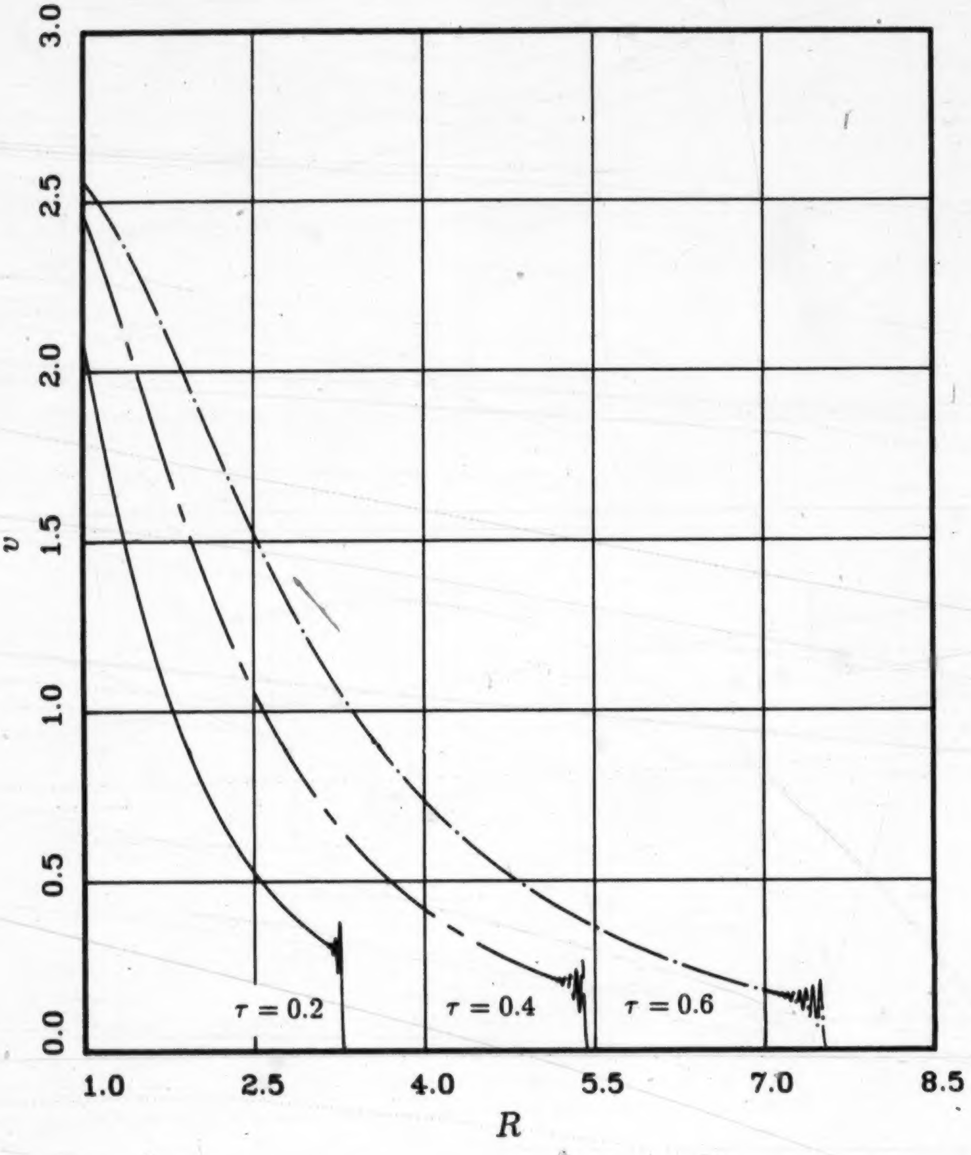

Figure 5.3: Spherical Cavity in an Unbounded Medium
Velocity at $\tau = 0.2$, 0.4 and 0.6
Modified Gaussian sef, $\nu = 0.495$
$p(\tau) = 10\,H(\tau)$

R at a fixed time, using the results in the region behind the numerical dispersion. Extrapolation is terminated when the jump conditions are satisfied. For spherically symmetric deformation, the termination condition is

$$[\, v\,]^2 = [P_r][\lambda_r], \tag{5.4}$$

which can be obtained by eliminating the shock velocity V_S, from (3.75a) and (3.75b). This relation can also be written as

$$v^2 = P_r\,(\lambda_r - 1), \tag{5.5}$$

noting that $v = P_r = 0$ and $\lambda_r = 1$ ahead of the shock.

The extrapolation procedure can be implemented either numerically or graphically, and for the present problem, no significant advantage is gained by a numerical approach. Figures 5.4 and 5.5 show the radial stretch and nominal radial stress (as obtained using (3.26a)), at $\tau = 0.2, 0.4, 0.6$, corresponding to the times used in figure 5.3. Table 5.1 lists the magnitudes of the jump quantities given in (5.4). These values were obtained using a graphical extrapolation procedure on enlarged-scale plots of P_r, λ_r and v. The discrepancy is within measurement uncertainty; the jump conditions are satisfied.

Numerical solutions which show the stretch components, velocity and dilatation at the cavity wall are given in figures 5.6 and 5.7 for compressible and incompressible media respectively. As expected, the material at the cavity wall is in compression; J is less than 1 and is almost constant. The effect of material compressibility is evident although the compressible and incompressible solutions are of a similar form.

A similar problem is considered in figure 5.8 which shows the tangential stretch at the inner cavity wall of a spherical cavity in an unbounded medium. A Heaviside

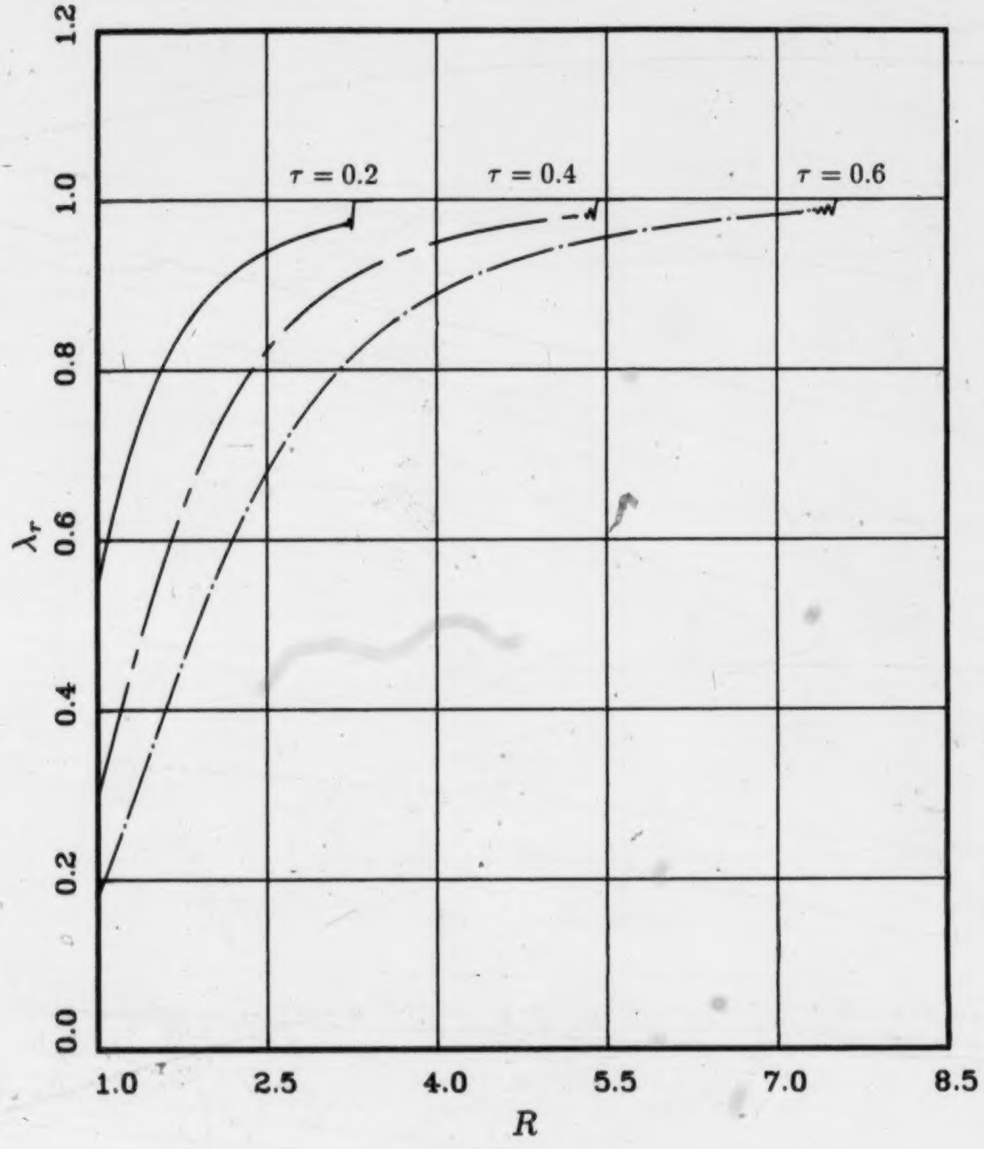

Figure 5.4: Spherical Cavity in an Unbounded Medium
Radial Stretch at $\tau = 0.2$, 0.4 and 0.6
Modified Gaussian sef, $\nu = 0.495$
$p(\tau) = 10\,H(\tau)$

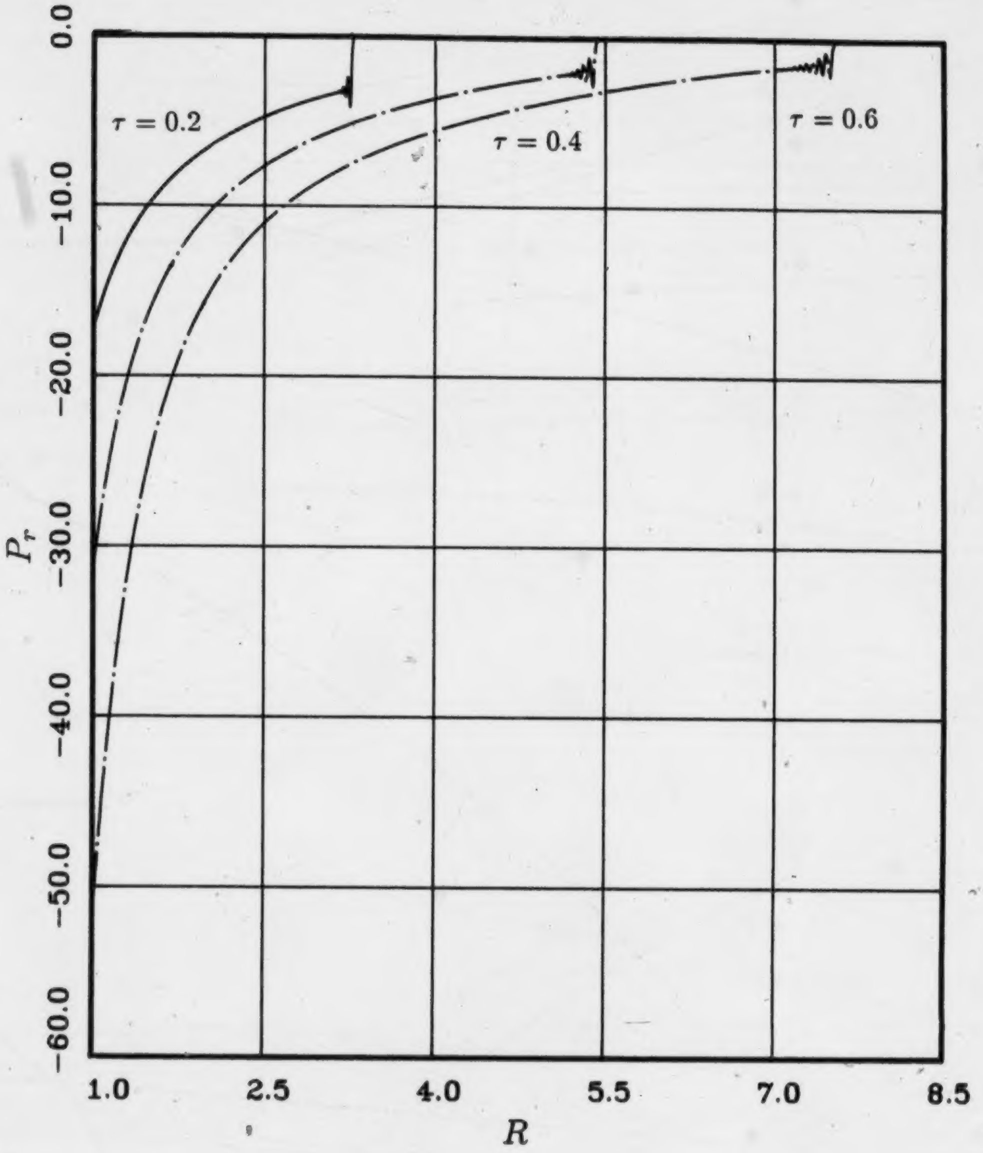

Figure 5.5: Spherical Cavity in an Unbounded Medium
Nominal Radial Stress at $\tau = 0.2$, 0.4 and 0.6
Modified Gaussian sef, $\nu = 0.495$
$p(\tau) = 10\,H(\tau)$

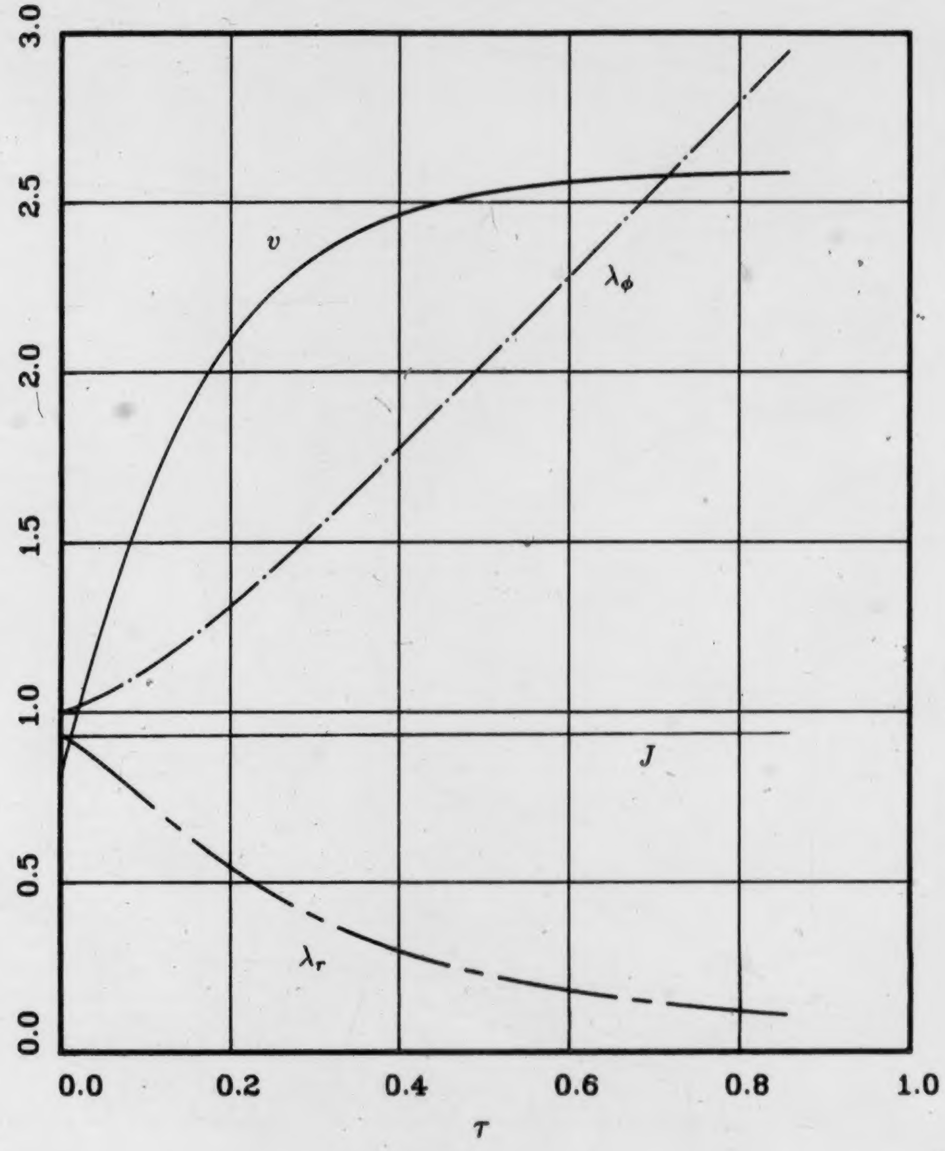

Figure 5.6: Spherical Cavity in an Unbounded Medium
Velocity, Stretch and Dilation at $R = R_i$
Modified Gaussian sef, $\nu = 0.495$
$p(\tau) = 10\,H(\tau)$

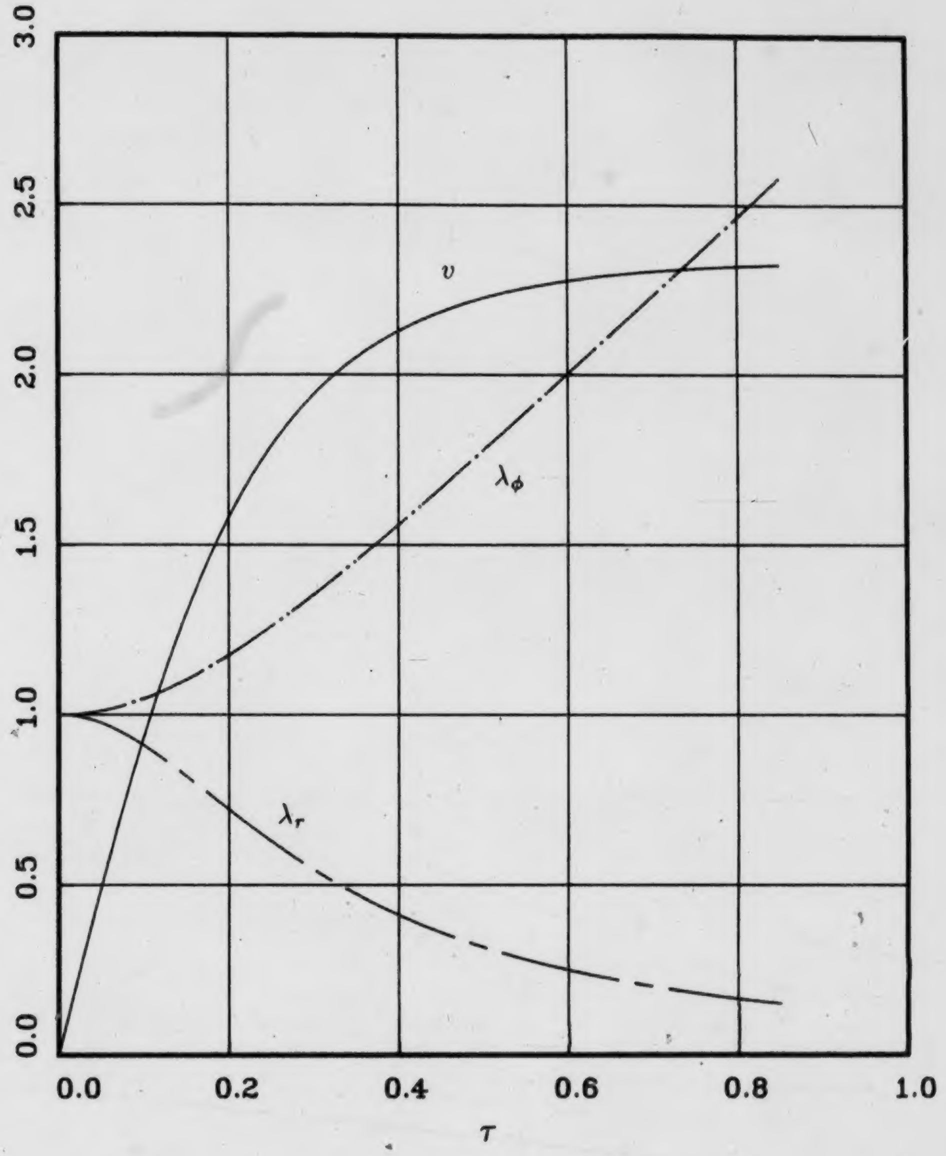

Figure 5.7: Spherical Cavity in an Unbounded Medium
Velocity and Stretch at $R = R_i$
neo-Hookean sef
$p(\tau) = 10\,H(\tau)$

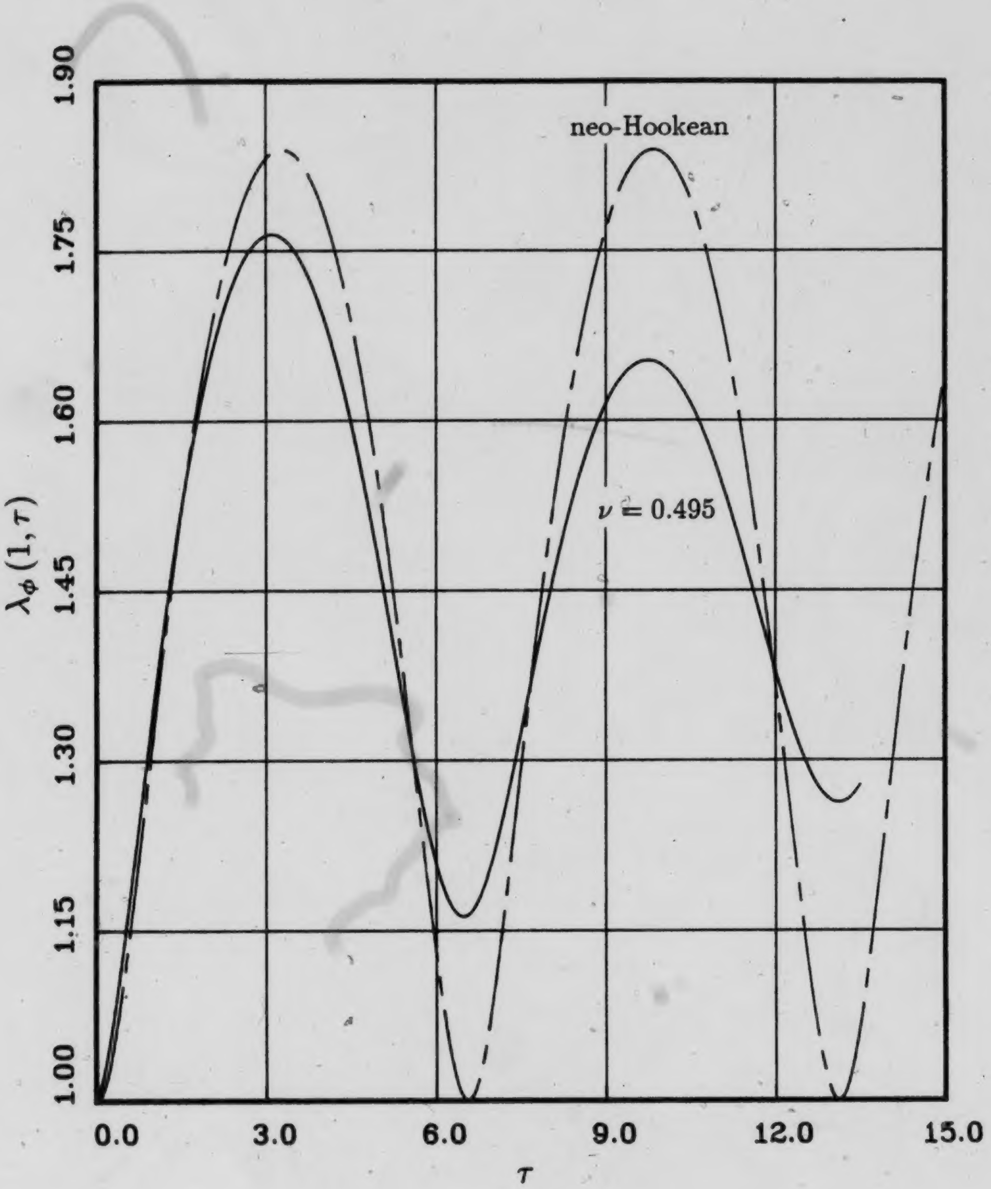

Figure 5.8: Spherical Cavity in an Unbounded Medium
Motion of the Cavity Wall
Modified Gaussian sef, $\nu = 0.495$ and neo-Hookean sef
$p(\tau) = H(\tau)$

		$\tau = 0.2$	$\tau = 0.4$	$\tau = 0.6$
From	$[\lambda_r]$	0.08589	0.03383	0.01825
Figures	$[P_r]$	3.20000	1.93333	1.43333
5.3-5.5	$[v]$	0.28667	0.17667	0.13500
Jump				
Relation	$[v]^2$	0.08218	0.03121	0.01823
Terms	$[P_r]\ [\lambda_r]$	0.08589	0.03383	0.01825

Table 5.1: Jump Discontinuities at Shock Fronts : Unbounded Medium

step function of pressure is applied with $q = 1$ and $\nu = 0.495$ for a modified Gaussian material. A longer time scale than that of figure 5.6 is used.

For the compressible material, the motion is a damped oscillation due to a dissipation of mechanical energy across the shock. The deformation is irreversible and there is a jump in entropy across the shock. There is no damping for the incompressible material provided the adiabatic approximation is adopted.

The constitutive relations used in the numerical solutions presented in this section, are based on isothermal stress-deformation formulations rather than more appropriate isentropic relations. Although this is an approximation, for the range of deformations considered, the error involved in using an isothermal stress-deformation rather than an isentropic stress-deformation relation is negligible. This is discussed in chapter 2.3. An example comparing deformation of a cylindrical tube using both an isothermal and an isentropic stress-deformation relation is shown in figure 2.5.

5.1.4 Sudden Application of Pressure : Spherical Shell

The numerical results of figure 5.9 are for the deformation of a spherical shell which is subjected to a Heaviside step function of pressure where $q = 1$, $\nu = 0.495$, and $R_o/R_i = 2$. A stress free boundary condition ($\sigma_r = 0$) is specified at $R = R_o = 2$. The figure shows the solutions for both a compressible material (as obtained using the hybrid scheme) and for an incompressible material (as obtained using a fourth-order Runge-Kutta scheme). The sawtooth form of the velocity is due to the reflection of a shock from the inner and outer shell surfaces.

The phase plane solution for a similar deformation of a spherical shell for which $q = 0.4$ and $q = 1.0$, is shown in figure 5.10. Solutions for deformation of both incompressible and compressible media are plotted. The solution for $q = 0.4$ is stable and the phase plane closes. The solution for $q = 1$ is unstable and the velocity increases monotonically until the shell bursts.

For a modified Gaussian material (2.24) with $\nu = 0.495$, the critical stability value of the magnitude of the suddenly applied pressure is near that of the incompressible material shown in figure 5.1 and is approximately $q_c = 0.7435$ when $R_o/R_i = 2$.

5.1.5 Sinusoidal Pulse : Unbounded Medium

Expansion of a spherical cavity in an unbounded medium, due to the application of a sinusoidal pulse, is shown in figure 5.11. The applied sinusoidal pulse is of magnitude $q = 10$ and duration $\tau_* = 0.1$ and the constitutive behaviour of the material is governed by the modified Gaussian sef (2.24) with $\nu = 0.495$.

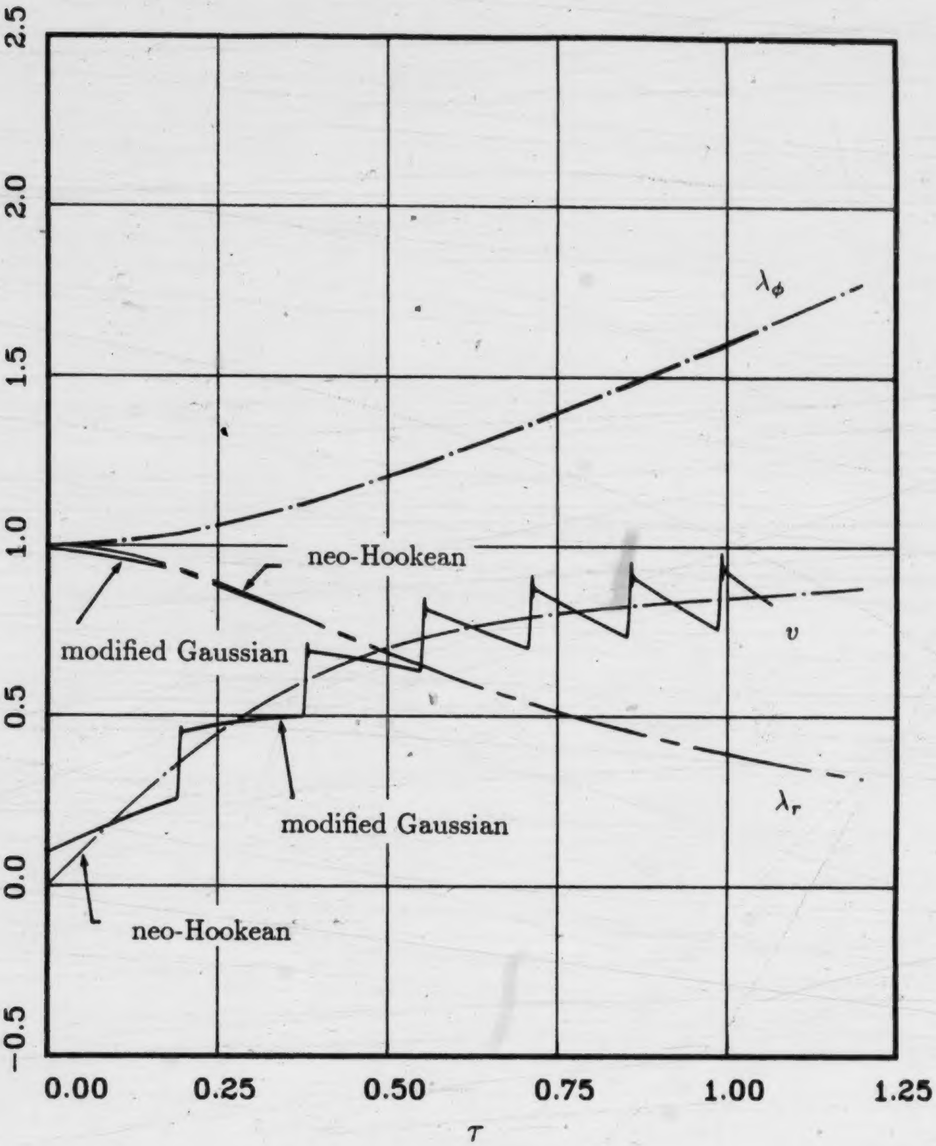

Figure 5.9: Spherical Shell, $R_o/R_i = 2$
Motion of the Inner Cavity Wall
Modified Gaussian sef, $\nu = 0.495$, and neo-Hookean sef
$p(\tau) = H(\tau)$

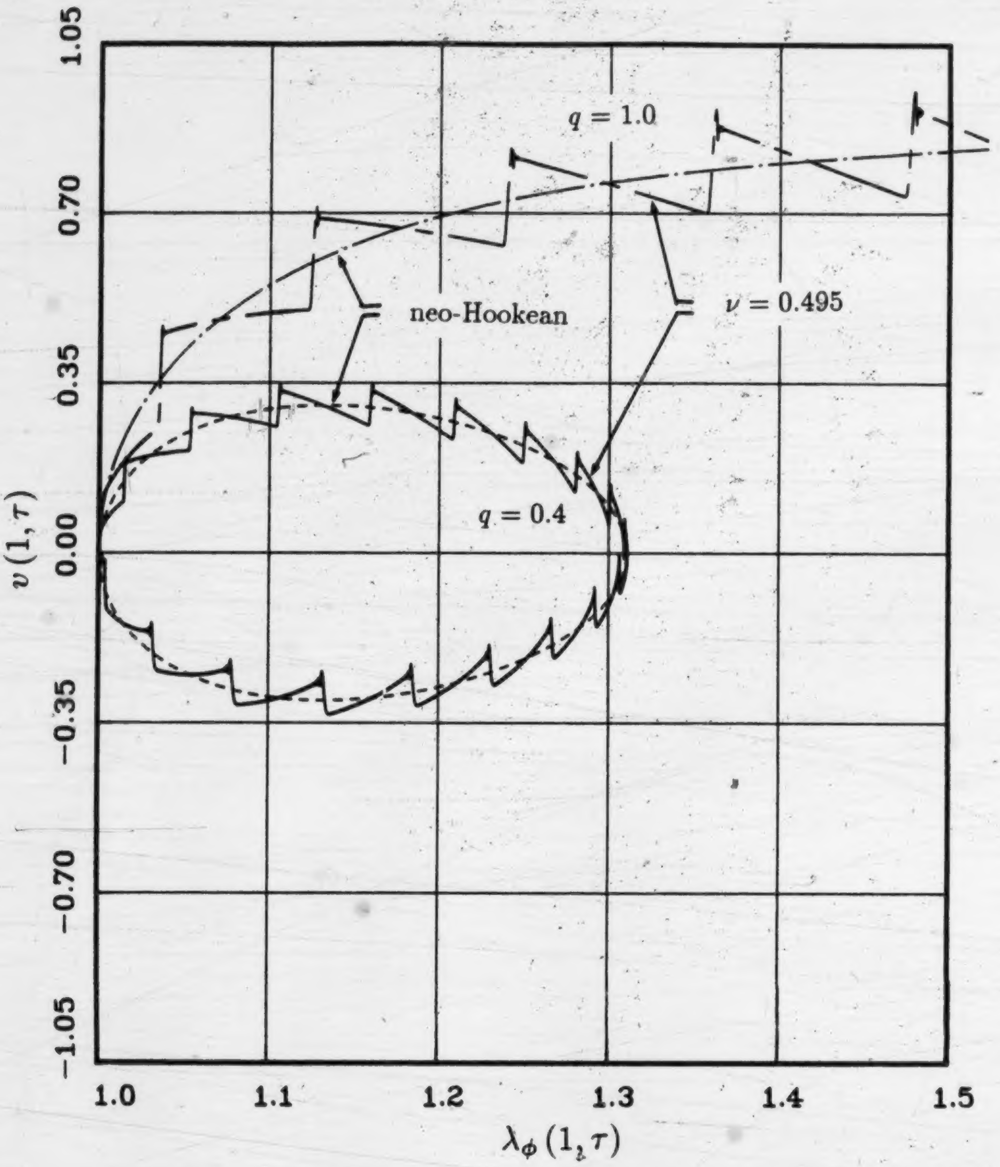

Figure 5.10: Phase Plane Solution for Spherical Shell, $R_o/R_i = 2$
Motion of the Inner Cavity Wall
Modified Gaussian sef, $\nu = 0.495$, and neo-Hookean sef
$p(\tau) = q\,H(\tau)$

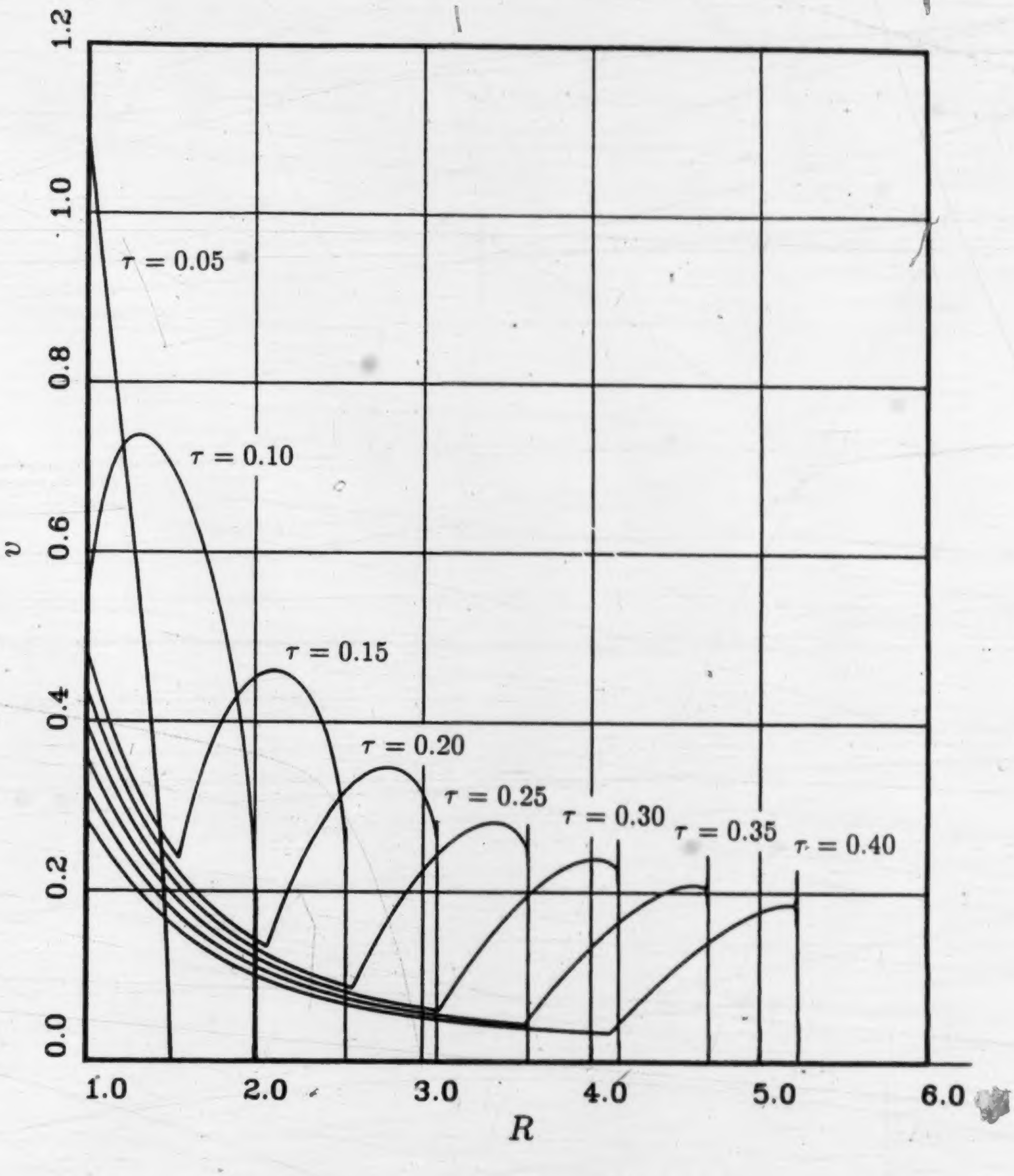

Figure 5.11: **Spherical Cavity in an Unbounded Medium**
Modified Gaussian sef, $\nu = 0.495$,
$p(\tau) = 10 \sin(\pi\tau/0.1)H(\tau)\, H(0.1 - \tau)$

The figure shows the propagation of the initial disturbance and the eventual breaking of the wave to form a shock. The stretch λ_ϕ, is continuous since no separation of the material occurs. The jump conditions for spherically symmetric deformation (3.45) are satisfied to an acceptable degree.

The wave breaks at an earlier time if the magnitude of the pulse is increased or if the Poisson ratio is decreased. The numerical scheme is not sensitive enough to indicate the exact position at which the wave breaks.

5.1.6 Comparison of Gaussian Strain Energy Functions

Numerical solutions for expansion of a spherical cavity in an unbounded medium were obtained for both the modified Gaussian sef (2.19), where $g(J)$ is based on experimental data for hydrostatic compression of solid rubber materials (Ogden, 1982), and for the Gaussian sef (2.21). For the range of deformations considered, the difference was found to be negligible for $\nu = 0.495$. However, for $\nu = 0.463$, which is a minimal value for solid rubber (Beatty and Stalnaker, 1986), the difference could be significant.

For example, figure 5.12 shows the solution for spherically symmetric deformation of an unbounded medium with $\nu = 0.463$ and $q = 1$ using both the modified Gaussian sef (2.19) and the Gaussian sef (2.21). The difference between the two strain energy functions is most significant for the velocity and radial stretch components at $\tau = 0$. A maximum difference of approximately 15% is evident in this case. The relation between the Gaussian and modified Gaussian strain energy functions is evident from the Taylor series expansion, discussed in section 2.2.2, and given by (2.20). As $J \rightarrow 1$, the difference between these strain energy functions decreases. For isochoric deformation, the Gaussian and modified Gaussian strain energy functions are the

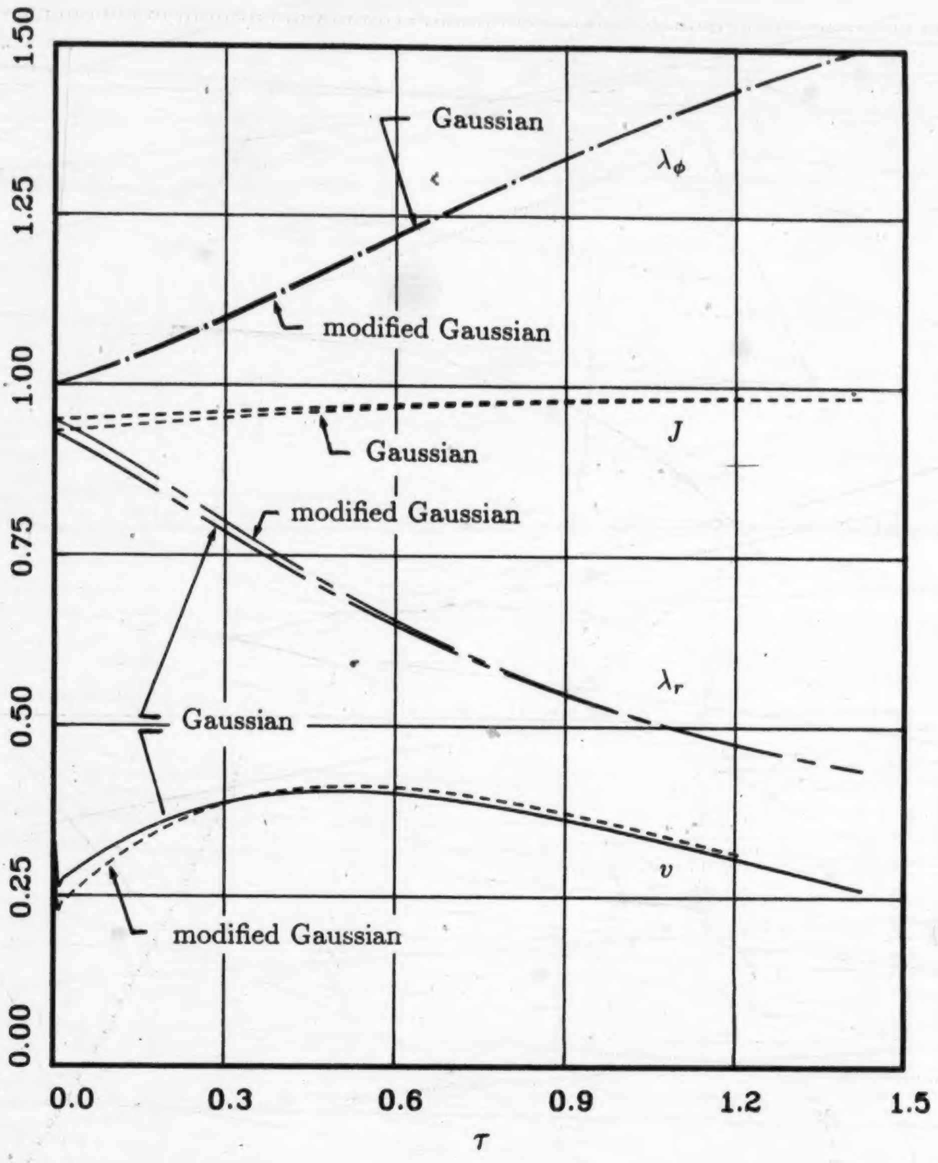

Figure 5.12: Spherical Cavity in an Unbounded Medium
Motion of the Inner Cavity Wall
Comparison of Gaussian Strain Energy Functions, $\nu = 0.463$
$p(\tau) = H(\tau)$

same; both reduce to the neo-Hookean sef.

5.1.7 Solutions for Blatz Strain Energy Function

The Blatz strain energy function, given by (2.32), describes the constitutive behaviour of a sponge rubber. Although a numerical solution for dynamic deformation is presented in the following figure, the use of the static properties of the sponge rubber for dynamic deformation may not be warranted. Thus, the solution presented here may not accurately represent the dynamic behaviour of a sponge material and should be interpreted with caution. This limitation of the Blatz sef is further discussed in chapter 2.2.4.

Figure 5.13 shows the radial and tangential stretches at the surfaces of a thick-walled spherical shell. A sudden application of pressure of magnitude $q = 0.25$ is applied at the inner surface and the outer surface is stress free. The tangential stretch at $R = R_i$ is equivalent to the radial displacement of the inner surface when R_i is taken to be 1.

Discontinuity in the slopes of the stretches is due to the reflection of the initial disturbance from the inner and outer walls of the spherical shell.

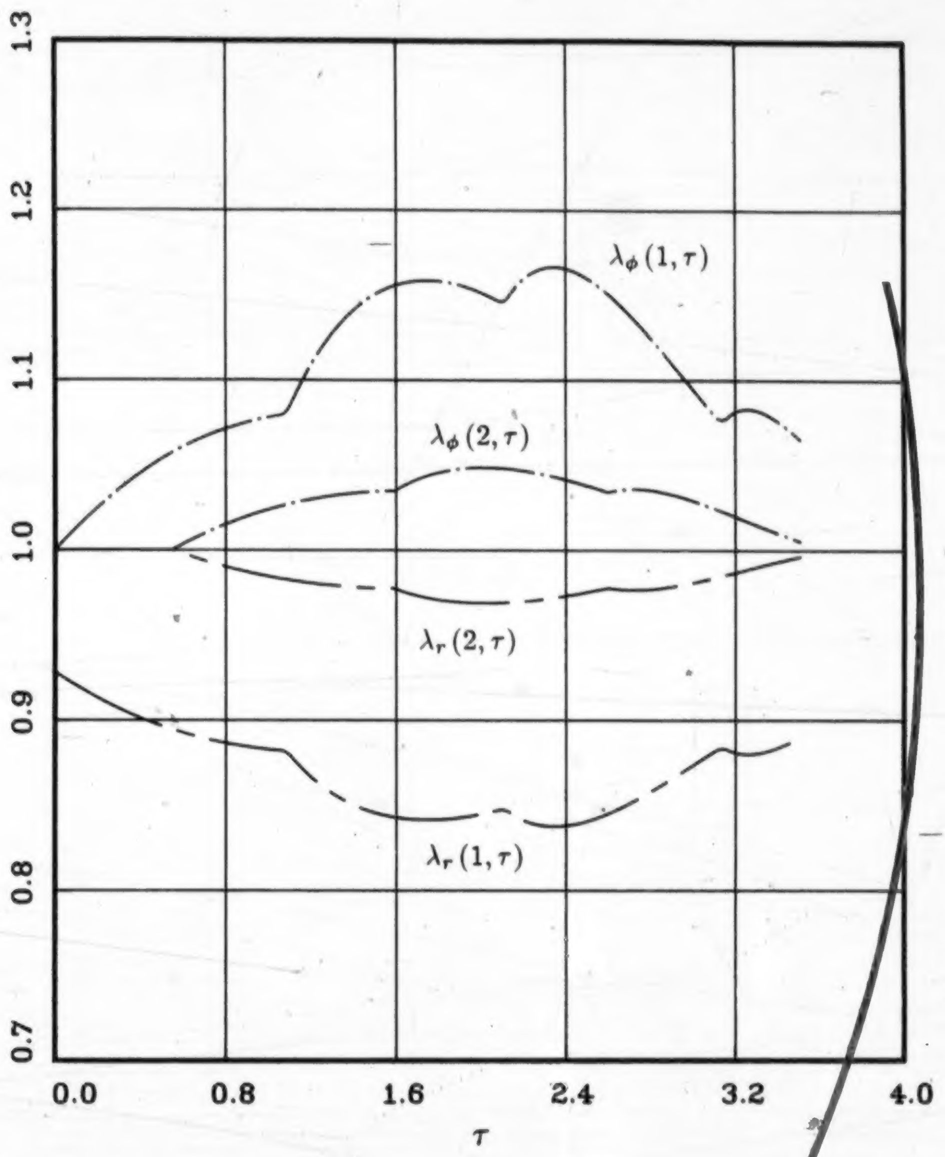

Figure 5.13: Spherical Shell, $R_o/R_i = 2$
Motion of the Inner Cavity Wall
Blatz sef
$p(\tau) = 0.25\,H(\tau)$

5.2 Cylindrically Symmetric Deformation

Numerical solutions presented in this section are for cylindrically symmetric problems in which the plane strain assumption is valid. As is the case for spherically symmetric deformation, the boundary condition due to the application of a spatially uniform pressure $p(\tau)$, is given in terms of either a Heaviside step function (5.1) or a sinusoidal pulse (5.2). The boundary surface at $R = R_o$ is assumed to be stress-free although other boundary conditions can also be implemented.

Numerical results for deformation of cylindrical tubes are presented for the radius ratio $R_o/R_i = 2$. It is assumed that this ratio is sufficiently large that the cylindrical tube remains symmetric throughout the deformation. Solutions are presented for both the Gaussian sef (2.27) and the modified Gaussian sef (3.60) with $\nu = 0.495$. Numerical solutions for higher Poisson ratios can be obtained, subject to the limitations of the hybrid numerical scheme as discussed in section 4.3.6.

Numerical solutions for the incompressible neo-Hookean sef (2.13) are also included.

5.2.1 Incompressible Cylindrical Tube

Governing equations for the finite expansion of an incompressible cylindrical tube are presented in section 3.2.2. Figure 5.14 shows the phase plane solution for the motion of the inner cavity wall where $R_o/R_i = 2$. The phase plane closes provided that the magnitude of the suddenly applied pressure is less than the critical value which for this radius ratio, is approximately $q_c = 0.685$. When q is less than the critical value, the motion of the cavity wall is periodic. When $q > q_c$, the motion is unstable and the stretch increases monotonically until the tube bursts.

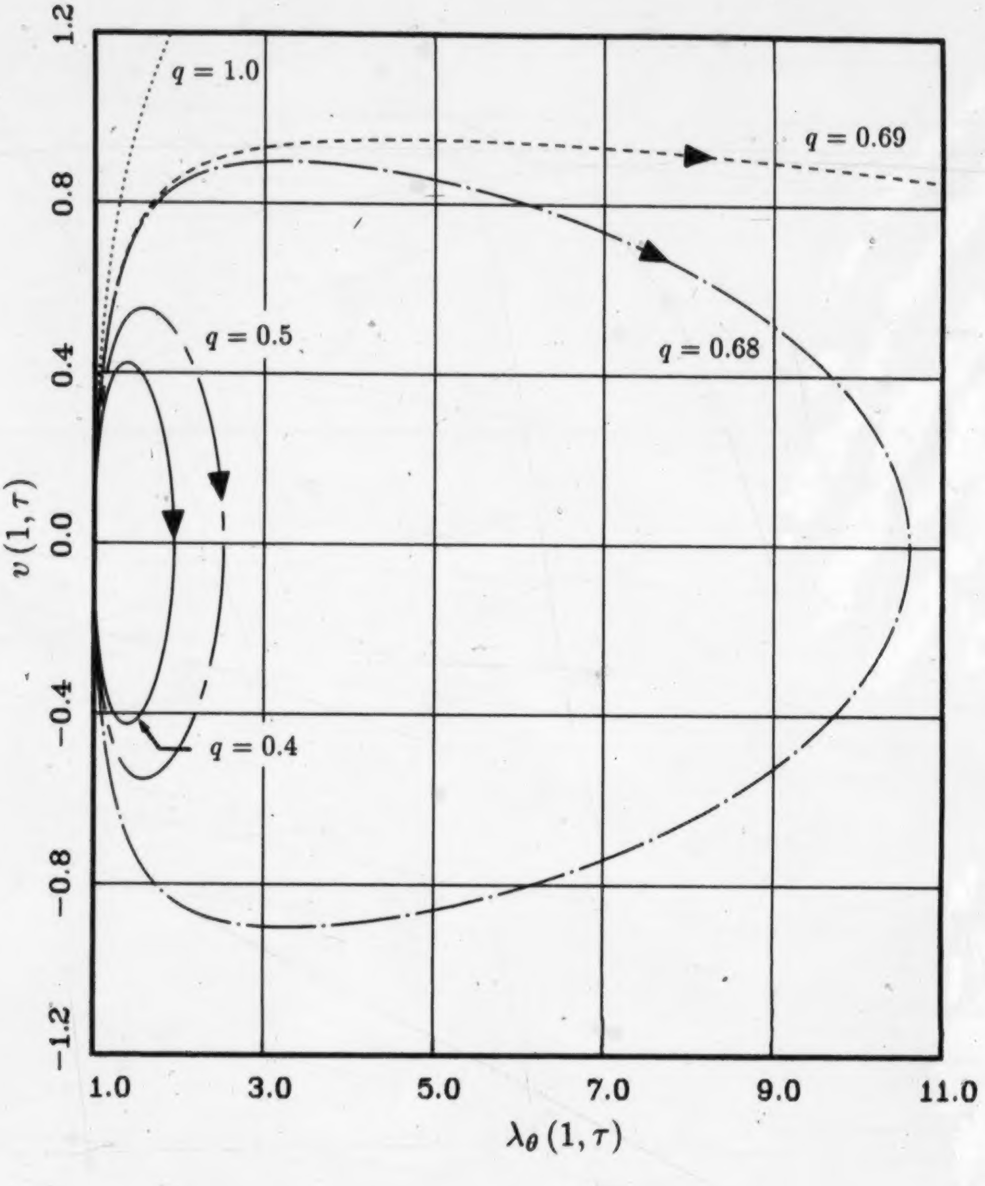

Figure 5.14: **Phase Plane Solution for Cylindrical Tube Motion of the Inner Cavity Wall neo-Hookean sef, $R_o/R_i = 2$ $p(\tau) = q\,H(\tau)$**

5.2.2 Sudden Application of Pressure

The phase plane solution for expansion of a cylindrical tube for which $R_o/R_i = 2$ is shown in figure 5.15 . The solution for the compressible material is obtained using the hybrid scheme with the modified Gaussian sef (3.60) and $\nu = 0.495$. The solution for the incompressible material is obtained using the neo-Hookean sef (2.13).

A sudden application of pressure of magnitude $q = 0.4$ is applied at the inner wall. This value of q is less than the critical value and the deformation is stable; the phase plane closes. For a compressible material with sef given by (3.60) and $\nu = 0.495$, the critical value of the magnitude of the suddenly applied pressure q_c, is near that of the incompressible tube shown in figure 5.14 and is approximately $q_c = 0.685$ when $R_o/R_i = 2$. The sawtooth form of the velocity is due to the reflection of a shock from the inner and outer surfaces of the tube.

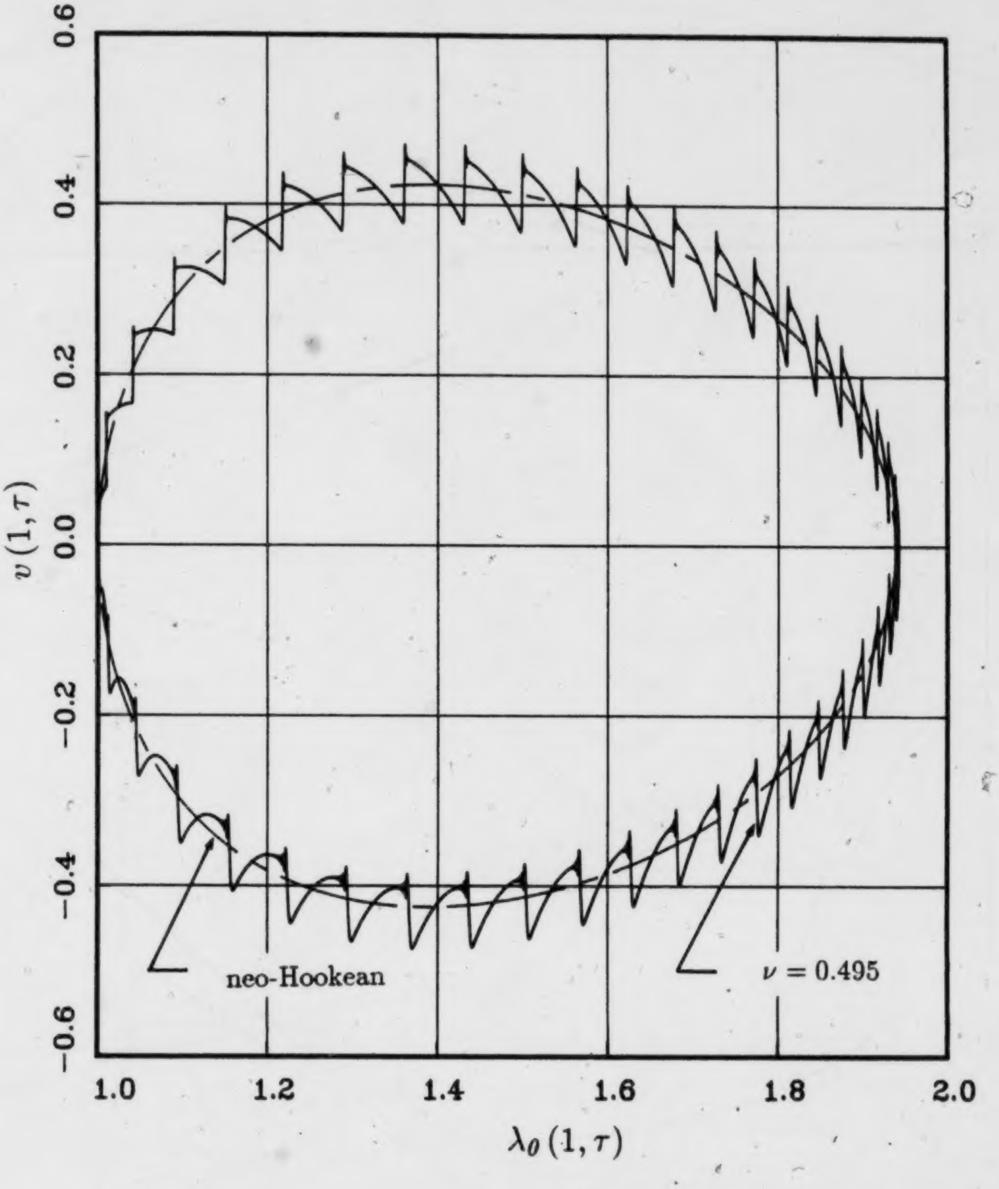

Figure 5.15: Phase Plane Solution for Cylindrical Tube, $R_o/R_i = 2$
Motion of the Inner Cavity Wall
Modified Gaussian sef, $\nu = 0.495$ and neo-Hookean sef
$p(\tau) = 0.4\,H(\tau)$

5.3 Plane Stress of Uniformly Prestressed Sheets

Numerical solutions presented in this section are for generalized plane stress deformation of uniformly prestressed sheets. A circular hole of nondimensional radius $R = 1$, (referred to the reference state) is suddenly punched in the sheet. This results in radial propagation of unloading waves. The initial stretch is given by (3.84).

Prestressed sheets of finite outer radius and prestressed unbounded sheets are both considered. For the finite sheets, the outer boundary at $R = R_o$ is rigidly fixed so that the boundary condition is $v(R_o, \tau) = 0$.

Since the hole is not punched instantaneously, solutions are obtained for a linear decrease of the nominal stress P_r at $R = 1$, from the initial value to zero, which occurs during a time τ_*. For the results presented here, $\tau_* = 0.05$, although the difference in the numerical results for this value and instantaneous plugging are negligible. The magnitude of τ_* is discussed by Rinehart and Pearson (1954) and by Mioduchowski et al. (1978).

Numerical results are obtained using the hybrid finite difference-characteristic scheme which is discussed in section 4.3. An incompressible material, given by the Mooney-Rivlin sef (2.14) is considered, with various α parameters. As discussed in section 3.3.1., only minor modifications are required to consider plane stress deformation of a compressible material.

5.3.1 Comparison with Method of Characteristics

Plane stress unloading waves in a prestressed sheet resulting from a suddenly punched hole, have been previously considered by Mioduchowski et al. (1978). These authors use the method of characteristics to obtain numerical solutions. The hybrid scheme numerical solutions presented in this section are compared with these results.

Figure 5.16 shows the stretch components and velocity at the edge of the suddenly-punched circular hole ($R = 1$) as a function of nondimensional time. A linear transition from the prestressed to the stress-free state occurs at the edge of the hole during the nondimensional time $\tau_* = 0.05$, as is given by (3.86). The constitutive behaviour of the material is described using the Mooney-Rivlin sef (2.14) with $\alpha = 0.75$.

The continuous curve shows the solution obtained by the hybrid scheme and the discrete data points show the method of characteristics solution of Mioduchowski, et al. (1978). There is good agreement between these two independent solutions for this nonlinear finite deformation problem.

5.3.2 Prestressed Finite Sheets

Consider the generalized plane stress unloading waves in a suddenly-punched, uniformly prestressed sheet. The sheet is of finite extent and the outer boundary at $R = R_o = 6$ is rigidly fixed so that $v(R_o, \tau) = 0$.

Figures 5.17-5.21 show the hybrid scheme numerical solution using a Mooney-Rivlin sef (2.14) with $\alpha = 0.6$ and $\tau_* = 0.05$ as given in section 3.3.2. These figures show the velocity and nominal stress components as a function of radius, at times $\tau = 2, 4, 6, 14$ and 16. The nominal stresses are obtained from the principal stretch components using (3.90) and are scaled by the magnitude of the initial stress $(P_r)_o$ using

$$\begin{aligned}\overline{P_\theta} &= \frac{P_\theta}{(P_r)_o}\\ \overline{P_r} &= \frac{P_r}{(P_r)_o} \qquad (5.6)\end{aligned}$$

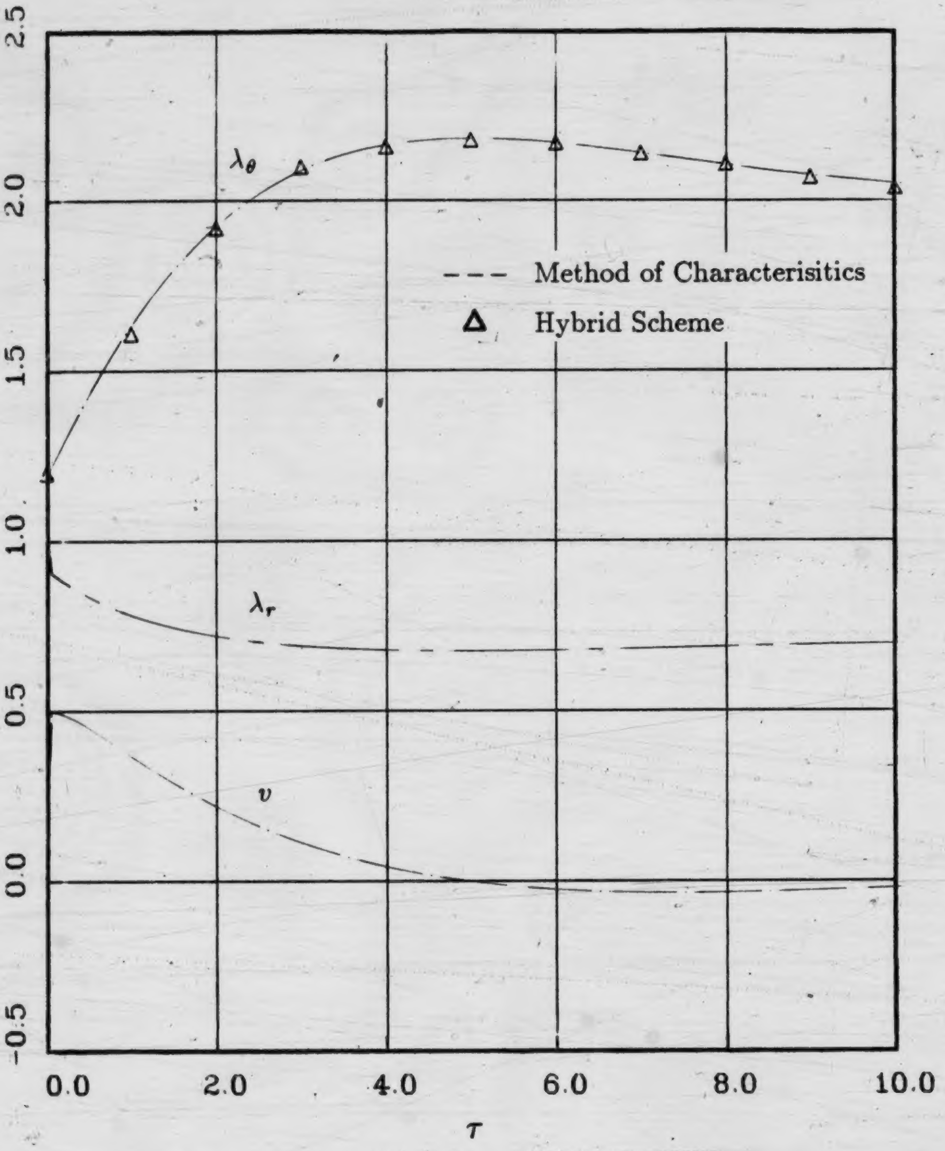

Figure 5.16: Plane Stress Deformation in an Unbounded Medium
Comparison of Hybrid Scheme with Method of Characteristics
Mooney-Rivlin sef, $\alpha = 0.75$, $\lambda_o = 1.2$, $\tau_* = 0.05$

where $(P_r)_o$ corresponds to the uniform initial stretch and is given by (3.91). Henceforth, these scaled quantities will be used although the overbar notation will be omitted.

The solution of figure 5.17 shows the propagation of the resulting shock at time $\tau = 2$, before reflection from the rigid boundary. The arrows indicate the direction of propagation. The material is in biaxial tension (positive P_r and P_θ) throughout the radius. The magnitude of the constant prestress ahead of the shock is 1 as given by the scaling relations (5.6).

Figure 5.18 shows the solution at time $\tau = 4$, after reflection from the rigid boundary. The result of the reflection is a decrease in the radial and tangential stress although both components of stress are still tensile at all radii. A shock is propagating radially inward.

The solution of figure 5.19 is at time $\tau = 6$, after reflection from the free edge of the circular hole. The velocity and stress are no longer discontinuous, although the radial stress is still positive and both components of stress are still tensile.

Figure 5.20 shows the solution at time $\tau = 14$ after several reflections from both the rigid outer boundary and the free edge of the hole. At this particular time, the velocity and stress are not discontinuous and the disturbance is propagating radially outward.

The solution of figure 5.21 is at time $\tau = 16$, after the next reflection from the rigid outer boundary. It is evident that a shock has again formed and is propagating radially inward.

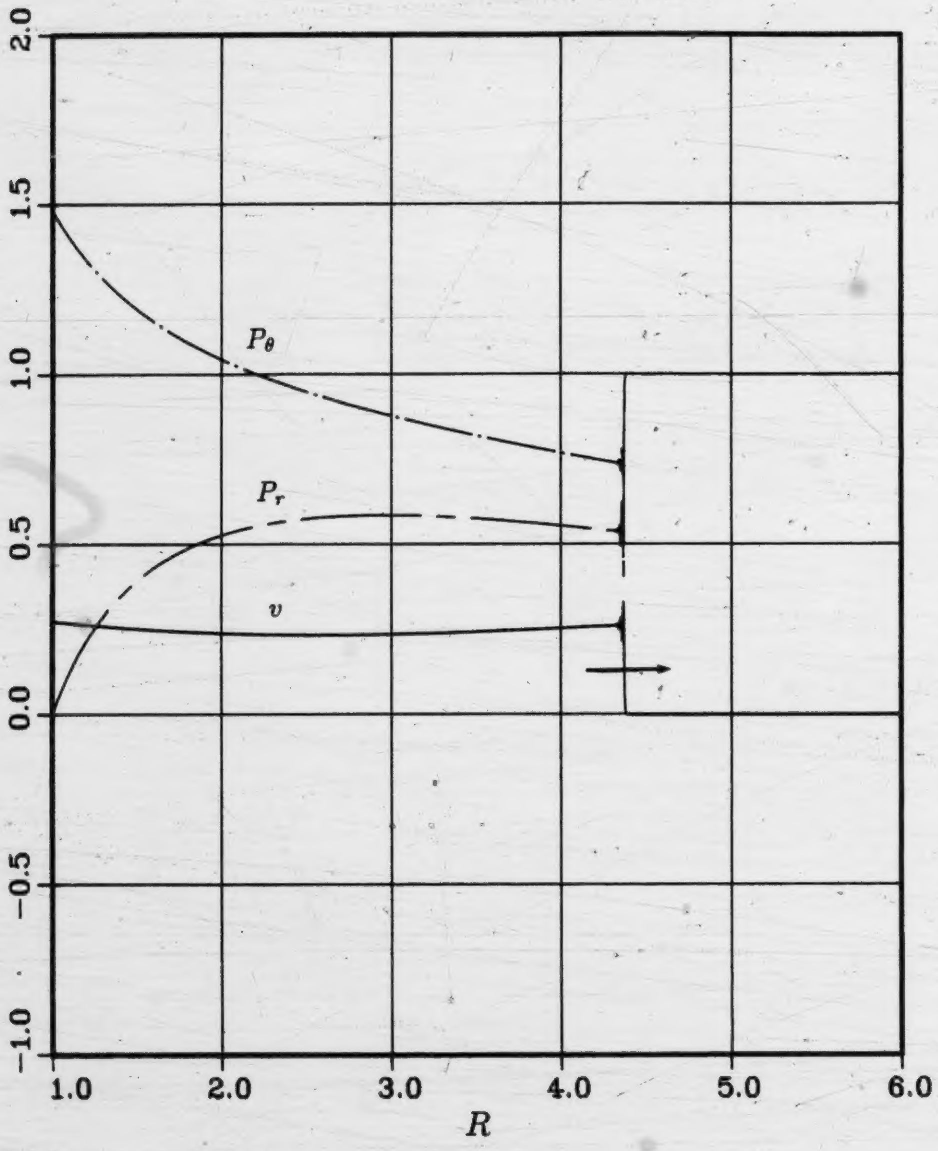

Figure 5.17: Plane Stress Deformation, $R_o/R_i = 6$, $v(6,\tau) = 0$
Solution Before Reflection, $\tau = 2$
Mooney-Rivlin sef, $\alpha = 0.6$, $\lambda_o = 1.2$, $\tau_* = 0.05$

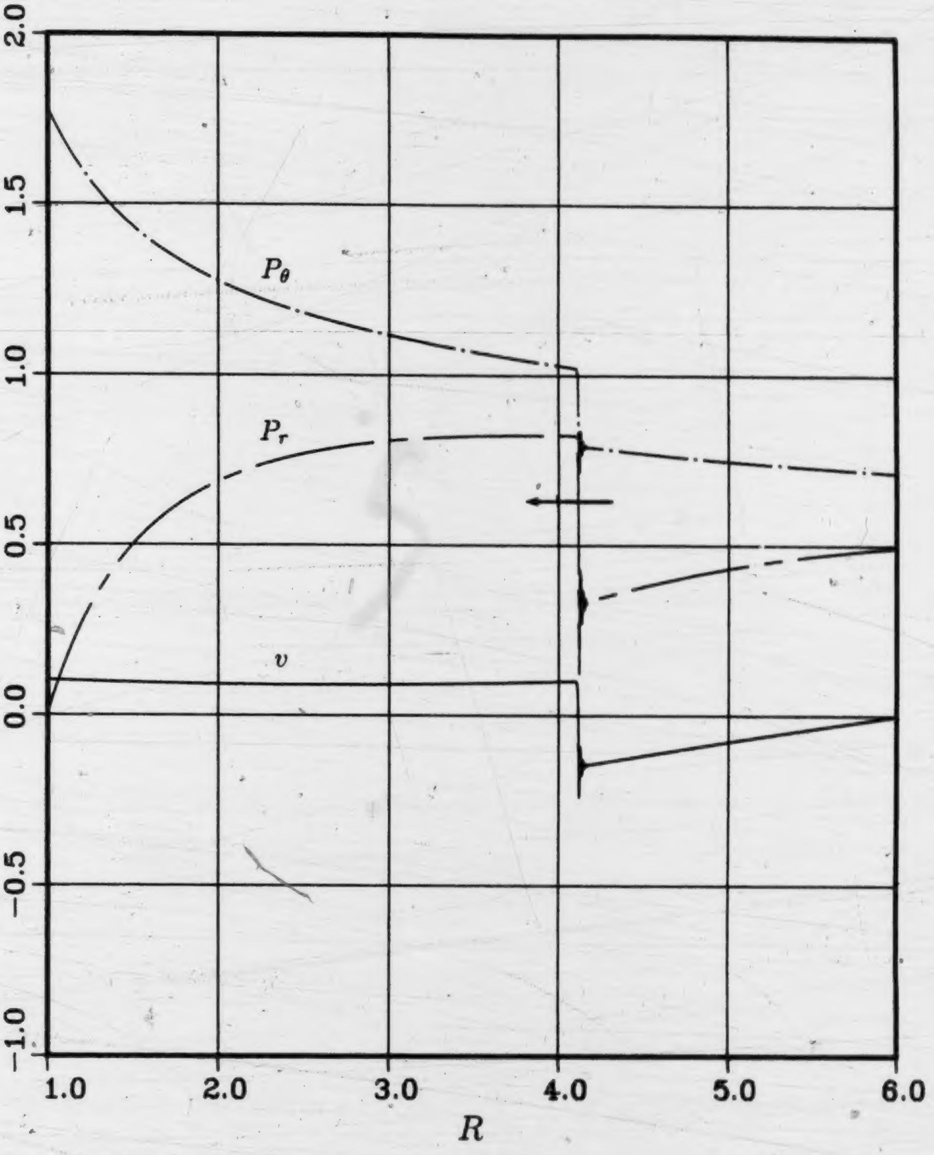

Figure 5.18: Plane Stress Deformation, $R_o/R_i = 6$, $v(6,\tau) = 0$
Solution After Reflection From Rigid Wall at $R = 6$, $\tau = 4$
Mooney-Rivlin sef, $\alpha = 0.6$, $\lambda_o = 1.2$, $\tau_* = 0.05$

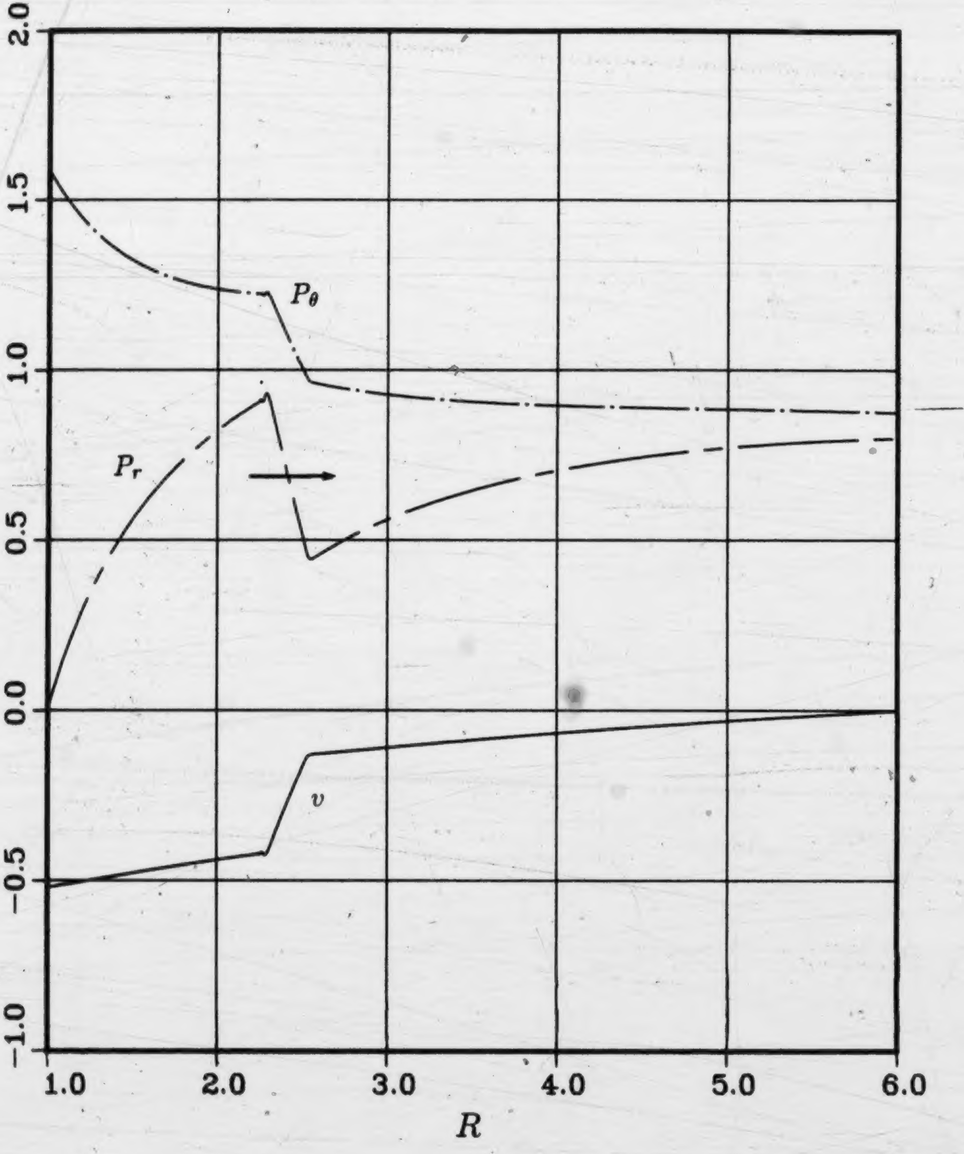

Figure 5.19: Plane Stress Deformation, $R_o/R_i = 6$, $v(6,\tau) = 0$
Solution After Reflection From Edge of Hole, $\tau = 6$
Mooney-Rivlin sef, $\alpha = 0.6$, $\lambda_o = 1.2$, $\tau_* = 0.05$

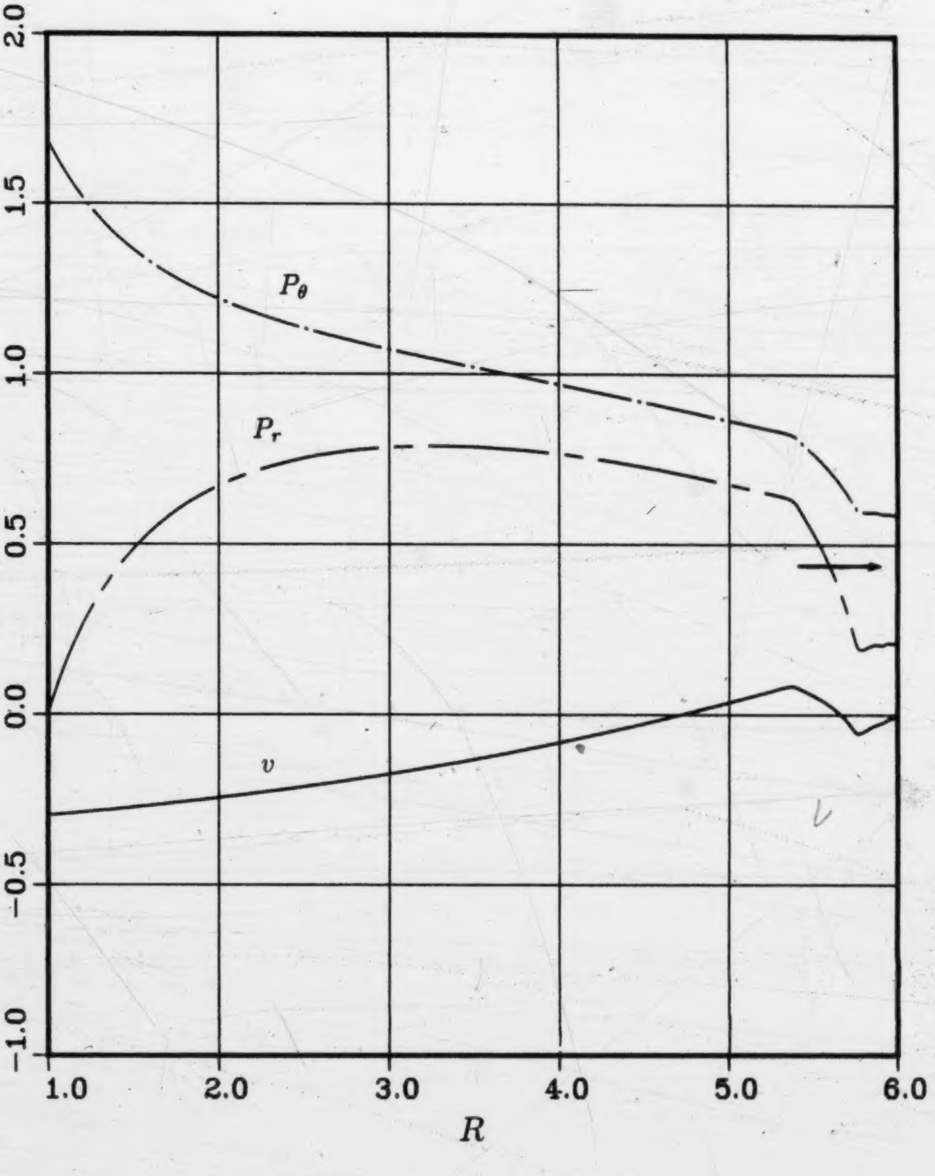

Figure 5.20: Plane Stress Deformation, $R_o/R_i = 6$, $v(6,\tau) = 0$
Solution After Several Reflections, $\tau = 14.0$
Mooney-Rivlin sef, $\alpha = 0.6$, $\lambda_o = 1.2$, $\tau_* = 0.05$

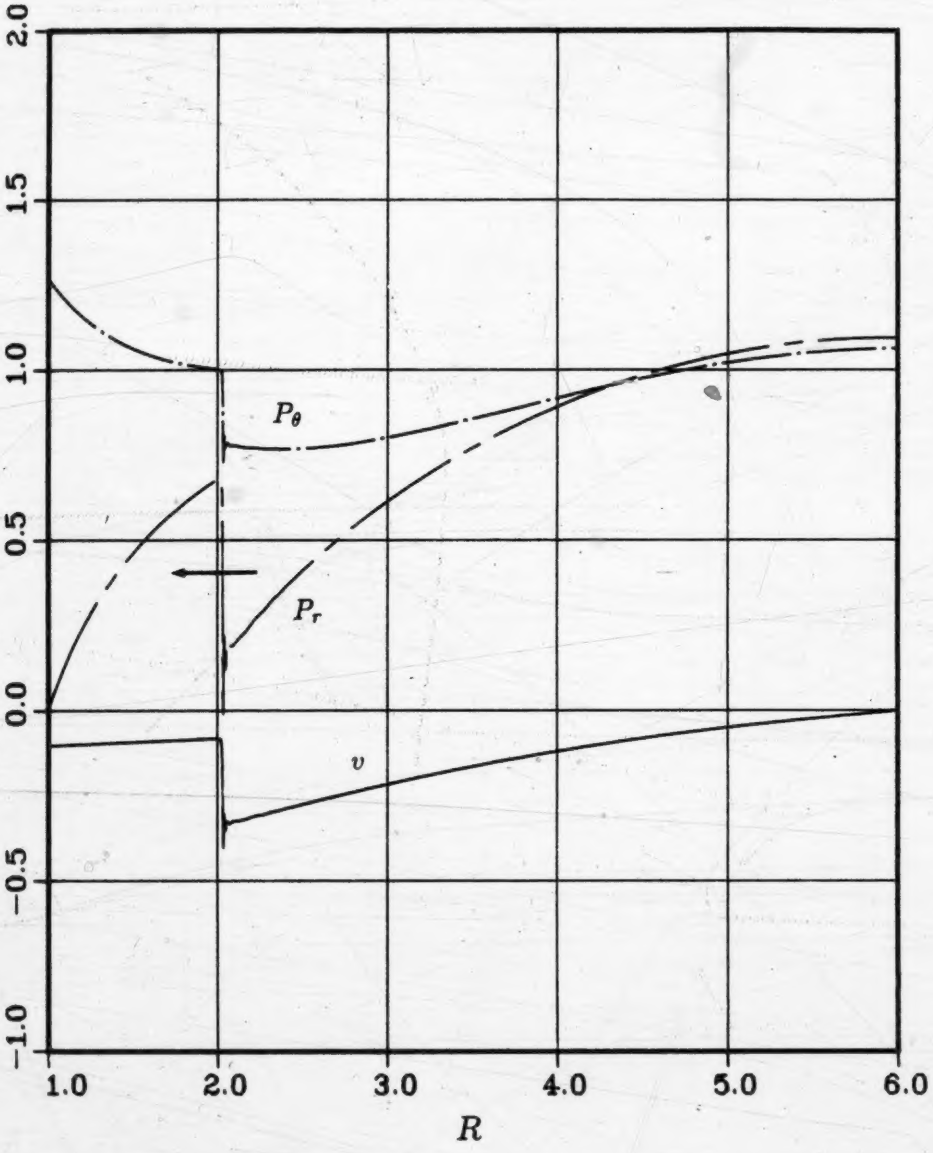

Figure 5.21: Plane Stress Deformation, $R_o/R_i = 6$, $v(6,\tau) = 0$
Formation of a Shock After Several Reflections, $\tau = 16.0$
Mooney-Rivlin sef, $\alpha = 0.6$, $\lambda_o = 1.2$, $\tau_* = 0.05$

5.3.3 Elastic Stability of Prestressed Finite Sheets

An important consideration for the validity of the numerical solutions for plane stress of a thin sheet as presented in this thesis, is that buckling or rippling of the sheet does not occur. This type of elastic instability violates the principal assumptions on which the governing equations are based. Numerical solutions for which a compressive stress exists, are questionable since it is unlikely that a thin rubberlike sheet can sustain a significant radial compressive stress without buckling.

The solutions shown in 5.22 and 5.23 are for a configuration which is identical to the previous problem with the exception that the rigidly constrained outer radius is at $R_o = 2$ rather than $R_o = 6$. The solution at time $\tau = 0.4$, before reflection from the rigid boundary, is shown in figure 5.22. Both the radial and tangential stresses are positive.

After reflection, at $\tau = 0.8$, the radial stress is negative as shown in figure 5.23. This radial compressive stress may cause the sheet to buckle; the solution shown in figure 5.23 may not be valid.

For plane stress deformation of prestressed sheets which are unloaded by a suddenly-punched circular hole, the existence of a compressive radial stress (after reflection) is dependent on the magnitude of the initial stretch and the radial extent of the sheet. If the outer radius is sufficiently large, the decrease in radial stress which occurs after reflection from the outer radius, will not result in a negative (compressive) stress. As a specific example, for a Mooney- Rivlin material with $\alpha = 0.6$, $\lambda = 1.2$ and $R_i = 1$, the outer radius must be larger than approximately 5 to avoid compressive radial stresses and thus potential buckling of the sheet.

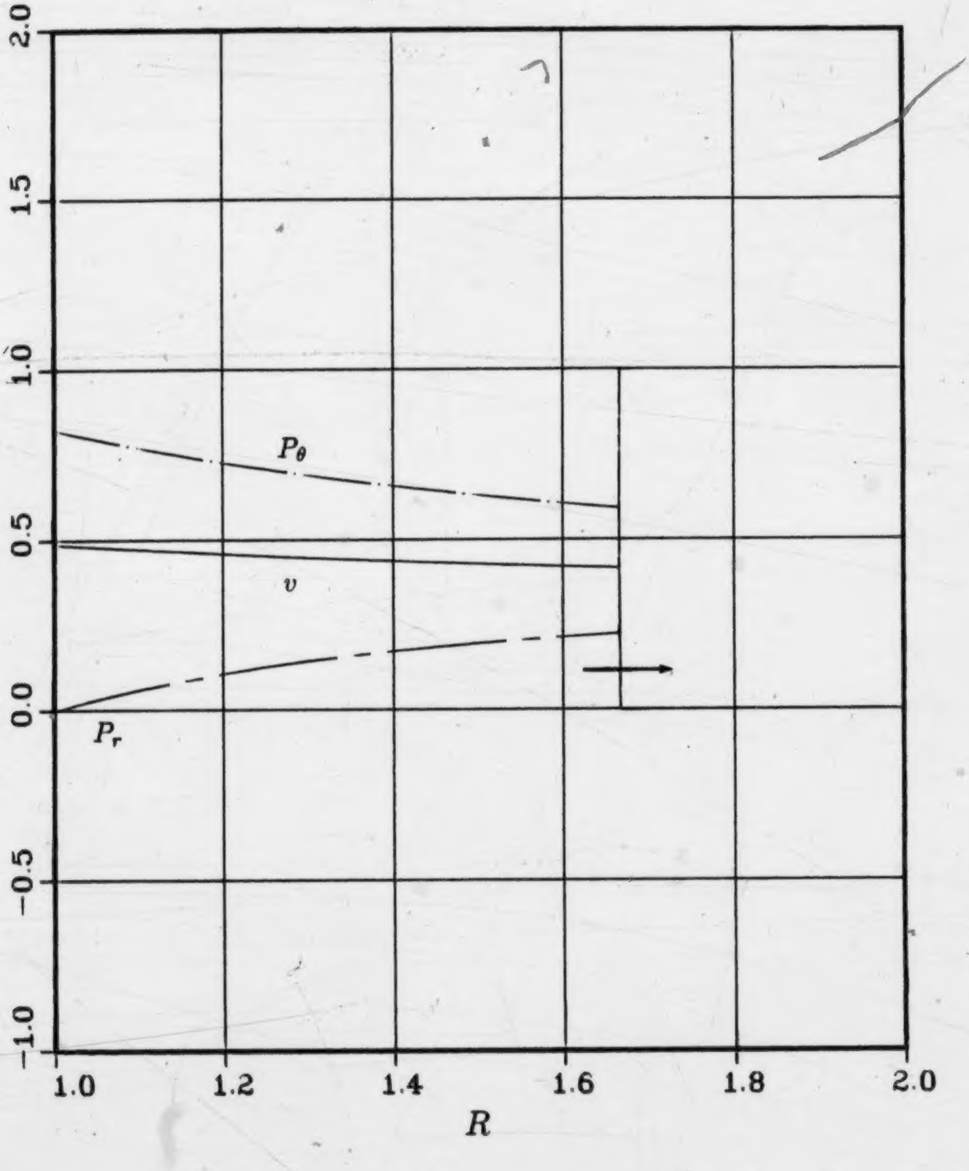

Figure 5.22: Plane Stress Deformation, $R_o/R_i = 2$, $v(2,\tau) = 0$
Solution Before Reflection, $\tau = 0.4$
Mooney-Rivlin sef, $\alpha = 0.6$, $\lambda_o = 1.2$, $\tau_* = 0.05$

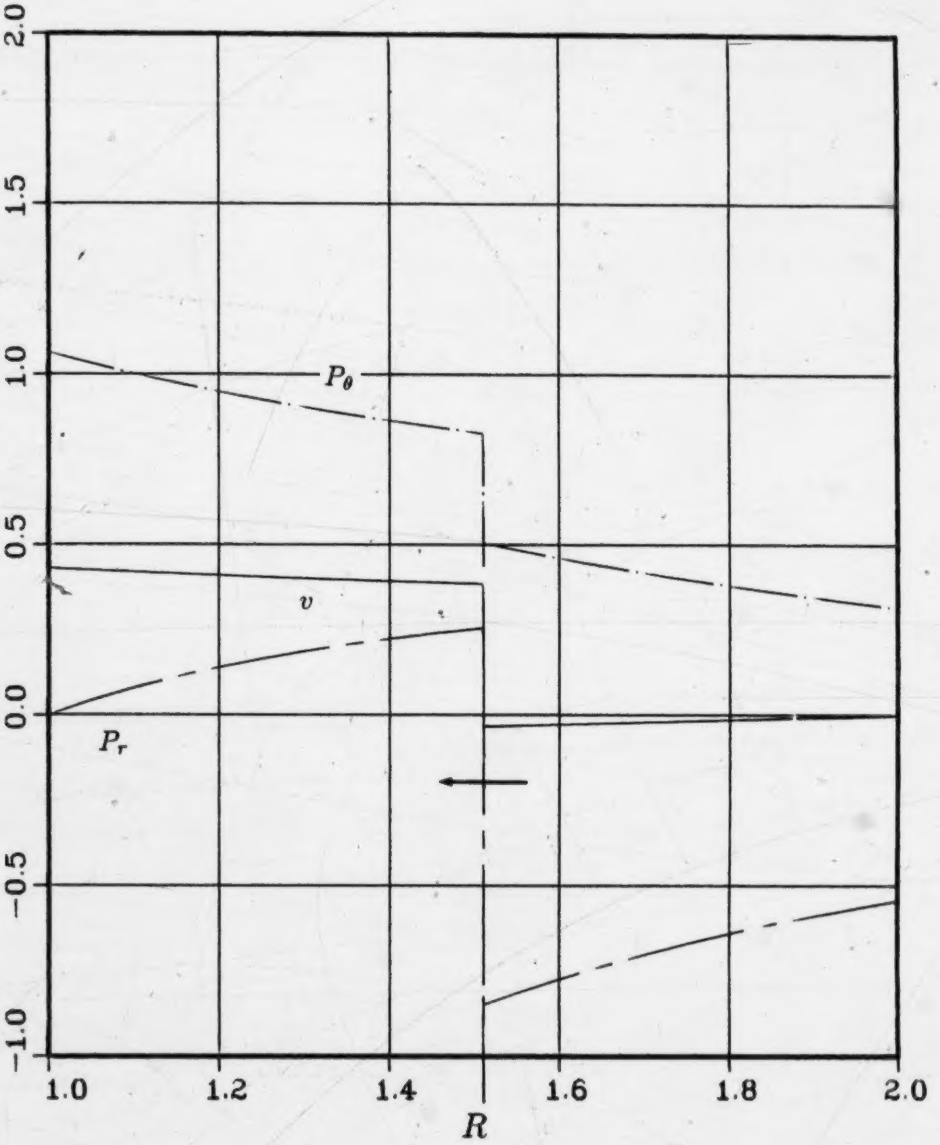

Figure 5.23: Plane Stress Deformation, $R_o/R_i = 2$, $v(2,\tau) = 0$
Solution After Reflection From Rigid Wall at $R = 2$, $\tau = 0.8$
Mooney-Rivlin sef, $\alpha = 0.6$, $\lambda_o = 1.2$, $\tau_* = 0.05$

5.4 Concentric Cylinders

The numerical solutions presented in this section are for plane strain expansion of two concentric cylinders which are subjected to a sudden application of pressure of magnitude q at the inner radius of the inner cylinder. Both cylinders are initially unstressed and it is assumed that they remain in contact during the deformation. The constitutive relations of both cylinders are obtained from the modified Gaussian sef given by (3.60). The notation of chapter 3.4 is adopted here; subscript 1 refers to the inner cylinder, subscript 2 refers to the outer cylinder and subscript $*$ refers to the interface.

Numerical solutions for two configurations are presented. The first of these is an extreme case for which the ratios of shear modulii and densities of the inner and outer cylinder have been chosen to illustrate the effects of significant changes in material properties. The second solution is for a more realistic choice of material properties. If the material properties of both cylinders are chosen to be the same, the solution reduces to the homogeneous case discussed in section 5.2.

Figures 5.24-5.26 show v, P_r, and λ_r respectively for the first configuration for which $\nu_1 = 0.48$, $\nu_2 = 0.495$, $\zeta = \rho_{02}/\rho_{01} = 2$, $\psi = \mu_2/\mu_1 = 7$, $R_i = 1$, $R_* = 1.25$, $R_o = 1.5$ and $q = 1$.[3] Arrows indicate the direction of propagation.

At $\tau = 0.025$ the disturbance is propagating outward and is still entirely within the inner cylinder. At $\tau = 0.05$ a reflected component is propagating inward and a transmitted component is propagating outward.

As is evident, the solutions satisfy continuity of v, λ_θ, and σ_r at the interface. When the density of the inner and outer cylinder are different, as they are for this

---

[3] Material properties are defined for infinitesimal deformation from the reference configuration, taken to be the undeformed state.

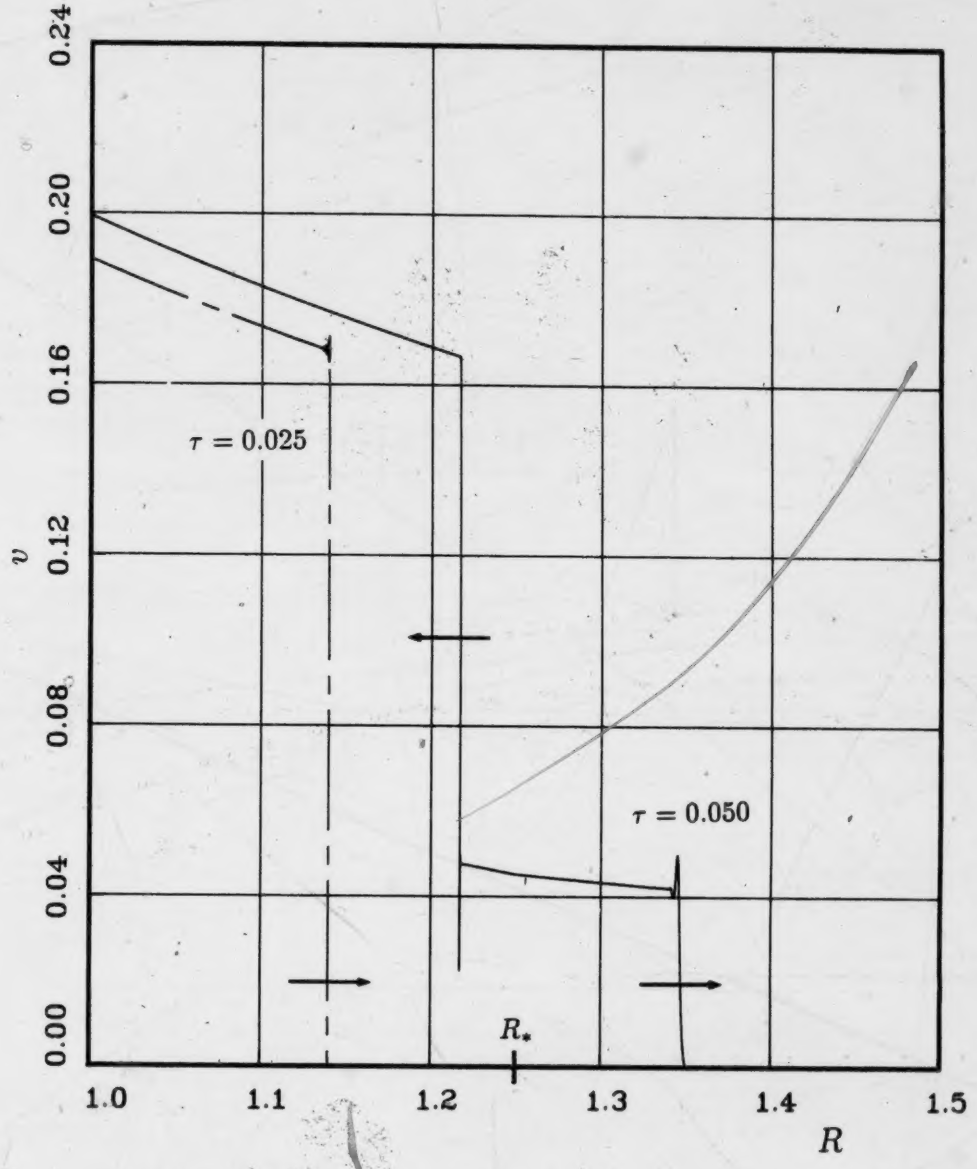

Figure 5.24: Concentric Cylinders, $\nu_1 = 0.48$, $\nu_2 = 0.495$, $\zeta = \rho_{02}/\rho_{01} = 2$, $\psi = \mu_2/\mu_1 = 7$, $R_i = 1$, $R_* = 1.25$, $R_o = 1.5$, $q = 1$.
Velocity at $\tau = 0.025$ and $\tau = 0.05$
Modified Gaussian sef

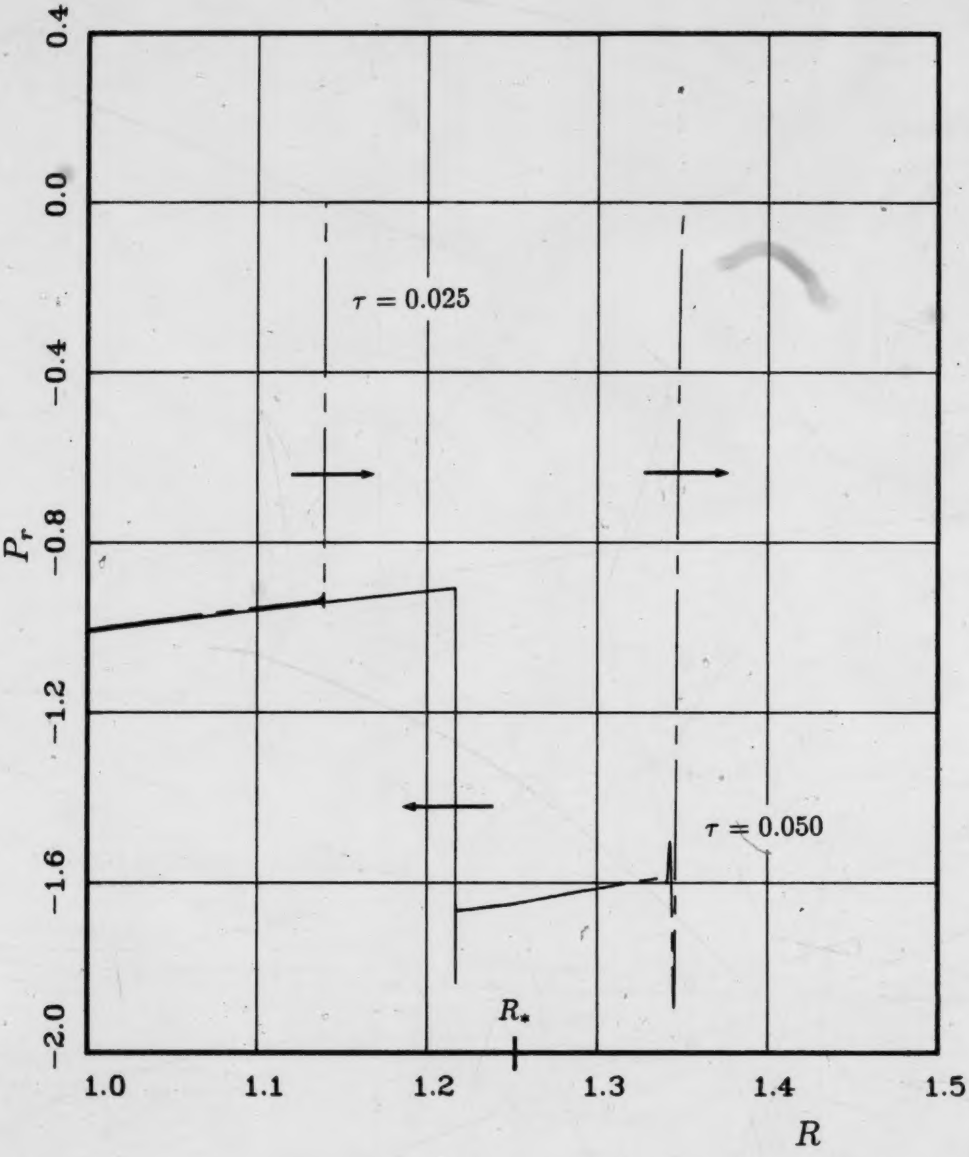

Figure 5.25: Concentric Cylinders, $\nu_1 = 0.48$, $\nu_2 = 0.495$, $\zeta = \rho_{02}/\rho_{01} = 2$, $\psi = \mu_2/\mu_1 = 7$, $R_i = 1$, $R_* = 1.25$, $R_o = 1.5$, $q = 1$.
Nominal Radial Stress at $\tau = 0.025$ and $\tau = 0.05$
Modified Gaussian sef

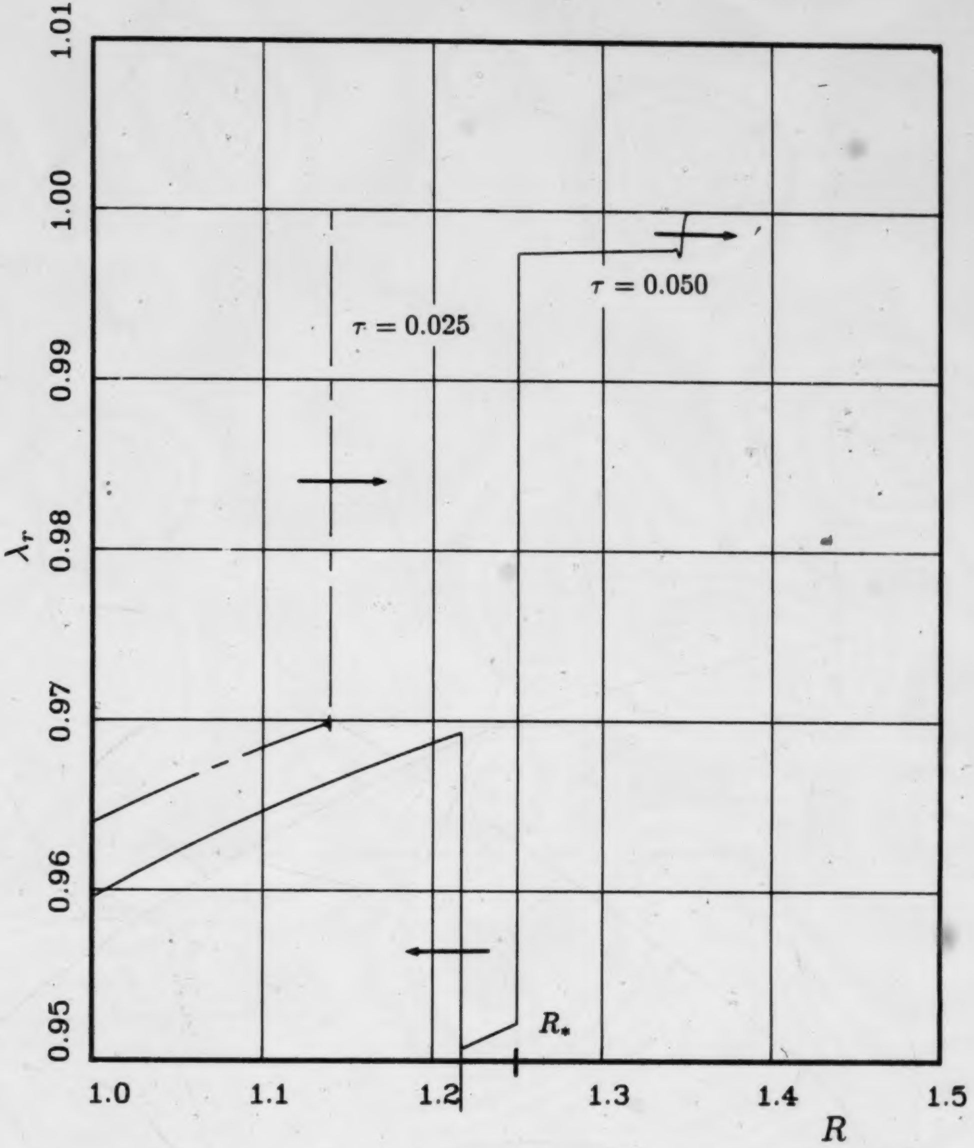

Figure 5.26: Concentric Cylinders, $\nu_1 = 0.48$, $\nu_2 = 0.495$, $\zeta = \rho_{02}/\rho_{01} = 2$, $\psi = \mu_2/\mu_1 = 7$, $R_i = 1$, $R_* = 1.25$, $R_o = 1.5$, $q = 1$.
Radial Stretch at $\tau = 0.025$ and $\tau = 0.05$
Modified Gaussian sef

example, the slope of the velocity is discontinuous at the interface.

The numerical dispersion and smearing which are evident at the shock fronts is spurious and is a consequence of both the crude grid size and the fact that the Courant number in the outer cylinder is significantly less than 1. The latter occurs because the spatial grid sizes for the inner and outer cylinder are fixed and are based on the initial conditions of the deformation. A discussion of this effect is presented in section 4.3.5. The jump conditions for the inner and outer cylinder are given in section 3.4.3 and are satisfied if an extrapolation procedure, similar to that discussed in section 5.1.3 is used to account for the numerical dissipation and dispersion.

Figure 5.27 shows the velocity as a function of R for a somewhat more realistic configuration for which $\nu_1 = 0.48$, $\nu_2 = 0.495$, $\zeta = \rho_{02}/\rho_{01} = 1$, $\psi = \mu_2/\mu_1 = 3$, $R_i = 1$, $R_* = 1.25$, $R_o = 1.5$ and $q = 1$. When $\zeta = 1$, the velocity is both function and slope continuous at the interface.

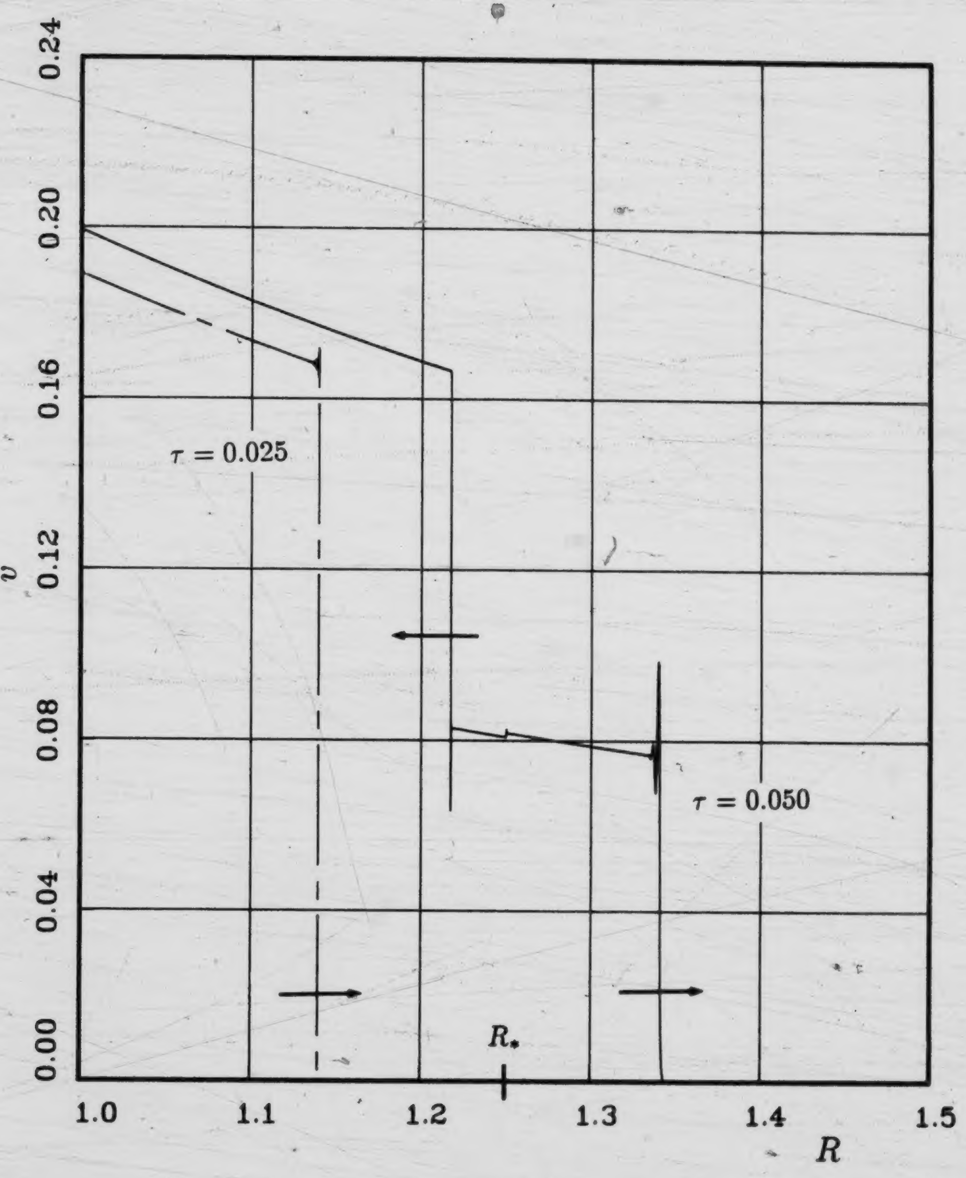

Figure 5.27: Concentric Cylinders, $\nu_1 = 0.48$, $\nu_2 = 0.495$, $\zeta = \rho_{02}/\rho_{01} = 1$, $\psi = \mu_2/\mu_1 = 3$, $R_i = 1$, $R_* = 1.25$, $R_o = 1.5$, $q = 1$.
Radial Stretch at $\tau = 0.025$ and $\tau = 0.05$
Modified Gaussian sef

Chapter 6

Concluding Remarks

The finite elasticity problems considered in this thesis are problems which involve one spatial dimension (radius). A significant extension of this research is to consider two and three dimensional problems in which spherical or cylindrical symmetry does not apply. The additional complexity of two and three dimensional problems is significant since additional dependent variables and governing equations are required to specify the problem.

Based on the success of the hybrid scheme for problems of one spatial dimension, an extension of this scheme for two and three spatial dimension problems may also prove successful. Extension of MacCormack's method for two and three dimensional problems is straightforward and is discussed by several authors including Anderson et al. (1984), MacCormack (1969) and Warming et al. (1973). However, like the one dimensional case, application of the appropriate boundary conditions may not be as easily accomplished and likely requires extension of the method of characteristics for first order PDE's in two and three dependent variables. A presentation of this extension is given by Zauderer (1983).

Another major extension of the thesis work is to consider problems involving simultaneous propagation of both thermal and mechanical disturbances. Part of the difficulty of this problem is in obtaining a suitable constitutive relation which describes the transport of heat in the medium. Fourier's law of heat conduction results in an infinite thermal propagation velocity.

The Maxwell relation (Achenbach, 1984) is a modification of Fourier's law which includes a term which is proportional to the time rate of change of heat flux. The addition of this term results in a finite thermal propagation velocity which, for a one-dimensional thermal propagation problem is $\pm\sqrt{\alpha/\tau}$ where α is the thermal diffusivity and τ is the relaxation time in the Maxwell relation.

An important consideration of this analysis is that limited experimental studies have been conducted to obtain the relaxation time τ. It's magnitude is presumed to be small although experimental measurements for a specific material are generally unavailable.

The computational difficulty of a combined mechanical and thermal propagation problem is related to the fact that the propagation speed of stress and thermal waves may differ by several orders of magnitude. This will cause excessive dispersion of the mechanical wave if the numerical stability criteria is based on the numerically largest characteristic velocity (dominated by the thermal wave velocity).

Most of the numerical solutions which are shown in various figures throughout this thesis, have taxed the limits of mainframe computing power currently available to the author (several hours on an Amdahl 5870 and Floating Point Systems FPS-164 Attached Processor). Using these facilities, a limited amount of numerical dispersion and dissipation is evident in the numerical solutions for the types of problems and range of deformation considered. Extension of this research in areas such as, problems of more than one space dimension, analysis of nearly incompressible media, or thermal wave propagation will require extensive use of a supercomputer.

References

Abbott, M.B., An Introduction to the Method of Characteristics, American Elsevier, New York. (1966)

Adams L.H., Gibson R.E., The compressibility of rubber, *Journal of the Academy of Sciences, Washington* **20**: 213-223, (1930)

Achenbach, J.D., Wave Propogation in Elastic Solids, North Holland Publishing Company, Amsterdam, (1984)

Anderson, D.A., Tannehill, J.C., Pletcher, R.H., Computational Fluid Mechanics and Heat Transfer, McGraw Hill Book Company. (1984)

Baumeister, T., Avallone, E.A., Baumeister III, T., Mark's Standard Handbook for Mechanical Engineers, McGraw Hill Book Company, New York. (1978)

Beatty, M.F., Stalnaker, D.O., The Poisson function of finite elasticity, *Journ. of Appl. Mech.* **53**: 807, (1986)

Bland, D.R., Nonlinear Dynamic Elasticity, Blaisdell Publishing Company, Waltham, Massachusetts, (1969)

Blatz, P.J., Application of large deformation theory to the thermomechanical behavior of rubberlike polymers-porous, unfilled, and filled, Rheology, Theory and Applications, Volume 5 Academic Press, New York. (1969)

Blatz, P.J., Ko, W.L., Applications of finite elasticity theory to the deformation of rubbery materials, *Trans. Soc. Rheo* **6**: 223, (1962)

Bridgman, P.W., The compression of 61 substances to $25,000 kg/cm^2$ determined by a new rapid method, *Proceedings of the American Academy of Arts and Sciences*, **76**: 9-24, (1945)

Chadwick, P., Thermomechanics of rubberlike materials, *Phil. Trans. Roy. Soc. A.*: 276, (1974a)

Chadwick, P., Aspects of the dynamics of a rubberlike material, *Q.J. Mech. appl. Math.* **XXVII** : 263-285, (1974b)

Chadwick, P., Creasy, C.F.M., Modified entropic elasticity of rubberlike materials, *J. Mech. Phys. Solids* **32**: 337, (1984)

Chou, P.C., Koenig, H.A., A unified approach to cylindrical and spherical elastic waves by method of characterisitics, *Journal of Applied Mechanics.* **33** : 159, (1966)

Davison, B., Propagation of plane waves of finite amplitude in elastic solids, *J. Mech. Phys. Solids* **14** : 249-270, (1966)

Fung, Y.C., Foundation of Solids Mechanics, Prentice-Hall, Inc., Englewood Cliffs, New Jersey. (1965)

Graff, K.F., Wave Motion in Elastic Solids, Ohio State University Press. (1975)

Gotlieb, T.T., Turkel, D., Boundary conditions for multistep finite-difference methods for time-dependent equations, *J. Comp. Phys.* **26**: 181, (1978)

Haddow, J.B., Mioduchowski, A., Analysis of expansion of a spherical cavity in unbounded hyperelastic medium by method of characteristics, *Acta Mechanica.* **23** : 219, (1975)

Haddow, J.B., Mioduchowski, A., Dynamic expansion of a compressible hyperelastic spherical shell, *Acta Mechanica.* **26**: 179-187, (1977)

Haddow, J.B., Lorimer, S.A., Tait, R.J., Nonlinear axial shear wave propogation in a hyperelastic incompressible solid, *ACTA Mechanica* **66** : 205-216, (1987a)

Haddow, J.B. Lorimer, S.A., Tait, R.J., Nonlinear combined axial and torsional shear wave propagation in an incompressible hyperelastic solid, *Int. J. Nonlinear Mechanics* **22**: 297, (1987b)

Hildebrand, F.B., Advanced calculus for applications, Prentice-Hall, Inc. Englewood Clifs, New Jersey. (1976)

Kestin, J., A Course in Thermodynamics - Volumes 1, 2, Blaisdell Publishing Company, Waltham, Massachusetts. (1966)

Knowles, J.K., Large amplitude oscillations of a tube of incompressible elastic material, *Quart. Appl. Math.* **18**: 71, (1960) Knowles, J.K., Jakub, M.T., Finite dynamic deformations of an incompressible elastic medium containing a spherical cavity, *Arch. Rat. Mech. Anal.* **18**: 89, (1965)

Kutler, P., Warming, R.F., Lomax, H., Computation of space shuttle flowfields using noncentered finite-difference schemes, *AIAA Journal* **11,2** : 196-204, (1973)

Levinson, M., Burgess, I.W., A comparison of some simple constitutive relations for slightly compressible rubber-like materials, *Int. J. Mec. Sci.***13** : 563-572, (1971)

MacCormack, R.W., The effect of viscosity in hypervelocity impact, *AIAA Paper* **69**: 354, (1969)

MacCormack, R.W., Numerical solution of the interaction of a shock wave with a laminar boundary layer, *Proceedings Second Intl. Conf. on Numerical Methods in Fluid Dynamics* : 151-163, (1971)

Miklowitz, J., Plane stress unloading waves emenating from a suddenly punched hole in a stretched elastic plate, *ASME J. of Applied Mech.* **27**: 165, (1960)

Mioduchowski, A., Haddow, J.B., Dynamic expansion of a spherical cavity in an unbounded hyperelastic medium, *ZAMM* **56**: 89, (1976)

Mioduchowski, A., Moodie, T.B., Haddow, J.B., Waves from suddenly punched hole in finitely stretched elastic sheet, *J. of Applied Mech.* **45**: 83, (1978)

Ogden, R.W., Elastic deformations of rubberlike solids, mechanics of solids, Ed. H.G. Hopkins and M.J.Sewell. *Pergamon Press*, (1982)

Ogden, R.W., Nonlinear Elastic Deformations, Ellis Horwood Limited, Chichester, England (1984)

Reinhart, J.S., Pearson, J., Behavior of metals under impulsive loads, *Journal of The American Society for Metals* (1954)

Sod, G.A., A survey of several finite difference methods for systems of nonlinear hyperbolic conservation laws, *Journal of Computational Physics* **27** : 1-31, (1978)

Sokolnikoff, I.S., Mathematical Theory of Elasticity, McGraw-Hill Book Company, New York. (1956)

Spencer, A.J.M., Continuum Mechanics, Longman Group Limited, Essex, England. (1980)

Warming, R.F., Kutler P., Lomax, H., Second and third order noncentered difference schemes for Nonlinear Hyperbolic Equations, *AIAA Journal* **11**: 189, (1973)

Whitham, G.B., Linear and nonlinear waves, Wiley-Interscience, New York. (1974)

Wood, L.A., Martin, G.M., *J. Res. Nat. Bur. Stand.* **68A**: 259-268, (1964)

Zauderer, E., Partial Differential Equations of Applied Mathematics, Wiley-Interscience Publication, New York. (1983)

Appendix A

Spherically Symmetric Deformation in Incompressible Materials

The dynamic deformation of an incompressible spherical shell is considered in this section. The analysis presented here is a modification of the analysis given by Knowles (1960) for the expansion of an incompressible cylindrical tube.

The dynamic deformation of an incompressible hyperelastic spherical shell is governed by a second order, nonlinear ordinary differential equation whose solution gives the position of a particular radius as a function of time. The ODE which is derived here, gives the position of the inner cavity wall as a function of time. A simple kinematic relation can be used to relate the position at any other radius with the position of the cavity wall.

The analysis is given for the neo-Hookean sef (2.13) although there is no difficulty in principle in considering other incompressible strain energy relations.

The nontrivial equation of motion for spherically symmetric deformation in which body forces are neglected, is given by (3.19) and is repeated below

$$\frac{\partial P_r}{\partial R} + \frac{2\,(P_r - P_\theta)}{R} = \rho_o\,\frac{\partial^2 r}{\partial t^2} \tag{A.1}$$

The velocity term has been written as $\partial r/\partial t$ using $r = r(R,t)$.

For an incompressible material, the nominal stress components are given by

$$\begin{aligned} P_r &= \frac{\partial}{\partial \lambda_r}(W - p{\lambda_\phi}^2\lambda_r) = \frac{\partial W(\lambda_r,\lambda_\phi)}{\partial \lambda_r} - p{\lambda_\phi}^2 \\ P_\phi &= \frac{1}{2}\frac{\partial}{\partial \lambda_\phi}(W - p{\lambda_\phi}^2\lambda_r) = \frac{1}{2}\frac{\partial W(\lambda_r,\lambda_\phi)}{\partial \lambda_\phi} - \frac{p}{\lambda_\phi} \end{aligned} \tag{A.2}$$

where p is an arbitrary Lagrangian multiplier which is not determined from the deformation. The incompressibility condition given by $J = \lambda_r \lambda_\theta{}^2 = 1$ has been used.

The neo-Hookean sef (2.13), for spherically symmetric deformation is

$$W = \frac{\mu}{2}\left\{\lambda_r{}^2 + 2\,\lambda_\phi{}^2 - 3\right\} \tag{A.3}$$

The nominal stress components obtained using (A.2) are

$$\begin{aligned} P_r &= \frac{\mu}{\lambda_\phi{}^2} - p\lambda_\phi{}^2 \\ P_\phi &= \mu\lambda_\phi - \frac{p}{\lambda_\phi} \end{aligned} \tag{A.4}$$

Substitution of these relations into the equation of motion (A.1) yields

$$-\lambda_\phi{}^2\frac{\partial p}{\partial R} + \frac{2\,\mu}{R}\left\{(\lambda_\phi{}^{-3} - 1)(\lambda_\phi - \lambda_\phi{}^{-2})\right\} = \rho\,\frac{\partial^2 r}{\partial t^2} \tag{A.5}$$

where

$$\frac{\partial}{\partial R}(\lambda_\phi) = \frac{\partial}{\partial R}\left(\frac{r}{R}\right) = \frac{1}{R}(\lambda_\phi{}^{-2} - \lambda_\phi) \tag{A.6}$$

has been used.

To apply the boundary conditions, it is convenient to introduce

$$Q = \frac{R}{r} = \frac{1}{\lambda_\phi} \tag{A.7}$$

Differentiation with respect to R, in terms of differentiation with respect to Q can be related using

$$\begin{aligned} \frac{\partial}{\partial R} &= \frac{dQ}{dR}\,\frac{\partial}{\partial Q} = \frac{d}{dR}(R\,r^{-1})\,\frac{\partial}{\partial Q} \\ &= \frac{(Q - Q^4)}{R}\frac{\partial}{\partial Q} \end{aligned} \tag{A.8}$$

Using (A.7) and (A.8), the equation of motion (A.5) can be written

$$-\frac{\partial p}{\partial Q} + 2\mu\,(Q^3 - 1) = \frac{rQ^2}{(1 - Q^3)}\,\rho\,\frac{\partial^2 r}{\partial t^2} \tag{A.9}$$

Since the material is incompressible,

$$r^3 - R^3 = r_i^3 - R_i^3 \qquad\qquad R_i \le R \le R_o \tag{A.10}$$

where R_i and R_o are the inner and outer radii of the shell in the reference state. Using this relation, the acceleration term of equation (A.9), $\partial^2 r/\partial t^2$, can be expressed in terms of $d^2 r_i/dt^2$, where r_i is the radius of the cavity wall in the deformed coordinate system. Differentiating both sides of equation (A.10) twice with respect to time and using (A.7) yields

$$\frac{\partial^2 r}{\partial t^2} = \left(\frac{1 - Q^3}{r_i^3 - R_i^3}\right)^{2/3} r_i \left\{ r_i \frac{d^2 r_i}{dt^2} + 2\left(\frac{dr_i}{dt}\right)^2 \left(1 - \frac{1 - Q^3}{r_i^3 - R_i^3} r_i^3\right)\right\} \tag{A.11}$$

Substitution of this relation into (A.9) yields

$$\begin{aligned} -\frac{\partial p}{\partial Q} \quad &+ \quad 2\,\mu\,(Q^3 - 1) \\ &= \frac{\rho\, Q^2 (r_i^3 - R_i^3)^{-1/3}}{(1 - Q^3)^{2/3}} r_i \left\{ r_i \frac{d^2 r_i}{dt^2} + 2\left(\frac{dr_i}{dt}\right)^2 \left(1 - \frac{1 - Q^3}{r_i^3 - R_i^3} r_i^3\right)\right\} \end{aligned} \tag{A.12}$$

If the inner and outer surfaces of the spherical shell are subjected to spatially uniform internal and external pressures $\Pi_i(t)$ and $\Pi_o(t)$ respectively, the boundary conditions can be written

$$\begin{aligned} \sigma_r(R_i, t) \quad &= \quad -\Pi_i(t) = \frac{1}{{\lambda_\phi}^2} P_r(R_i, t) = Q^2 P_r(R_i, t) \\ \sigma_r(R_o, t) \quad &= \quad -\Pi_o(t) = \frac{1}{{\lambda_\phi}^2} P_r(R_o, t) = Q^2 P_r(R_o, t) \end{aligned} \tag{A.13}$$

Using equation (A.4a), these boundary conditions can also be written

$$
\begin{aligned}
-p+\mu\,Q_i^4 &= -\Pi_i(t) \qquad for \qquad Q_i=\frac{R_i}{r_i}\\
-p+\mu\,Q_o^4 &= -\Pi_o(t) \qquad for \qquad Q_o=\frac{R_o}{r_o}
\end{aligned} \tag{A.14}
$$

If equation (A.12) is integrated with respect to Q and the boundary condition (A.14a) is applied, the hydrostatic pressure p must satisfy

$$
\begin{aligned}
-p \quad &+ \quad \frac{\mu\,Q^4}{2}-2\mu\,Q\\
&= \quad -\frac{\mu\,Q_i^4}{2}-2\,\mu\,Q_i+\frac{\rho r_i^3}{(r_i^3-R_i^3)^{1/3}}\frac{d^2r_i}{dt^2}\int_{Q_i}^{Q}\frac{\eta^2}{(1-\eta^3)^{2/3}}d\eta\\
&+ \quad \frac{2\,\rho r_i}{(r_i^3-R_i^3)^{1/3}}\left(\frac{dr_i}{dt}\right)^2\int_{Q_i}^{Q}\frac{\eta^2}{(1-\eta^3)^{2/3}}\left(1-\frac{(1-\eta^3)}{(r_i^3-R_i^3)}r_i^3\right)d\eta\\
&- \quad \Pi_i(t)
\end{aligned} \tag{A.15}
$$

If equation (A.15) is evaluated at $Q = Q_o$ and the boundary condition given by (A.14b) is used, the differential equation for $r_i(t)$ is

$$
\begin{aligned}
2\,\mu(Q_o-Q_i) \quad &+ \quad \frac{\mu}{2}(Q_o^4-Q_i^4)\\
&+ \quad \frac{\rho r_i^3}{(r_i^3-R_i^3)^{1/3}}\frac{d^2r_i}{dt^2}\int_{Q_i}^{Q_o}\frac{\eta^2}{(1-\eta^3)^{2/3}}d\eta\\
&+ \quad \frac{2\,\rho r_i}{(r_i^3-R_i^3)^{1/3}}\left(\frac{dr_i}{dt}\right)^2\int_{Q_i}^{Q_o}\frac{\eta^2}{(1-\eta^3)^{2/3}}\left(1-\frac{(1-\eta^3)}{(r_i^3-R_i^3)}r_i^3\right)d\eta\\
&= \quad \Pi_i(t)-\Pi_o(t)
\end{aligned} \tag{A.16}
$$

The incompressibility condition (A.10) can be used to eliminate r_o in the definition of Q_o as given by

$$
Q_o=\frac{R_o}{r_o}=\frac{R_o}{(R_o^3-R_i^3+r_i^3)^{1/3}} \tag{A.17}
$$

If the integration in (A.16) is performed, the resulting differential equation is

$$\hat{A}\frac{d^2r_i}{dt^2} + \hat{B}\left(\frac{dr_i}{dt}\right)^2 + \hat{C} = \Pi_1(t) - \Pi_o(t) \tag{A.18}$$

where

$$\begin{aligned}
\hat{A} &= \frac{\rho r_i^2}{(r_i^3 - R_i^3)^{1/3}}\left\{(1 - Q_i^3)^{1/3} - (1 - Q_o^3)^{1/3}\right\} \\
\hat{B} &= \frac{2\,\rho r_i}{(r_i^3 - R_i^3)^{1/3}}\left\{(1 - Q_i^3)^{1/3} - (1 - Q_o^3)^{1/3}\right. \\
&\quad \left. + \frac{r_i^3}{4(r_i^3 - R_i^3)}\left\{(1 - Q_o^3)^{4/3} - (1 - Q_i^3)^{4/3}\right\}\right\} \\
\hat{C} &= 2\mu(Q_o - Q_i) + \frac{\mu}{2}(Q_o^4 - Q_i^4)
\end{aligned} \tag{A.19}$$

Consider a nondimensional scheme given by

$$\overline{\Pi} = \frac{\Pi}{\mu} \qquad\qquad \tau = \frac{t}{R_i}\sqrt{\frac{\mu}{\rho}} \tag{A.20}$$

which corresponds to the scheme used in Section 3.1.2 for deformation of compressible materials. Defining λ_1 as

$$\lambda_1 = \lambda_\phi(R_i, t) = r_i/R_i \tag{A.21}$$

the ordinary differential equation corresponding the deformation of an incompressible spherical shell for the neo-Hookean sef is

$$A\frac{d^2\lambda_1}{d\tau^2} + B\left(\frac{d\lambda_1}{d\tau}\right)^2 + C = \overline{\Pi}_1(\tau) - \overline{\Pi}_0(\tau) \tag{A.22}$$

where

$$\begin{aligned} A &= \frac{\lambda_1^2}{(\lambda_1^3-1)^{1/3}}\left\{(1-Q_i^3)^{1/3}-(1-Q_o^3)^{1/3}\right\} \\ B &= \frac{2\lambda_1}{(\lambda_1^3-1)^{1/3}}\left\{(1-Q_i^3)^{1/3}-(1-Q_o^3)^{1/3}\right\} \\ &+ \frac{\lambda_1^4}{2\,(\lambda_1^3-1)^{4/3}}\left\{(1-Q_o^3)^{4/3}-(1-Q_i^3)^{4/3}\right\} \\ C &= 2\,(Q_o-Q_i)+\frac{1}{2}(Q_o^4-Q_i^4) \end{aligned} \tag{A.23}$$

The nonlinear ODE (A.22) can be solved using a $4th$ order Runge-Kutta Technique. The solutions presented in this thesis are for $\Pi_o(\tau)=0$ although there is no difficulty in using a non-zero external pressure.

For the special case in which $R_o \to \infty$, that is, deformation of a spherical cavity in an unbounded medium,

$$Q_o=\frac{R_o}{r_o}\to 1 \qquad as \qquad \frac{R_o}{R_i}\to\infty \tag{A.24}$$

The ordinary differential equation (A.22) is applicable with $\Pi_o(\tau)=0$ and

$$\begin{aligned} A &= \frac{\lambda_1^2}{(\lambda_1^3-1)^{1/3}}(1-Q_i^3)^{1/3} \\ B &= \frac{2\,\lambda_1}{(\lambda_1^3-1)^{1/3}}(1-Q_i^3)^{1/3}-\frac{\lambda_1^4}{2\,(\lambda_1^3-1)^{4/3}}(1-Q_i^3)^{4/3} \\ C &= 2\,(1-Q_i)+\frac{1}{2}(1-Q_i^4) \end{aligned} \tag{A.25}$$

Appendix B

Finite Elasticity Terminology

For problems of spherical symmetry, it is convenient to use spherical polar coordinates denoted by r, θ, ϕ in the deformed coordinate system and R, Θ, Φ in the reference (undeformed) coordinate system. An analogous cylindrical polar coordinate system denoted by r, θ, z and R, Θ, Z is convenient for problems of cylindrical symmetry.

Spherically symmetric homogeneous deformation of body B, from its reference configuration B_o, is given by (Ogden, 1984)

$$\begin{aligned} r &= r(R,t) \\ \theta &= \Theta \\ \phi &= \Phi \end{aligned} \tag{B.1}$$

Cylindrically symmetric homogeneous deformation is given by

$$\begin{aligned} r &= r(R,t) \\ \theta &= \Theta \\ z &= Z \end{aligned} \tag{B.2}$$

The deformation gradient tensor F is a two point tensor with components $F_{i\alpha}$. In spherical polar coordinates, the components of F are (Spencer, 1980)

$$F = \left\{ \begin{array}{ccc} \frac{\partial r}{\partial R} & \frac{1}{R}\frac{\partial r}{\partial \Theta} & \frac{1}{R\,sin\Theta}\frac{\partial r}{\partial \Phi} \\ r\frac{\partial \theta}{\partial R} & \frac{r}{R}\frac{\partial \theta}{\partial \Theta} & \frac{r}{R\,sin\Theta}\frac{\partial \theta}{\partial \Phi} \\ r\,sin\theta\frac{\partial \phi}{\partial R} & \frac{r\,sin\theta}{R}\frac{\partial \phi}{\partial \Theta} & \frac{r\,sin\theta}{R\,sin\Theta}\frac{\partial \phi}{\partial \Phi} \end{array} \right\} \tag{B.3}$$

and in cylindrical polar coordinates, the components of F are

$$F = \left\{ \begin{array}{ccc} \frac{\partial r}{\partial R} & \frac{1}{R}\frac{\partial r}{\partial \Theta} & \frac{\partial r}{\partial Z} \\ r\frac{\partial \theta}{\partial R} & \frac{r}{R}\frac{\partial \theta}{\partial \Theta} & r\frac{\partial \theta}{\partial Z} \\ \frac{\partial z}{\partial R} & \frac{1}{R}\frac{\partial z}{\partial \Theta} & \frac{\partial z}{\partial Z} \end{array} \right\} \tag{B.4}$$

If the deformation is spherically or cylindrically symmetric, only the diagonal components of (B.3) and (B.4) respectively are non-zero.

By the polar decomposition theorem, the deformation gradient tensor F may be uniquely decomposed into either of the products

$$\begin{aligned} F &= R\,U \\ F &= V\,R \end{aligned} \tag{B.5}$$

where R is a second order orthogonal tensor and U and V are symmetric positive definite second order tensors. U and V are called the right and left stretch tensors respectively, and R is called the rotation tensor. For the special case of spherically and cylindrically symmetric deformation, $R = I$ where I is the identity tensor. Since U is symmetric and positive definite, it's principal values $(\lambda_1, \lambda_2, \lambda_3)$ are real and positive. The principal values of V are the same as those of U.

A suitable measure of finite deformation is given by either the right Cauchy-Green deformation tensor C or the left Cauchy-Green deformation tensor B, where

$$\begin{aligned} C &= F^T F \\ B &= F\,F^T \end{aligned} \tag{B.6}$$

The relation between tensors C and B and U and V can be obtained using (B.5) and (B.6)

$$C = F^T F = U\,R^T R\,U = U^2$$

$$C = F\,F^T = V\,R\,R^T\,V = V^2 \tag{B.7}$$

The principal stretches $\lambda_1, \lambda_2, \lambda_3$ are invariants which are intrinsic to the deformation and are principal values of U and V. Since $C = U^2$ and $B = V^2$, the principal values of C and B are λ_1^2, λ_2^2 and λ_3^2. Other combinations of these principal stretches are also invariant and it is convenient to define the strain invariants

$$\begin{aligned} I_1 &= tr\, C = tr\, B = \lambda_1^2 + \lambda_2^2 + \lambda_3^2 \\ I_2 &= \frac{1}{2}\{(tr\, C)^2 - tr\, C^2\} = \frac{1}{2}\{(tr\, B)^2 - tr\, B^2\} = \lambda_2^2\lambda_3^2 + \lambda_1^2\lambda_2^2 + \lambda_3^2\lambda_1^2 \\ I_3 &= det\, C = det\, B = \lambda_1^2\lambda_2^2\lambda_3^2 \end{aligned} \tag{B.8}$$

The dilatation J is given by

$$J = \lambda_1\lambda_2\lambda_3 \tag{B.9}$$

and can be written in terms of the deformation gradient F

$$J = \sqrt{I_3} = \sqrt{det\, C} = \sqrt{det(F^T F)} = det\, F \tag{B.10}$$